UNIVERSIDAD NACIONAL DEL LITORAL

Facultad de Bioquímica y Ciencias Biológicas

TECHNISCHE UNIVERSITÄT DRESDEN

Bereich Mathematik und Naturwissenschaften

Thesis presented as part of the requirements of UNL,
to obtain the Academic Degree
Doctor in Biochemistry and Applied Biology / Doctor Rerum Naturalium

STUDY OF THE NOVEL OXR PROTEIN FAMILY IN PLANTS

Regina Mencia

Argentine Director: Prof. Dr. Elina Welchen
German Director: Prof. Dr. Jutta Ludwig-Müller

Places of execution: Laboratorio de Biología Molecular-Instituto de Agrobiotecnología del Litoral-UNL-CONICET and Institut fuer Botanik-TU Dresden

-2019-

Acknowledgments

It is a great pleasure to express my gratitude and appreciation to Prof. Dr. Elina Welchen and Prof. Dr. Jutta Ludwig-Müller for their supervision during my PhD work.

Also, I would like to thank CONICET and CUAA-DAHZ-DAAD for financial support, the IAL-FCBC-UNL for providing an excellent working place, and my colleagues from the LBM.

I would further like to thank FBCB-UNL and TU Dresden for accepting me into their PhD program.

Part of this work was published in:

Francisco Colombatti*, Regina Mencia*, Lucila Garcia, Natanael Mansilla, Sergio Alemano, Andrea M Andrade, Daniel H Gonzalez, Elina Welchen. The mitochondrial oxidation resistance protein AtOXR2 increases plant biomass and tolerance to oxidative stress. Journal of Experimental Botany, Volume 70, Issue 12, 1 June 2019, Pages 3177–3195, https://doi.org/10.1093/jxb/erz147

*both authors share the first authorship.

Submitted: Regina Mencia, Gabriel Céccoli, Georgina Fabro, Pablo Torti, Francisco Colombatti, Jutta Ludwig-Müller, Maria Elena Alvarez, Elina Welchen. Arabidopsis OXR2 increases plant defense acting on the activity of the salicylic acid pathway.

Table of Contents

List of Abbreviations

AA	antimycin A
aa	amino acid
ABI4	abscisic acid-insesitive-4
AHK	Arabidopsis histidine kinase
AHP	histidine phosphotransfer proteins
ANAC	no apical meristem/arabidopsis transcription activation factor/cup-shaped cotyledon transcription
AOX	alternative oxidase
ARR	Arabidopsis response regulator
ATP	adenosine triphosphate
bp	base pair
BSA	bovine serum albumin
CaMV	cauliflower mosaic virus
CAT	catalase
CcO	cytochrome c oxidase
CDKE1	cyclin-dependent kinase E1
cDNA	complementary DNA
CFU	colony-forming unit
CG-MS	gas chromatography–mass spectrometry
Chl	chlorophyll
CKs	cytokinins
CKX	cytokinin oxidase
CLSM	confocal microscopy
Col 0	Columbia 0
COX2	cytochrome c oxidase subunit 2
DAI	days after inoculation
DAS	days after sowing
DHAR	dehydroascorbate reductase
DI	disease index
DNA	deoxyribonucleic acid

DPI	days postinfection
DW	dry weigth
E. coli	*Escherichia coli*
ER	endoplasmic reticulum
et al.	*et alii*/and others
ETI	effector-triggered immunity
Fig.	figure
Fv/Fm	maximun dark-adapted quantum photosynthetic efficiency of photosystem II
FW	fresh weight
G6PDH	glucose-6-phosphate 1-dehydrogenase
GFP	green fluorescent protein
GMO	genetic modified organism
GPX	glutathione peroxidase
GR	glutathione reductase
GUS	ß-glucuronidase
H2DCFDA	2',7'-dichlorodihydrofluorescein diacetate
HAI	hours after inoculation
HEPES	4-(2-hydroxyethyl)-1-piperazineethanesulfonic acid
HPLC	High-performance liquid chromatography
HR	hypersensitive reaction
HRE2	hypoxia responsive ethylene response factor2
HRP	horseradish peroxidase
HSP23.5	heat shock protein 23.5
i.e.	*id est*/that is
ICS1	isochorismate synthase
IgG	immunoglobulin G
iP	isopentenyl-adenine
iPR	isopentenyl-adenine riboside
IPT	isopentenyltransferase
JA	jasmonic acid
KB	King's B medium

KIN10	sucrose non-fermenting1 (SNF1)-related protein kinase
LB	Luria-Bertani medium
LD	long day
MAMP	microbe-associated molecular patterns
Mbp	mega base pair
MDAR	monodehydroascorbate reductase
MeSA	methylsalicylic acid
miRNA	micro RNA
mRFP	monomeric red fluorescent protein
MRR	mitochondrial retrograde regulation
MS	Murashige and Skoog medium
mtROS	mitochondrial ROS
MUG	4-methyl umbelliferyl glucuronide
MV	methyl viologen
MYB29	MYB domain protein 29
NADP	nicotinamide adenine dinucleotide phosphate
NBT	nitroblue tetrazolium
NIMIN	NIM1-interacting
NPR1	nonexpressor of PR genes
NTR	NADPH-thioredoxin reductase
OM66	outer mitochondrial membrane protein of 66 kDa
OXR	oxidation resistance
P. brassicae	*Plasmodiophora brassicae*
P. syringae	*Pseudomonas syringae pv. tomato*
PAD	phytoalexin deficient
PAMP	pathogen-associated molecular patterns
PAP	30-phosphoadenosine-50-phosphate
PC	plastocyanin
PCR	polymerase chain reaction
POX	peroxidase
PR	pathogenesis-related gene 1
PRR	pattern recognition receptors

PRXs	peroxiredoxins
PSII	photosystem II
Pst DC 3000	*Pseudomonas syringae pv. Tomato DC3000*
PTI	pattern triggered immunity
PVDF	polyvinylidene fluoride
RI	relative ion intensity
RNA	ribonucleic acid
ROS	reactive oxygen species
RT-qPCR	real-time polymerase chain reaction
SA	salicylic acid
SAD_4	salicylic acid-D_4
SAL1	phosphatase-like protein
SAR	systemic acquired resistance
SDS	sodium dodecyl sulfate
SDS-PAGE	sodium dodecyl sulfate–polyacrylamide gel electrophoresis
SEM	standard error of the mean
SHAM	salicylhydroxamic acid
sid2	induction deficient 2
eds	enhanceddisease susceptiblity
SOD	superoxide dismutase
T-DNA	transfer DNA
TF	transcription factor
TGA	basic leucine zipper (bZIP) type TGACGTCA cis-element-binding protein
TLDc	Tre2/Bub2/Cdc16 (TBC), lysin motif (LysM), domain catalytic
TMRM	tetramethyl rhodamine methyl ester
tZ	trans-zeatin (tZ)
tZR	trans-zeatin riboside
UGT74E2	UDP-glycosyl transferase 74E2
UPOX	upregulated by oxidative stress
UV-B	ultraviolet B
v/v	volume/volume

w/v	weight/volume
WB	western blot
WRKY	WRKY DNA-binding protein
ws	Wassilewskija
Wt	wild type
x	times
X-gluc	5-Bromo-4-chloro-1H-indol-3-yl ß-D-glucopyranosiduronic acid

Amino acid code

A	Ala	Alanine	M	Met	Methionine
C	Cys	Cysteine	N	Asn	Asparagine
D	Asp	Aspartic Acid	P	Pro	Proline
E	Glu	Glutamic Acid	Q	Gln	Glutamine
F	Phe	Phenylalanine	R	Arg	Arginine
G	Gly	Glycine	S	Ser	Serine
H	His	Histidine	T	Thr	Threonine
I	Ile	Isoleucine	V	Val	Valine
K	Lys	Lysine	W	Trp	Tryptophan
L	Leu	Leucine	Y	Tyr	Tyrosine

Abstract

OXidation Resistance (OXR) is a family of eukaryotic proteins characterized by the presence of the highly conserved TLDc (TBC (Tre2/Bub2/Cdc16), LysM (lysine motif), domain catalytic) domain at the C-terminal half. Although the mechanism by which OXR proteins exert their action is still unknown, they have been associated with the prevention of oxidative damage in mammals and in response to pathogens and immune-associated inflammatory responses in different animal models. The purpose of this thesis is to study the presence and the role of OXR proteins in plants, particularly in *Arabidopsis thaliana*.

Six OXR proteins were identified in Arabidopsis and the analysis was focused on 2 members of this family: AtOXR2 and AtOXR5. Their subcellular localisation was confirmed by CLSM using fluorescent tags and observed AtOXR2 in mitochondria while AtOXR5 was found in the apoplast on the assayed conditions.

To study the function of these proteins, plants that constitutively overexpress *AtOXR2* or *AtOXR5* (OXR2, OXR5) and T-DNA knockout mutants (*oxr2*, *oxr5*) were obtained and analysed throughout their life cycle under normal growth conditions. OXR2 plants exhibited a larger size, higher biomass and prolonged vegetative stage that renders in higher plant production. OXR5 and *oxr2* loss-of-function mutants did not show distinct features in comparison to wild type (Wt) plants and *oxr5* unexpectedly showed some characteristics similar to OXR2 plants, like an increased number of leaves and a delayed transition to the reproductive phase. Besides, OXR2 plants possess an increased respiration rate, a lower mitochondrial membrane potential and accumulate ROS in comparison with Wt plants grown in long day (LD) conditions.

AtOXR2 transcript is induced by different compounds that produce oxidative stress in plants, such as MV, AA, SA and also when plants were faced with hemibiotrophic pathogens like *Pseudomonas syringae* pv. *tomato* DC3000. OXR2, Wt, *oxr2* and *oxr5* plants behaviour, growth phenotypes and their responses to different abiotic stressors like MV and AA was tested. In these experiments, OXR2 plants were more resistant and, on the contrary, both loss-of-function mutants were more sensitive.

Also, plants with altered levels of *AtOXR2* and *AtOXR5* were exposed to two different plant pathogens: the hemibiotrophic bacterium Pst DC3000 and the biotrophic protist *Plasmodiophora brassicae*. OXR2 plants showed increased resistance to both pathogens compared to Wt plants and the opposite behaviour was observed in *oxr2* and *oxr5* mutants. In agreement, plants with altered expression of *AtOXR2* accumulated different levels of the pathogen response hormone SA. The increased basal pathogen-defence phenotype was dependent on an intact SA synthesis and SA activation and signaling pathways, due to it is loss in *ics1*/*sid2* and *npr1* mutant backgrounds.

In order to explain the fact that OXR2 plants exhibit both increased biomass and pathogen resistance the hormone CKs was studied. OXR2 plants accumulate CKs and *oxr2.2* displays a lower amount. The growth phenotypes found for OXR2 plants were lost in mutant plants with loss-of-function in proteins related to CKs syntheses (*ipt1357*+OXR2) and signalling (*ahp1234*+OXR2). In plants with gain-of-function in catabolic enzymes (CKX1+OXR2 and CKX2+OXR2) a partial reversion of the root length phenotype and also the increased sensitivity towards Pst DC3000 was detected. It seems likely that the accumulation of CKs in OXR2 plants could be partially due to a decrease in CKX activity.

Overall, new pieces of evidences about the role of OXR proteins in Arabidopsis are provide. These evidences aim to reinforce the role of OXR plant-proteins in oxidative stress responses as was proposed in different animal models. Still, more studies are required to disclose specific mechanism of action of TLDc proteins. Furthermore, the characteristics conferred to plants by the overexpression of *AtOXR2*, like increased yield and resistance to pathogens, makes it valuable for agro-biotechnological purposes.

Resumen

La familia de proteínas eucariotas OXR *(OXidation Resistance)* se caracteriza por la presencia del dominio TLDc altamente conservado en la mitad C-terminal, sin actividad específica asignada. Se ha descrito previamente su papel en la prevención del daño celular por estrés oxidativo y en respuesta a enfermedades relacionas con patógenos en animales. En esta Tesis nuestro objetivo fue estudiar la presencia y el papel de las proteínas OXR en *Arabidopsis thaliana*.

Identificamos seis proteínas OXR en Arabidopsis y nos centramos en el análisis de 2: AtOXR2 y AtOXR5. Confirmamos su localización subcelular por CLSM usando reporteros fluorescentes y vimos que AtOXR2 se expresa en mitocondrias, mientras que AtOXR5 se localiza en el apoplasto, en condiciones normales de crecimiento.

Analizamos parámetros de crecimiento a lo largo del ciclo de vida, de plantas con altos niveles de expresión de *AtOXR2* o *AtOXR5* (OXR2, OXR5) y mutantes nulas por inserciones de T-DNA en ambos genes (*oxr2, oxr5*). Las plantas OXR2 exhibieron un mayor tamaño, mayor biomasa y una etapa vegetativa prolongada, lo que se tradujo en una mayor producción de semillas. Las mutantes OXR5 y *oxr2* no mostraron características distintivas en comparación con las plantas Wt y las plantas *oxr5* mostraron algunas similitudes a las plantas OXR2, como un mayor número de hojas y un retraso en la transición al estadío reproductivo. Además, las plantas OXR2 presentaron una mayor tasa de respiración mitocondrial, menor potencial de membrana mitocondrial y acumulación de ROS en comparación con las plantas cultivadas en condiciones normales.

Particularmente *AtOXR2* es inducido en plantas Wt desafiadas con diferentes compuestos que producen estrés oxidativo y también cuando se enfrentan al patógeno Pst DC3000. Luego, analizamos los fenotipos de crecimiento de las plantas OXR2, Wt, *oxr2* y *oxr5* y sus respuestas a MV y AA. En estos experimentos, las plantas OXR2 fueron más resistentes y, por el contrario, ambos mutantes con pérdida de función fueron más sensibles.

Además, enfrentamos plantas con niveles alterados de *AtOXR2* y *AtOXR5* a dos patógenos de plantas diferentes: Pst DC3000 y *Plasmodiophora brassicae*. Las plantas OXR2 mostraron una mayor resistencia a ambos patógenos en comparación con las plantas Wt. El comportamiento opuesto se observó en las plantas mutantes *oxr2* y *oxr5*. De acuerdo con este resultado, las plantas con expresión alterada de *AtOXR2* acumularon diferentes niveles de la hormona SA. El fenotipo de aumento basal de defensas frente a patógenos depende de la presencia de la vía de síntesis y señalización de SA, debido a la supresión presentada cuando se analizan plantas mutantes con pérdida de función en estos procesos (*ics1/sid2* y *npr1)*.

Para explicar el hecho de que las plantas OXR2 exhiben una mayor biomasa y resistencia a aumentada a patógenos, estudiamos la hormona CKs. Las plantas OXR2 acumulan CKs y las *oxr2.2*, por el contrario, presentan menos cantidad. Los fenotipos de crecimiento presentados por las plantas OXR2 se perdieron en plantas mutantes con de pérdida de función en la síntesis (*ipt1357*+OXR2) y en la señalización de CKs (*ahp1234*+OXR2). En plantas con ganancia de función en el catabolismo de CKs (CKX1+OXR2 y CKX2+OXR2) detectamos una reversión parcial del fenotipo de longitud de raíz y una mayor sensibilidad hacia Pst DC3000. Es probable que la acumulación de CK en las plantas OXR2 se deba en parte a la disminución de la actividad de CKX.

En general, proporcionamos nuevas evidencias sobre el papel de las proteínas OXR en Arabidopsis. Estas evidencias apuntan a reforzar el papel de las proteínas vegetales OXR en respuestas al estrés oxidativo. Además, las características conferidas a las plantas por la sobreexpresión de *AtOXR2*, resultan muy atractivas para ser utilizadas con fines agrobiotecnológicos.

Zusammenfassung

OXidationsresistenz (OXR) ist eine Familie von eukaryotischen Proteinen, die durch das Vorhandensein von hochkonserviertem TLDc (TBC (Tre2 / Bub2 / Cdc16), LysM (Lysinmotiv), Domänenkatalyse) in der C-terminalen Hälfte gekennzeichnet ist. Obwohl der Mechanismus, durch den OXR-Proteine ihre Wirkung ausüben, noch unbekannt ist, wurden sie mit der Verhinderung oxidativer Schäden bei Säugetieren und als Reaktion auf Krankheitserreger und immunassoziierte Entzündungsreaktionen in verschiedenen Tiermodellen in Verbindung gebracht. In dieser Arbeit untersuchen wir das Vorhandensein und die Rolle von OXR-Proteinen in Pflanzen, insbesondere in *Arabidopsis thaliana*.

Wir haben sechs OXR-Proteine in Arabidopsis identifiziert und uns auf die Analyse von zwei Mitgliedern dieser Familie konzentriert: AtOXR2 und AtOXR5. Wir bestätigten ihre subzelluläre Lokalisation durch CLSM unter Verwendung fluoreszierender Markierungen und beobachteten AtOXR2 in Mitochondrien, während AtOXR5 unter den untersuchten Bedingungen im Apoplasten gefunden wurde.

Um die Funktion dieser Proteine zu untersuchen, haben wir Pflanzen hergestellt und analysiert, die *AtOXR2* oder *AtOXR5* (OXR2, OXR5) und T-DNA-Knockout-Mutanten (*oxr2*, *oxr5*) während ihres gesamten Lebenszyklus unter normalen Wachstumsbedingungen überexprimieren. OXR2-Pflanzen wiesen eine größere Größe, höhere Biomasse und ein längeres vegetatives Stadium auf, was zu einer höheren Pflanzenproduktion führte. OXR5 und *oxr2*-Funktionsverlustmutanten zeigten im Vergleich zu Wt-Pflanzen keine besonderen Merkmale, und *oxr5* zeigte unerwartet ähnliche Merkmale wie OXR2-Pflanzen, wie eine erhöhte Anzahl von Blättern und einen verzögerten Übergang zur Fortpflanzungsphase. Außerdem zeigten OXR2-Pflanzen eine erhöhte Atmungsrate, ein niedrigeres Mitochondrienmembranpotential und akkumulierten ROS im Vergleich zu Wt-Pflanzen, die unter Langtag-Bedingungen angezogen wurden.

Das *AtOXR2*-Transkript wird durch verschiedene Verbindungen induziert, die pflanzlichen oxidativen Stress auslösen, wie MV, AA, SA, und auch, wenn Pflanzen mit hemibiotrophen Pathogenen wie *Pseudomonas syringae* pv. *Tomaten* DC3000 konfrontiert waren. Wir testeten das Verhalten von OXR2, Wt, *oxr2* und *oxr5*-Pflanzen, die Wachstumsphänotypen und ihre Reaktionen auf verschiedene abiotische Stressfaktoren wie MV und AA. In diesen Experimenten waren OXR2-Pflanzen resistenter und im Gegensatz dazu waren beide Mutanten mit Funktionsverlust sensitiver.

Wir sahen uns auch Pflanzen mit veränderten *AtOXR2*- und *AtOXR5*-Spiegeln an, die mit zwei verschiedenen Pflanzenpathogenen inokuliert wurden: Pst DC3000 und *Plasmodiophora brassicae*. OXR2-Pflanzen zeigten im Vergleich zu Wt-Pflanzen eine erhöhte Resistenz gegen beide Krankheitserreger und das gegenteilige Verhalten wurde bei *oxr2* und *oxr5*-Mutanten

beobachtet. In Übereinstimmung damit akkumulierten Pflanzen mit veränderter Expression von *AtOXR2* unterschiedliche Spiegel des Hormons SA, was in Pathogenantworten involviert ist. Der erhöhte basale Pathogen-Abwehr-Phänotyp war abhängig von einer intakten SA-Synthese sowie SA-Aktivierungs- und Signalwegen, da er in *ics1/sid2*- und *npr1*-Mutanten verloren geht.

Um die Tatsache zu erklären, dass OXR2-Pflanzen sowohl eine erhöhte Biomasse- als auch eine Pathogenresistenz aufweisen, untersuchten wir die Hormongruppe der Cytokinine (CKs). OXR2-Pflanzen akkumulieren CKs und *oxr2.2* weisen eine geringere Menge auf. Die von OXR2-Pflanzen gezeigten Wachstumsphänotypen gingen in Pflanzen mit Funktionsverlust in Proteinen verloren, die mit CKs-Synthesen (*ipt1357*+OXR2) und Signalübertragung (*ahp1234*+OXR2) zusammenhängen. In Pflanzen mit erhöhter Menge an katabolischen Enzymen (CKX1+OXR2 und CKX2+OXR2) wurde eine teilweise Umkehrung des Wurzellängenphänotyps sowie eine erhöhte Empfindlichkeit gegenüber Pst DC3000 festgestellt. Es ist wahrscheinlich, dass die Anreicherung von CKs in OXR2-Pflanzen teilweise auf eine verringerte CKX-Aktivität zurückzuführen ist.

Insgesamt liefern wir neue Belege für die Rolle von OXR-Proteinen bei Arabidopsis. Diese Nachweise zielen darauf ab, die Rolle von OXR-Pflanzenproteinen bei der Reaktion auf oxidativen Stress zu stärken, wie dies in verschiedenen Tiermodellen vorgeschlagen wurde. Es sind noch weitere Studien erforderlich, um den spezifischen Wirkungsmechanismus von TLDc-Proteinen aufzudecken. Darüber hinaus machen die Eigenschaften, die Pflanzen durch die Überexpression von *AtOXR2* erhalten, wie ein höherer Ertrag und eine erhöhte Resistenz gegen Krankheitserreger, es für agro-biotechnologische Zwecke wertvoll.

1. Introduction

1.1 OXR proteins

Recently was described the **OXR** (***OXidation Resistance***) family of proteins [1], with homologues previously identified in yeast [2], Drosophila [3], Anopheles [4], Zebrafish [5], *C. elegans* [6], Mouse [7], Cattle [8] and Humans [9].

The main characteristic of this protein family is the presence of a highly conserved region in the carboxy-terminal half, which contains a TLDc domain (Tre2/Bub2/Cdc16 (TBC), lysin motif (LysM), domain catalytic, IPR006571, PF07534, SM00584). This domain was found only in eukaryotic organisms [10] and it does not have a specific function or mechanism of action until now elucidated.

While the specific function of the TLDc domain is not yet clarified, the role of TLDc containing proteins is undaunted of critical importance for essential cellular functions. Naturally occurring mutations in these proteins lead to severe neurological disorders in humans [11,12], and loss-of-function mutations cause a reduction in the lifespan of mice [13], Drosophila [3], *C. elegans* [6] and Mosquitos [4]. On the contrary, over-expression of several members of the OXR family increase the lifespan and post-stress survival in mouse [14] and human cells [11]. Moreover, Oxr1 was proposed as a neuroprotective factor in neurodegenerative disorders [4,6,13] by, almost in part, regulating mitochondrial morphology [15]. More recently, *Oxr1* silencing has been identified in different types of human cancer, due to epigenetic alterations, like aberrant promoter methylation [16] or by being targeted by different microRNAs [17,18].

Several reports have associated TLDc proteins to oxidative damage prevention under stress conditions, either by direct protection of DNA damage in bacteria [1] or by conferring to the organism the ability to surpass oxidative conditions [1,4,19]. Even though TLDc proteins studied until now do not possess direct ROS scavenging activity, they are able to regulate the expression of the cellular antioxidant machinery [20–22].

Regarding the subcellular localisation of these type of proteins, they are found in different cellular compartments like mitochondria, cytosol and nucleus [2,9,19].

There is scarce evidence about the role of TLDc domain-containing proteins in plants. There is only one report [23] showing that *IbTLD* from sweet potato is one of the targets of the wounding-induced microRNA *miR828*, which regulates the expression of antioxidant enzymes and defence responses against abiotic stress.

Due to the relevance of different family members in several eukaryotic organisms already demonstrated, it was decided to analyse the presence and the role of OXR family proteins in plants using the plant model organism *Arabidopsis thaliana*.

1.2 Plant stress responses

Arabidopsis thaliana is a small vascular plant from the *Brassicaceae* family. This family includes several crops of agricultural relevance, like rapeseed, cabbage, sprouts and cauliflower. Arabidopsis was first described in 1577 in the Harz mountains in northern Germany by Johann Thal and its present name was given in 1842 by Gustav Heynhold [24]. The short lifecycle (of about six weeks between germination to mature seed, Fig. 1), its small diploid genome (of 135 Mbp distributed on five chromosomes) and the availability of a broad range of gene knockout mutant collections, makes the Arabidopsis plant an advantageous model organism to study gene function.

Plants are sessile organism and they need to surpass environmental adversities like extreme temperatures, water deficit or flooding, sun radiation, herbivores and pathogen attack, among others. To overcome these stress situations, plants have evolved a series of response mechanism.

Under stress conditions, reactive oxygen species (ROS) are generated and may cause cellular damage but also act as signalling molecules. Upon enhanced ROS accumulation, low molecular weight antioxidant like tocopherols, carotenoids, ascorbate and glutathione are synthesized [25]. Ascorbate and glutathione are the main ROS scavengers. There are also enzymes with ROS-detoxification activity such as catalase (CAT), superoxide dismutase (SOD), glutathione reductase (GR), glutaredoxin (GRX) and thioredoxin (TRX), which protect plants from oxidative damage caused by an excess of ROS (Fig. 2) [26]. This complex system maintains the redox homeostasis within the cell and allows ROS-triggered signalling.

At homeostatic levels, ROS act as signalling molecules responsible for orchestrating numerous cellular activities related to post-translational protein modifications, gene expression and hormonal regulation [27,28].

Due to the presence of electron transport chains, chloroplast and mitochondria are the primary sources of ROS in plants [29,30]. Particularly in mitochondria, there are energy decoupling systems represented by the alternative oxidase (AOX) [31] and the uncoupling proteins [32] that alleviate ROS generation particularly under stress conditions.

In a stress situation, plants have to modify their metabolisms and defences. A fine coordination must exist in order to provide the energy need for the plant in order to overcome the stress situations. Mitochondria, chloroplasts and nuclei must coordinate their functions. Thus, the signalling from mitochondria to nucleus is known as mitochondrial retrograde regulation (MRR).

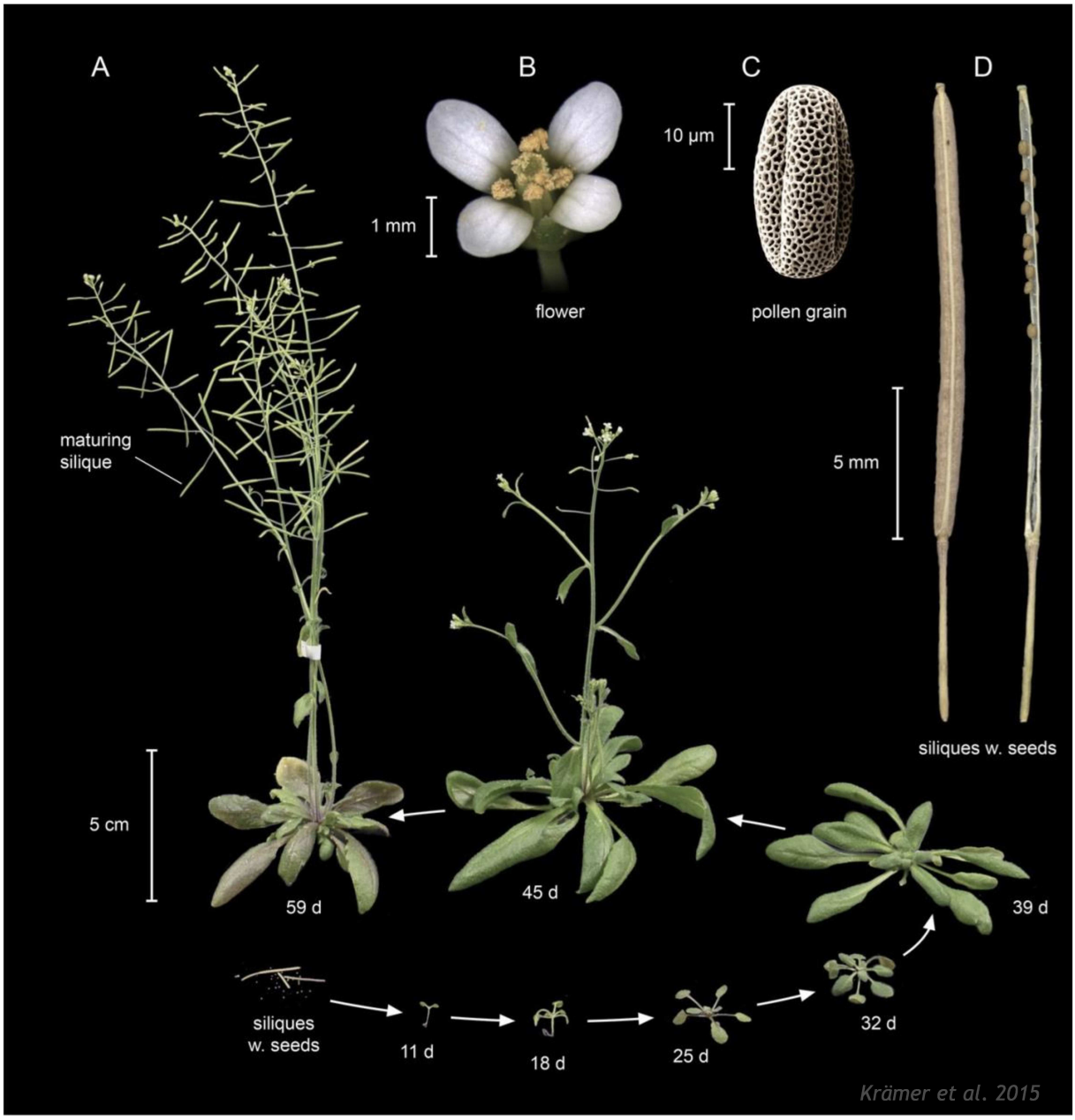

Figure 1: Life cycle of *Arabidopsis thaliana*. (A) *A. thaliana* of the accession Columbia (Col) at different stages of its life cycle, from seed (bottom left) to seedling (11 days), to vegetative growth (39 days), and to reproductive growth (45 days). Photographs of (B) a flower, (C) a pollen grain (scanning electron micrograph), and (D) mature siliques (seed pods; left: closed; right: open with a few remaining unshattered seeds) at higher magnification. *Adapted from Krämer et al. (2015, [24]).*

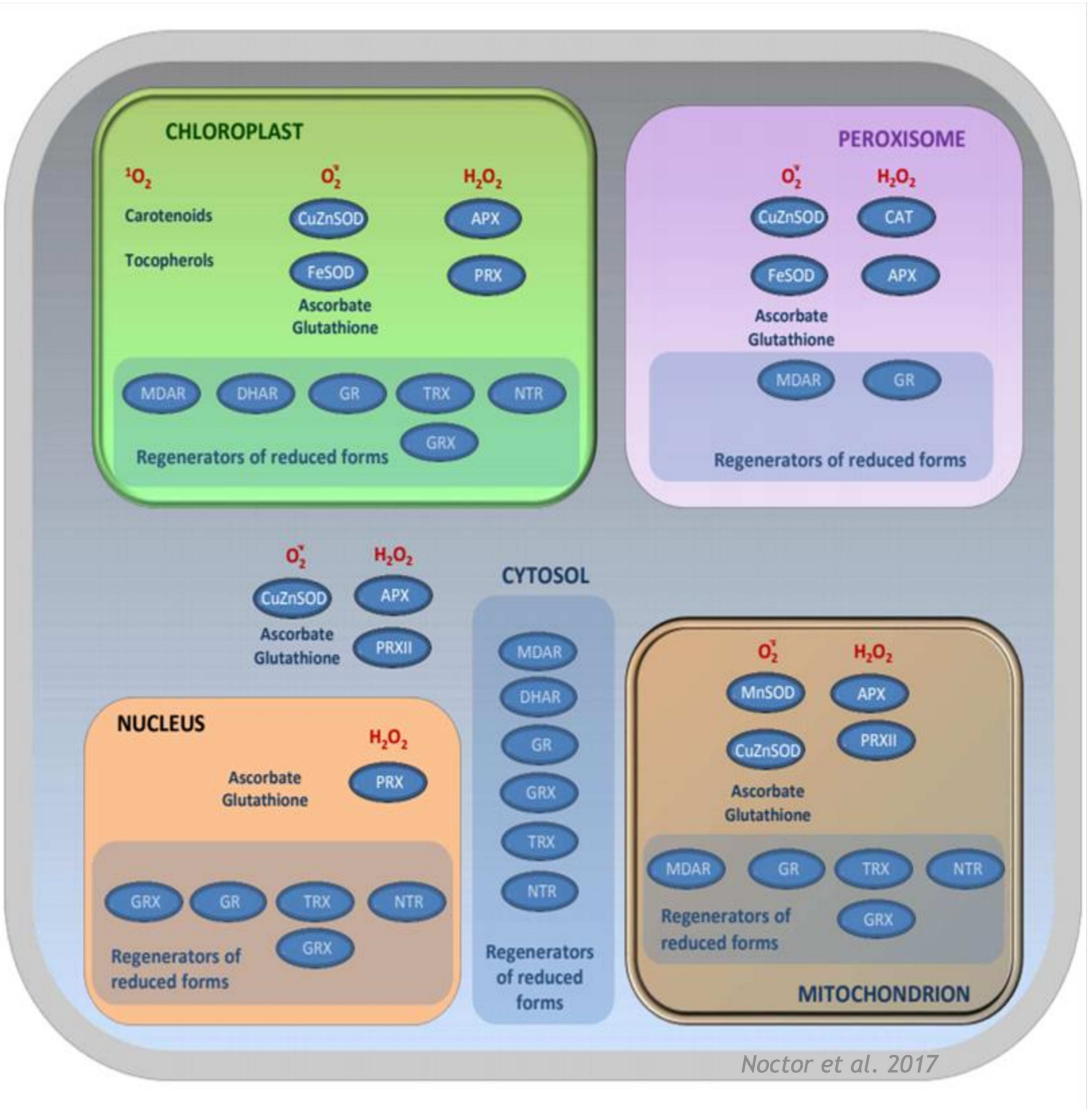

Figure 2: Plant antioxidative systems and where they are found within the cell. The figure summarizes available information for Arabidopsis on the subcellular localisation of antioxidative enzymes and related proteins. The information is not exhaustive, and other proteins may be involved. APX, ascorbate peroxidase. CAT, catalase. DHAR, dehydroascorbate reductase. GR, glutathione reductase. GRX, glutaredoxin. MDAR, monodehydroascorbate reductase. NTR, NADPH-thioredoxin reductase. PRX, peroxiredoxin. SOD, superoxide disumatase. TRX, thioredoxin. *Adapted from Noctor et al. (2017, [25]).*

1.2.1 Mitochondrial retrograde signalling

Mitochondrial respiration is essential for bioenergetics in aerobic organism, plants mitochondrial electron transport chain (miETC) show distinct features than other organism including the presence of AOX [126]. In plants, COX or cyanide-sensitive respiration is related with the proton gradient formation thus allowing the ATP synthesis by the ATP-synthase, while AOX or SHAM sensitive respiration diffuses the electron flow modulating ATP synthesis and other processes related to primary and secondary metabolism (Fig. 3) [37].

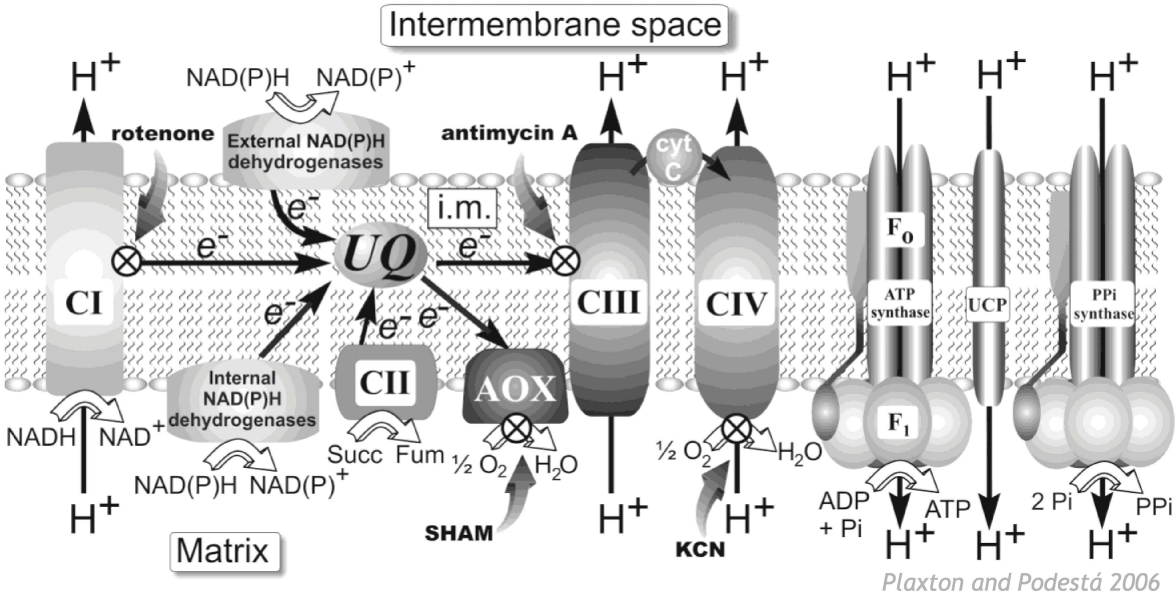

Figure 3: Organization of the electron transport processes occurring within the inner membrane. of plant mitochondria. The illustration provides detail of the cytochrome pathway (electrons flow to complex IV), which generates the electromotive force for ATP synthesis, and the non-energy conserving pathway (electrons pass directly to O_2 through AOX). CI, complex I or NADH dehydrogenase; CII, complex II or succinate dehydrogenase; CIII, complex III or cytochrome bc1 complex; CIV, complex IV or cytochrome oxidase. Crosses inside circles indicate sites of inhibition for different inhibitors of the miETC like rotenone, SHAM, antimycin A and KCN. *Adapted from Plaxton and Podestá (2006, [126]).*

Mitochondria play a critical role in sensing the environment, and their capacity to maintain cellular metabolism during stress was closely connected with the crop yield [33]. Upon mitochondrial perturbation, the expression of several proteins is induced. One of these proteins is AOX, which is used as marker for MRR [34]. AOX expression decreases ROS formation generated from the mitochondrial respiratory chain (mtROS) upon stress and helps maintaining the plant's performance [35,36]. mtROS, calcium and changes in mitochondrial redox status might act as signals for MRR [37–39].

One of the first MRR regulators described was the transcription factor ABI4, which interacts with the AOX-promoter to inhibit its expression [31]. Other regulators have been described as well, like the endoplasmic reticulum (ER)-bound NAC transcription factor, ANAC017 and ANAC013 [35]. ANAC017 appears to be a master regulator, its transcript abundance is stable under different conditions and the protein is released from the ER-membrane upon mitochondrial perturbation to initiate MRR. Furthermore, ANAC017 regulates ANAC013 [40] (Fig. 4).

The transcription factor MYB29, UDP-GLYCOSYL TRANSFERASE 74E2 (UGT74E2), and the kinase CDKE1 also regulates AOX expression and affect auxin signalling, thus revealing the antagonism between mitochondrial stress signalling and the growth signalling mediated by auxin [41]. Other characteristic genes that respond to mitochondrial dysfunction are

HYPOXIA RESPONSIVE ETHYLENE RESPONSE FACTOR2 (HRE2) and HEAT SHOCK PROTEIN 23.5 (HSP23.5) which altogether form the "mitochondrial dysfunction regulon" [42,43].

The crosstalk between MRR and another hormone, salicylic acid (SA) is also an example of mitochondrial sensing and response upon stress particularly in pathogen responses. Mitochondrial proteins like OM66 and AOX are regulated by the SA signalling pathway, apparently through some members of the WRKY transcription factor class [40]. Moreover, several WRKY transcription factors are also induced upon mitochondrial dysfunction and form part of the MRR [45,46].

WRKY transcription factors may also explain the connection between mitochondria and chloroplasts upon stress [40]. The expression of the WRKY proteins is up-regulated in response to ROS or ROS-generating stimuli, imbalances in redox homeostasis, and endogenous ROS-dependent processes like senescence. Although it is not known if ROS directly activates the enhancement of WKRY expression, there is a lack of information regarding how WRKY genes receive and transmit ROS signalling [47]. The involvement of the chloroplastic retrograde signalling protein PAP in MRR has not yet been described. However, SAL1, which regulates PAP levels is present in both, chloroplasts and mitochondria, and loss of functions mutants showed transcriptome signatures similar to many mitochondrial mutants. This suggests a role in mitochondrial retrograde signalling of this pathway and the connection between the two organelles [44].

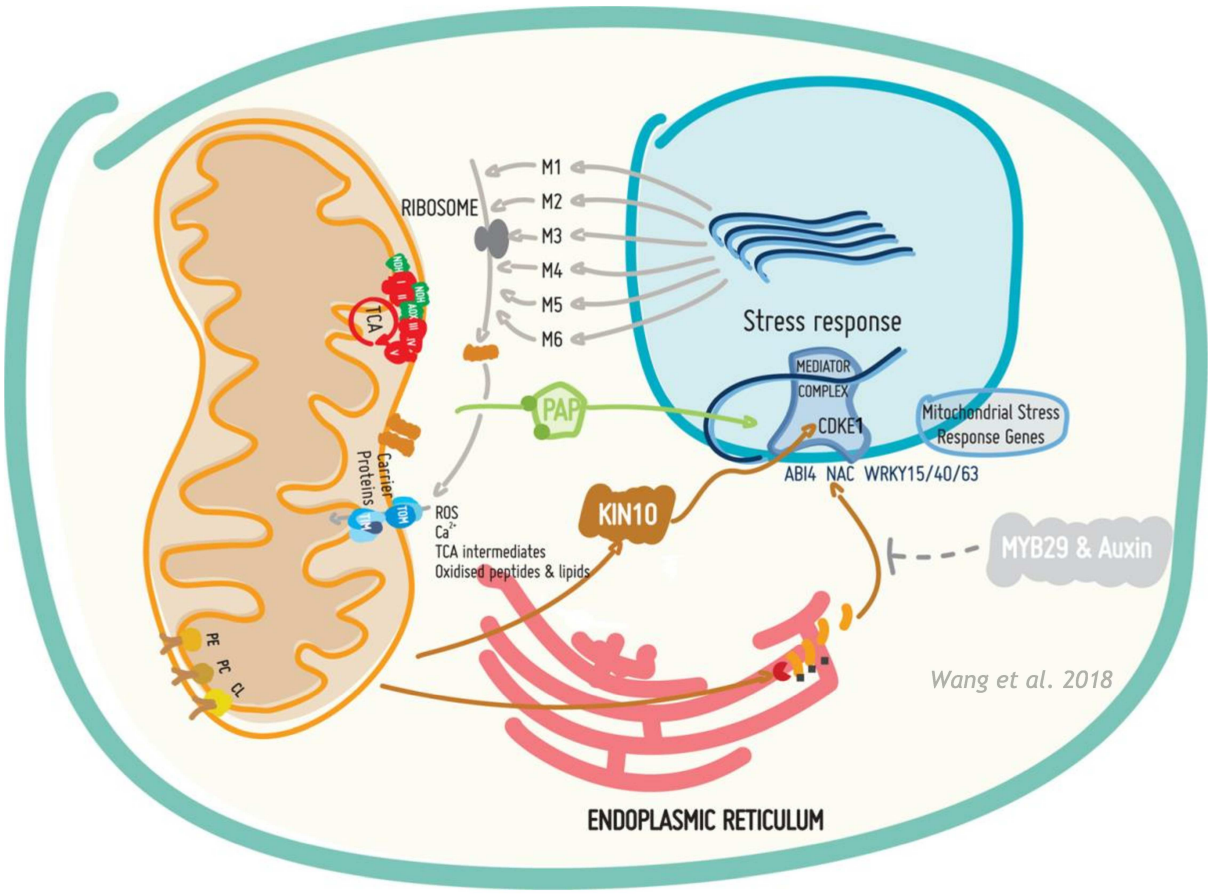

Figure 4: Overview of known pathways regulating the expression of genes encoding mitochondrial proteins. For mitochondrial retrograde signalling a number of regulatory components have been identified: transcription factors (ABI4, WRKY, NAC, MYB29), kinases (KIN10, CDKE1), in addition to plant hormones, ROS, calcium, metabolites and modified proteins or lipids. 3′-phosphoadenosine 5′-phosphate (PAP) initially identified as being involved in chloroplast retrograde signalling is also likely to be produced in mitochondria as the 3′(2′),5′-bisphosphate nucleotidase SAL1 regulating PAP levels is targeted to both mitochondria and chloroplasts. Analyses of global genes expression patterns putatively identified six main modules regulating mitochondrial gene expression representing anterograde regulatory pathways. The NAC transcription factors are targeted to the endoplasmic reticulum and released by proteolytic cleavage. Both MYB29 and auxin act at an unknown level to turn off the stress-induced expression of AOX1a. NAC, WRKY and ABI4 transcription factors bind directly to the AOX1a promoter. *Adapted from Wang et al. (2018, [40]).*

1.3 Plant pathogen responses

Plants are in contact with microbes like viruses, bacteria, fungi, oomycetes, and nematodes, many of which are pathogenic (i.e. are able to cause disease). Crop losses due to different disease are estimated to be between 10 and 30% of the potential harvest, but in cases of severe outbreaks the losses can be greater [48]. Nevertheless, plant disease is the exception rather than the rule since plants have evolved to resist most of the infections. Plants are able to set up a variety of immune responses according to the pathogen type to overcome infection and these responses are mainly orchestrated by plant hormones.

Over the last century scientists have contributed to obtain a relatively coherent idea of the molecular interactions that take place in plants upon pathogen infection, particularly

how plants recognize and respond to pathogens. The zigzag model is the most accepted to describe plant immune responses, although it does not apply equally to all pathogens nor can it explain all interactions (Fig. 5). In this model the initial recognition and response to the pathogen comes first, this is called pattern-triggered immunity (PTI). During PTI plants recognizes conserved molecular structures associated to the pathogen (PAMPs, MAMPs) and mounts a defensive response. In some cases, pathogens can overcome PTI by secreting small molecules or proteins called effectors that can suppress the plant immune response; this is called effector-triggered susceptibility (ETS). Sometimes, as consequence of the effector release, plants trigger a second wave of plant immune responses called effector-triggered immunity (ETI) [49].

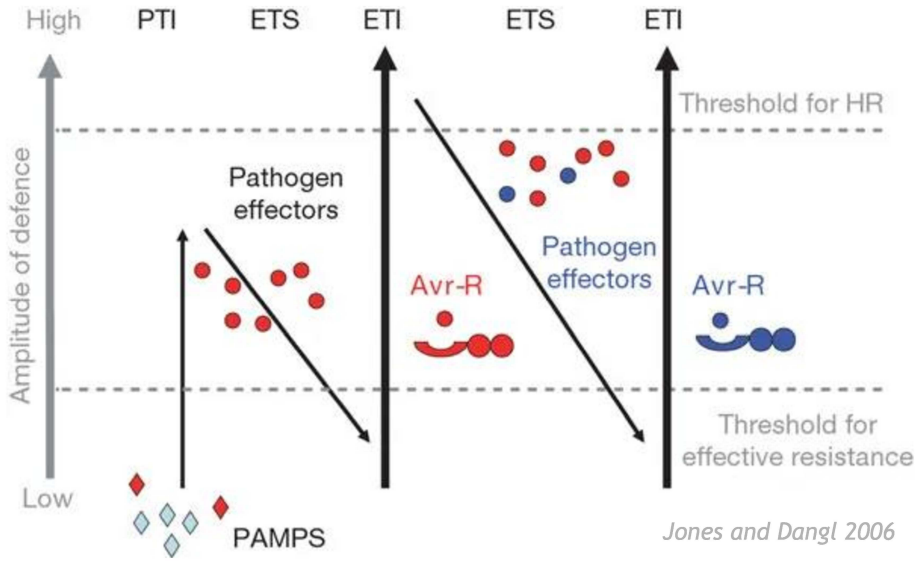

Figure 5: The zigzag model illustrates the quantitative output of the plant immune system. In this scheme, the ultimate amplitude of disease resistance or susceptibility is proportional to [PTI – ETS1ETI]. In phase 1, plants detect microbial/pathogen-associated molecular patterns (MAMPs/ PAMPs, red diamonds) via PRRs to trigger PAMP-triggered immunity (PTI). In phase 2, successful pathogens deliver effectors that interfere with PTI, or otherwise enable pathogen nutrition and dispersal, resulting in effector-triggered susceptibility (ETS). In phase 3, one effector (indicated in red) is recognized by an NB-LRR protein, activating effector-triggered immunity (ETI), an amplified version of PTI that often passes a threshold for induction of hypersensitive cell death (HR). In phase 4, pathogen isolates are selected that have lost the red effector, and perhaps gained new effectors through horizontal gene flow (in blue)—these can help pathogens to suppress ETI. Selection favours new plant NB-LRR alleles that can recognize one of the newly acquired effectors, resulting again in ETI. *Adapted from Jones and Dangl (2006, [49]).*

At the site of pathogen infection, local defence responses occur like the hypersensitive response (HR). The HR is a form of programmed cell death (PCD) mediated by a rapid increase of ROS, called oxidative burst. The HR acts by killing the pathogens within the infected cells and thus contributing to plant immunity. Plants deficient in HR show increased sensitivity towards biotrophic pathogens. The oxidative burst causes cell wall cross-linking that ends up sealing the infected tissues and in consequence helping to prevent pathogen

spread. Accumulation of ROS promotes SA synthesis and also works synergistically with SA in promoting defence responses. Furthermore, some defence genes are induced by ROS even in the absence of SA [50].

Another type of response occurs upon pathogen infection, a systemic and broad-spectrum immunity called systemic acquired resistance (SAR). SAR provides protection in distant parts of the plants which had not yet being exposed to the pathogen attack. In these tissues faster and stronger defence mechanism are triggered since the cells appear to be in a "prepared" state. Several molecules have been proposed as putative SAR signals that are able to move from the infection point through the rest of the plant activating the response, one of the main candidates is methyl salicylate (MeSA) [51].

In addition, plants can remain in a "primed" state, this phenomenon enables cells to respond to very low levels of a stimulus in a more rapid and robust manner than non-primed cells. Thus, primed plants show faster and/or stronger, activation of defence responses when subsequently challenged by microbes, insects, or abiotic stress, and this is frequently linked to the development of local and systemic immunity and stress responses [52]. Priming is associated with epigenetic modifications that can even be passed to the next generation [51,52].

1.3.1 The pathogen-response hormone salicylic acid

Upon pathogen attack, plants synthesize and accumulate the phytohormone SA. This accumulation also occurs in response to some abiotic stresses like heat, ozone, and UV light. The majority of the SA produced in these conditions is formed by the isochorismate synthase (ICS). The *ICS1* gene was characterized in Arabidopsis by the analysis of the loss-of-function mutants *salicylic acid induction deficient2* (*sid2*) and *enhanced disease susceptility16* (*eds16*). These mutants fail to accumulate SA upon pathogen infection and show enhanced susceptibility to pathogens but can be rescued with exogenous SA [53]. ICS is encoded by a single gene in most plants. Particularly Arabidopsis has two, *ICS1* is the major determinate of SA accumulation and *ICS2* is a minor contributor. Loss-of-function mutants in both genes does not completely abolish SA synthesis, confirming the presence of an alternate route for SA production.

Downstream of pathogen perception, positive regulators of SA accumulation have been identified genetically. For example, *EDS1* and *PHYTOALEXIN DEFICIENT4* (*PAD4*) loss-of-function mutants show enhanced susceptibility, this susceptibility can be rescued by exogenous addition of SA. Therefore, these two genes appear to be required for pathogen resistance acting upstream of SA accumulation [54].

The pathogen recognition, or SA application, leads to a massive change in gene expression. Up to 25% of the Arabidopsis genome is affected locally and up to 10% in systemic tissues. These induced genes are mainly involved in SA accumulation or SA signalling leading to an amplification of the signal. Finally, the next wave of transcriptional targets encode proteins with direct anti-microbial or defence effects. The over accumulation of SA-induced transcripts can cause diverse negative phenotypes in plants, like dwarfing, reduced fertility, and sometimes spontaneous cell death. For this, these genes are subject to strong negative as well as positive regulation. The PR1 gene has been used as a marker by which to study SA-induced transcription. Thanks to the work of many laboratories, we know that the tight transcriptional control of this gene involves complex and sophisticated negative and positive controls, including transcription factors and chromatin remodelling [54].

NONEXPRESSOR OF PATHOGENESIS-RELATED GENES1 (*NPR1*) is one of the major contributors to SA signal transduction. Loss-of-function in NPR1 plants (*npr1*) are extremely sensitive towards pathogen attack, *PR* gene expression and immunity responses are completely abolished, on the contrary *NPR1*-overexpressing plants show enhanced resistance. NPR1 encodes a protein with two protein–protein interaction domains: an ankyrin repeat domain and a BTB/POZ (broad complex, Tramtrack, and bric-a-brac/pox virus and zinc finger) domain. In the cytoplasm, NPR1 forms redox-sensitive oligomers. Under oxidizing conditions, NPR1 forms intermolecular disulfide-bonded multimers through conserved Cys residues. Under reducing conditions, NPR1 monomerizes and the monomers can translocate into the nucleus where NPR1 acts promoting plant immunity through its action as a transcriptional co-activator and the inhibition of inhibitors (Fig. 6). NPR1 action is further modulated by its interactions with the transcriptionally repressive NIMIN proteins and is subject to regulatory phosphorylation and proteolysis. It is hypothesized that continual proteolytic turnover in the nucleus may allow the plant to rapidly switch off the defence response as well as maintain a very low level of transcription in non-inducing conditions [55–57].

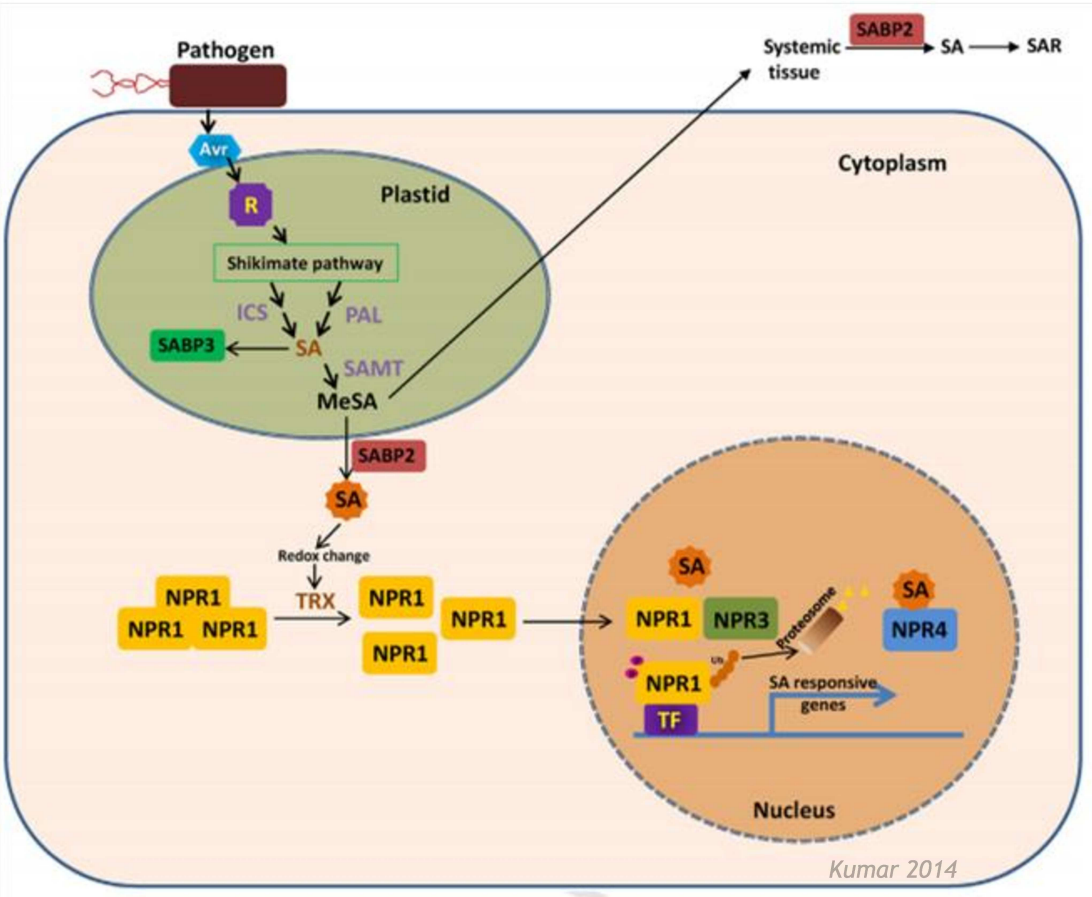

Figure 6: A model showing activation of SA signaling in a plant cell. Pathogen attack results in increased biosynthesis of SA via ICS/PAL pathway in plastids. SA methyltransferase (SAMT) catalyzes conversion of SA to MeSA which diffuses into the cytoplasm where it is converted back to SA by the esterase activity of SABP2. Increased SA levels in the cytoplasm disrupts the oligomeric NPR1 into its monomers which then migrate to the nucleus to activate transcription of SA responsive defense genes including PR genes. NPR1 is phosphorylated upon its interaction with transcription factors. Proteosome mediated degradation of phosphorylated NPR1 trigger's expression SA responsive genes. *Adapted from Kumar (2014, [58])*.

1.3.2 *Pseudomonas syringae* as a pathogen model

P. syringae is a bacterial pathogen that is responsible for bacterial speck diseases on different plants types, including *Arabidopsis thaliana*. *P. syringae* is classified into pathovars (pathogenic varieties) that correspond to their hosts.

P. syringae release effectors upon plant infection, and thus activates ETI. It is also able to synthesize the non-host-specific polyketide toxin coronatine, which is produced by strains belonging to at least five pathovars of *P. syringae* including Pst DC3000. Coronatine structurally mimics the plant hormone jasmonate (JA), which antagonizes SA. Coronatine plays multiple roles during *P. syringae* infection, including the facilitation of bacterial invasion through stomata, the promotion of bacterial multiplication and persistence *in planta*, the induction of disease symptoms, and the enhancement of disease susceptibility

in uninfected parts of the plant, partly by repressing SA-mediated responses due to the antagonistic activity of JA [59].

1.3.3 *Plasmodiophora brassicae*

Plasmodiophora brassicae causes clubroot, a major disease of Brassica oil and vegetable crops worldwide. *P. brassicae* is a plasmodiophorid, obligate biotrophic protist in the eukaryotic kingdom of Rhizaria. Clubroot disease causes enormous agricultural losses during outbreaks.

Plasmodiophorids have a complex, not fully understood, life cycle that consists of different zoosporic stages, the formation of plasmodia inside host cells, and resting spore formation (Fig. 7). To infect the plants first the haploid resting spore releases a zoospore in to the soil, then the zoospore is able to infect the root hairs and form multinucleate plasmodia. Those develop several single-nucleate secondary zoospores, which are released into the soil beginning a new infection cycle. A fusion of those secondary zoospores is assumed to occur occasionally. Zoospores invade the root cortex, in which secondary multinucleate plasmodia develop. How and when karyogamy is taking place is not exactly known, but meiosis appears to occur in the plasmodia before resting spore formation. The presence of plasmodia provokes abnormal cell enlargement (hypertrophy) and uncontrolled cell division (hyperplasia) leading to the development of the characteristic galls that obstruct nutrient and water transport. In infected root tissue, different developmental stages of the plasmodiophorids occur simultaneously [60].

Resting spores have the capacity to survive long periods of time in soil and then activate by different stimuli to trigger infection. This makes it difficult to avoid the apparition of the disease in previously infected fields.

P. brassicae appears to be able to modify hormonal homeostasis in host plants, infected tissues show unbalance of at least four plant hormones: CKs, SA, auxins and JA. The infection of Arabidopsis with *P. brassicae* induced the expression of *ICS1* and loss of function mutants in synthesis and signalling of SA showed increased sensitivity toward *P. brassicae* infection [61–63]. Thus, SA appears to be of particularity importance to guarantee pathogen success in infection and disease resistance.

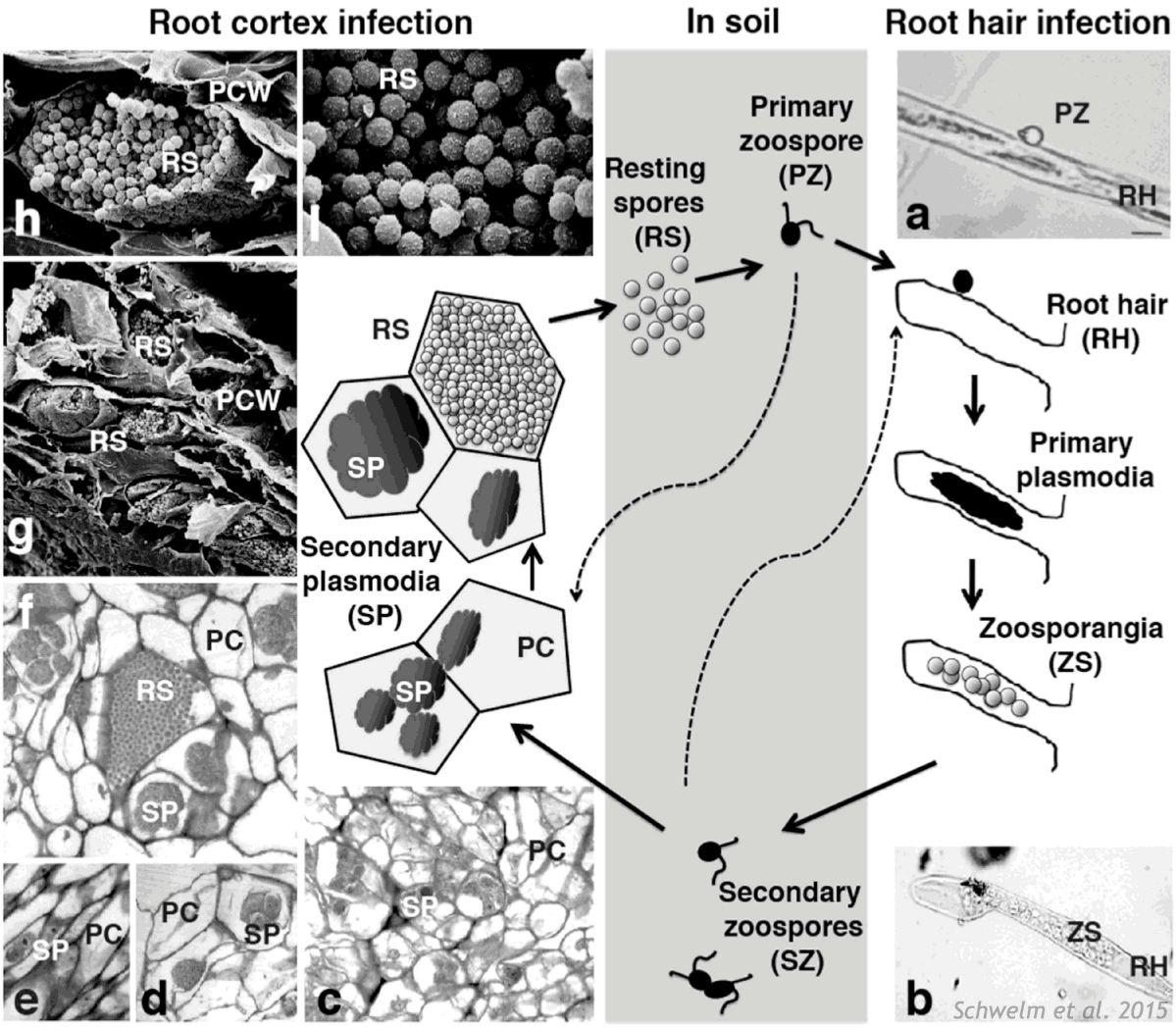

Figure 7: The life cycle of *Plasmodiophora brassicae*. A biflagellate primary zoospore (PZ) is released from each resting spore (RS). When the PZ reaches the surface of a root hair (RH) (a), it penetrates the cell wall and forms primary plasmodia in the root hairs. After a number of nuclear divisions, the plasmodia cleave into zoosporangia (ZS), developing and releasing secondary zoospores (SZ) (b). Occasional fusion of SZ has been suggested. PZ or SZ can penetrate root cortex cells, in which the pathogen develops into secondary plasmodia (SP) (c–f). Proliferation of SP is associated with cellular hypertrophy, causing a swollen root or club phenotype. After a number of nuclear divisions, the secondary plasmodia develop into multinuclear plasmodia and finally into resting spores (f–i), which are released into the surrounding soil when plants decay. RS=Resting spore, PZ=Primary zoospore, RH=root hair, ZS=Zoosporangia, SZ=Secondary zoospore, SP=Secondary plasmodia. PC=Plant cell, PCW=Plant cell wall. *Adapted from Schwelm et al. (2015, [60]).*

1.4 The plant hormone cytokinin

Cytokinins (CKs), which were named for their ability to promote cytokinesis [64], are well known growth-inducing phytohormones. CKs are involved in numerous developmental processes like cell division, the release of lateral buds from apical dominancy, nutrient mobilization, development and function of chloroplasts, and positively controlling the leaf longevity [65–67].

CKs are adenine derivatives with isopertenoid or aromatic side chains, being the first type the more abundant mainly trans-zeatin (tZ) and isopentenyl-adenine (iP). Isopentenyltransferases (IPTs) catalyse the rate limiting step for CKs biosynthesis: the isopentenylation of adenine using ADP, ATP and tRNA as substrates. After the riboside forms (tZR and iPR) are converted to active CKs by direct removal of the riboside catalysed by lonely guy enzymes (LOGs) or by gradual removal of the phosphate groups [67, 173] (Fig. 8).

Degradation pathways requires CK dehydrogenases (CKXs), which remove CK unsaturated isoprenyl side chains. CKs degradation has been proven to play an important regulatory role in plant hormone homeostasis [173].

The CKs signal is conveyed by a two-component signalling system, also called the histidyl-to-aspartyl system or His–Asp phosphorelay, which is found in bacteria as well as in plants and fungi, but not in animals. The first component of the CKs signalling cascade is the membrane-spanning histidine kinase [68] containing an extracellular CHASE (cyclases/histidine kinases-associated sensing extracellular) domain, which passes the phosphate to the histidine phosphotransfer proteins (AHPs) that further convey the signal into the nucleus to the last component: type B response regulators (ARRs). These work as transcription regulators and affect expression of the CKs target genes including type A response regulators (ARR-A), which inhibit the phosphotransfer from the AHPs to the type B response regulators (ARR-B) and thus work as a negative feedback loop (Fig. 8).

Many plant pathogens secrete CKs or induce CKs production in host plants. However, the other side of the coin is that CKs also mediate plant resistance against many types of pathogens [69–72]. Several lines of evidence support a role for CKs in plant-pathogen interactions mainly through the regulation of SA responses. According to the model, the accumulation of CKs as perceived through receptor AHKs and activation of ARR2, a type-B ARR, mediates Arabidopsis immunity. Mechanistically, ARR2 interacts with the b-ZIP transcription factor TGA3 (TGA1A-related gene 3) and binds to the promoters of defence-related genes [69].

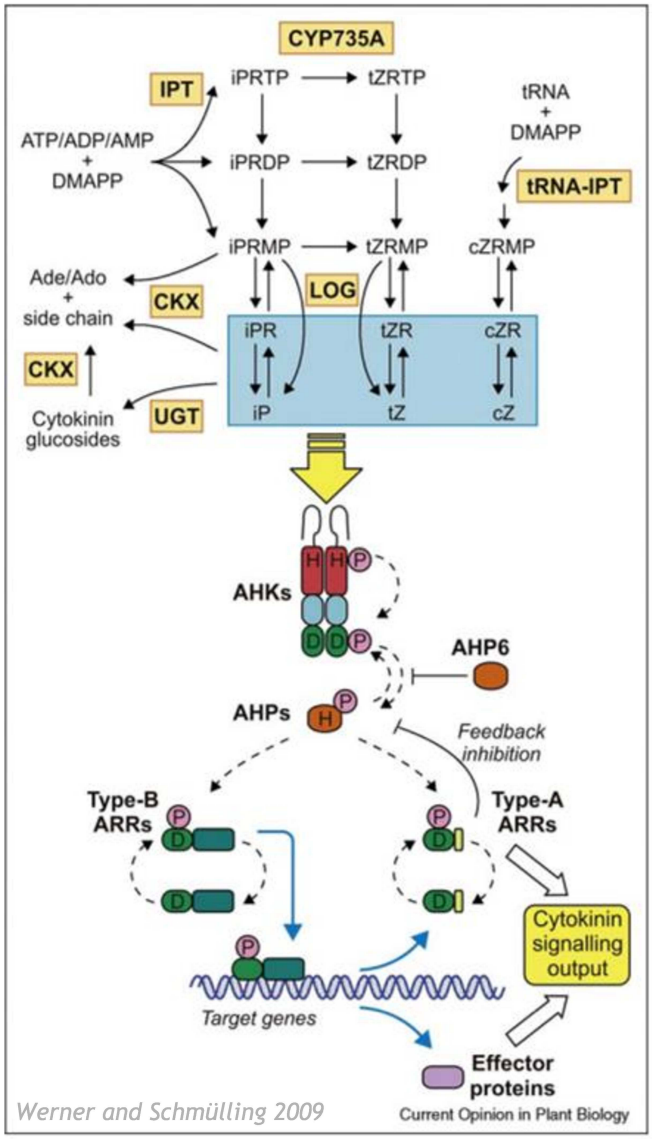

Figure 8: Schematic model of cytokinin biosynthesis, metabolism and core steps of the cytokinin signalling pathway. Biosynthesis of iP-cytokinins and tZ- cytokinins is initiated by adenosine phosphate-isopentenyltransferases (IPTs) to form iP-nucleotides which can be converted to the corresponding tZ-nucleotides by cytochrome P450 monooxygenases (CYP735As). iPRTP, iPRDP and the corresponding tZ-nucleotides are dephosphorylated by phosphatases, and iPRMP and tZRMP can be directly converted to active free bases by cytokinin nucleoside 50-monophosphate phosphoribohydrolases (LOGs). cis-Zeatin (cZ) cytokinins, which in some plant species are the major cytokinin metabolites, are synthesized in Arabidopsis exclusively by tRNA-IPTs which utilize tRNAs as prenyl acceptors. Biologically active cytokinins, highlighted in blue, are inactivated by cytokinin oxidases/ dehydrogenases (CKXs) and by conjugation to sugar moieties through glycosyltransferases (UGTs). A histidine (H)/aspartate (D)-phosphorelay (indicated by dotted arrowed lines) through a two-component signalling cascade is initiated by the binding of biologically active cytokinin to a CHASE domain of histidine kinase receptors (AHKs) and autophosphorylation of a His-residue in the protein kinase domain (red). The phosphoryl group is transferred via the Asp-residue of the receptor receiver domain (green) to a conserved His of the histidine phosphotransfer proteins (AHPs). Non-activated CRE1/AHK4 possesses phosphatase activity that dephosphorylates AHPs. AHP6, lacking the conserved His-residue, inhibits the phosphoryl transfer, presumably by interacting with activated receptors and/or response regulators. AHP proteins relay the signal to B-type or A-type response regulators (ARRs). B-type ARRs, which contain a C-terminal DNA-binding domain (turquoise), are transcription factors regulating expression of their target genes including A-type ARRs. One function of the A-type ARRs is to repress signalling in a negative feedback loop. Together with other effector proteins, they determine the signalling output of the pathway. *Adapted from Werner and Schmülling (2009, [67]).*

1.5 Increasing plant biomass and production

Plants enrich our lives in many ways, but with the continuous increase of the human population their use as food is essential to ensure alimentation, energy production and survival. The current agricultural practices are not enough to produce the amount of food required by us all. Current studies affirm that to prevent starvation the production of food must increase 70% by 2050, when the world population may stabilize at 9 billion. Increasing the land-surface to growing this additional food could be an option, but is necessary to adapt the actual crops to the new environmental conditions and/or grow more food on the same area (km^2) that we currently cultivate, improving the crop yield at maximum [73].

So far, agricultural technologies and plant breeding had managed this problem by increasing the crop yield. Unfortunately, this could be not enough for attending the food-requirements of the future population. In the last two decades, plant scientists have been studying the way to increase plant productivity by improving plant stress tolerance, nutrient usage and pathogen resistance, mainly by obtaining genetic modified crops (GMOs: genetically modified organism) by using biotechnological approaches [74].

Photosynthesis is the main driving force for the growth and biomass in plant production. Photosynthesis provides energy and carbon essential for the biosynthesis of metabolites required for plant living and growth. For this reason, CO_2 assimilation is one of the main targets of research aimed for improving crop productivity [75]. Furthermore, other biological processes could be optimized to gain biomass and yield by using GMOs, like nutrient supply or carbohydrate transport and allocation. It is possible to manipulate diverse molecules that play critical roles in plant growth and development like miRNAs, transcription factors (TFs), proteins that regulate cell division and expansion, as well as phytohormones. Environmental stress limits crops yield so obtaining stress-tolerant plants via genetic engineering is a crucial goal of biotechnology [33].

1.5.1 Obtaining plants resistant to stress

As mentioned before, plants are exposed to different environmental stresses like excess or lack of water, pathogens or herbivores, climate change and deficit of nutrients in the soil. Obtaining plants able to resist these stress situations is crucial to determinate crop productivity in changing climate conditions. Therefore, many plants scientist focus in achieving transgenic plants with increased resistance to abiotic stress like metal toxicity, extreme temperatures, excess light, drought, salinity, nutrient deficiency, hypoxia or UV-B

radiation. All these, provokes ROS accumulation and redox homeostasis disruption, resulting in cellular damage caused by oxidative stress.

Upon stress situations the photosynthetic apparatus is still very efficient in capturing light, while other processes are more sensitive to fail in these circumstances. This results in an imbalance between light absorption and energy utilisation in metabolism [76]. As we previously saw, many enzymatic and non-enzymatic antioxidants are synthesized to counteract the harmful effects of ROS in response to abiotic stresses [26,77]. Finally, different abiotic stress condition often triggers common responses in plants (like synthesis of osmoprotectants, differential expression of several TFs or phytohormones-mediated responses). Taken this knowledge as an advantage, to obtain transgenic plants with elevated levels of antioxidants, osmoprotectants or TFs is a common strategy to increase resistance to a variety of abiotic stresses [78].

With regard to pathogen resistance, the increased pathogen tolerance often comes with a penalty in growth. Plants must decide between growth or defense [79–81]. Different approaches have been taken to obtain plants with increased resistance, many of them target the hormone mediated responses or the capacity to detect PAMPs or MAMPs by plants [82]. Obtaining crops with increased pathogen resistance and with no penalty in growth is one of the goals of the modern agrobiotechnology.

2. Objectives

2.1 Main goals

Increase the knowledge about the functions and the mechanism of action of members of the OXR protein family in plants. Evaluate the possible connections between the roles of AtOXR proteins, their subcellular localisation and the mechanism by which they regulate different aspects of plant development like ROS homeostasis, synthesis and signalling of hormonal pathways and the mechanisms of plant-pathogen interaction in plants.

2.2 Specific goals

- Evaluate the transcriptional profile of AtOXR2 under normal growth conditions and in response to different stress.
- Analyse the subcellular localisation of AtOXR2 and AtOXR5.
- Analyse the phenotypic characteristic of plants with altered levels of AtOX2 and AtOXR5.
- Analyse the response of plants with altered levels of AtOXR2 and AtOXR5 to both biotic and abiotic stress conditions.
- Analyse the impact of different levels of AtOXR proteins on the Salicylic Acid (SA) and Cytokinins (CKs) synthesis and hormonal signalling pathways.

3. Materials and Methods

3.1 Plant material and growth conditions

Arabidopsis thaliana (ecotype Columbia, Col 0) was used throughout this study unless otherwise specified. A list of all the mutant and transgenic plants used is given in Table A1 of the Appendix.

Transgenic plants were obtained by stable transformation with *Agrobacterium tumefaciens* (labelled with "+" in case of plants expressing more than one transgene or mutation) or by manual crossing (labelled with "x" in case of plants expressing more than one transgene or mutation). Homozygous T-DNA mutants were confirmed by PCR using specific primers (Appendix, Table A2).

Plants were grown on soil at 22-24ºC under long-day (LD) conditions at a light intensity of 100 $\mu mol.m^{-2}.s^{-1}$. Alternately, plants were grown on Petri dishes with MS medium (0,5x MS, 0,8% (w/v) agar, 1% (w/v) sucrose). For root growth analysis plants were grown on vertical 14 cm square plates.

Plant phenotypic characterization was performed according to the parameters established by Boyes *et al.* (2001, [83]), using ten individual plants of each genotype per biological triplicate.

Growth time was expressed as days after sowing (DAS).

3.2 Gene cloning and generation of transgenic Agrobacterium for plant transformation

Plants expressing AtOXR2 under the control of the CaMV 35S constitutive were previously obtained in the work group and were described by Colombatti (2016, [172]).

To obtain plants expressing AtOXR5 under the control of the CaMV 35S constitutive promoter a fusion of AtOXR5 to mRFP, a 1659 bp *SalI*/*BamHI* fragment was amplified from cDNA using specific oligonucleotides (Table A2) and cloned into the pBi212 vector.

To obtain plants expressing a fusion of AtOXR5 to mRFP, a 1659 bp *SalI*/*BamHI* fragment was amplified from cDNA using specific oligonucleotides (Table A2) and cloned into pEntry3c vector (Invitrogen) and then transferred to the destination binary vector pGWB554 [84].

To obtain a NPR1-GFP construct the NPR1 coding sequence was amplified (1820 pb) using specific primers (Table A2) and cloned into the pDONR221 (Invitrogen) vector. Then it was transferred into the binary destination vector pFK-242 (from the Gateway-compatible pGREEN-IIS vector series) using the Gateway system (Invitrogen)), to express NPR1 under the control of the CaMV 35S constitutive promoter.

The DNA clones were transferred to *Agrobacterium tumefaciens* strain LBA4404 for plant transformation by the floral dip procedure [85].

E. coli strain DH5α (supE44ΔlacU169 (Φ80lacZΔM15) hsdR17 recA1 endA1 gyrA96 (Na1r) thi-1 relA1) was use for gene cloning. Bacterial cultures were grown at 37ºC on Luria-Bertani (LB) medium (10 $g.l^{-1}$ flesh peptone, 5 $g.l^{-1}$ yeast extract, 5 $g.l^{-1}$ NaCl) with the respective antibiotics according to the construct. Agrobacterium was grown at 28ºC on LB medium.

3.3 RNA isolation and analysis

RNA samples were prepared with TRIZOL RNA Isolation Reagent (Life Technologies). RT-qPCR analysis was performed according to O'Connell (2002, [86]). Quantitative PCR was performed on an aliquot of the cDNA with specific primers (Table A2) using the StepOnePlus® Real-Time PCR System [87]. For gene expression calculation the Ct method was used with *ACTIN2/8* as reference genes [171].

3.4 Dark-induced senescence

The method described by Zhang et al. (2017, [45]) was used for dark-induce senescence experiments. Briefly: detached leaves from four-week-old plants growth on LD conditions were incubated in a wet chamber in full darkness for 2 days. After that, the chlorophyll content was quantified and this value was used as a marker of senescence progression and expressed relative to the corresponding mock treatment (detached leaves incubated in wet chamber on LD) for each genotype.

3.5 Stress treatments

For UV-B (5 $mW.cm^{-2}$, UVP 34-0042-01 lamp) exposure, whole rosettes of three-week-old plants grown on soil were used. For MV treatments, seedlings were grown on MS medium supplemented with 0.1 µM or 1 µM MV. Plates were vertically set and root length was recorded every day. For AA treatment, two-week-old seedlings were transferred to MS medium supplemented with 50 µM AA and harvested in biological triplicate at 1 h and 3 h after treatment. For SA treatment 10 DAS seedlings grown on MS were flooded with 0,50 mM SA plus 0,025% (v/v) Silwet L-77 for 5 minutes and samples were taken at 1 h, 4 h, and 6 h after treatment in triplicates pools for GUS detection or RT-qPCR analysis. For analysis of gene expression, samples were immediately frozen in liquid nitrogen and stored at -80ºC until use.

3.6 Pathogen treatments

3.6.1 Pseudomonas infection

Flood-inoculation with Pst DC3000 on petri dishes was performed according to Isihga et al. (2011, [88]) with small variations. Briefly, plants grown on MS with water-agar 0,8% (w/v) on top were grown for 10 days in LD conditions. Infection was carried out incubating the seedlings 5 minutes with a bacterial suspension (5×10^8 CFU.ml^{-1}, 0,9% NaCl and 0,025% Silwet L-77) or mock solution (0,9% (w/v) NaCl and 0,025% (v/v) Silwet L-77), 3 DAI bacterial populations were measured. Internal bacterial populations were evaluated from at least 3 biological replicates and each replicate represent a pooled sample of 3 independent seedlings from a single experiment grown on a single petri-dish. Inoculated seedlings are collected by cutting the hypocotyls to separate the parts above the agar (whole rosette). After measurement of the seedlings weight, they were surface-sterilized by incubation with 5% (v/v) H_2O_2 for 5 min. After washing three times with sterile distilled water samples were homogenized in 1 mL sterile distilled water using a mortar and pestle and diluted samples were plated onto KB (see below)-Agar medium containing 50 µg.ml^{-1} Kanamycin and 50 µg.ml^{-1} Rifampicin. Two days after plating of diluted samples, the bacterial colony forming units (CFU) were counted. The CFU was normalized as CFU.mg^{-1} using total weight of inoculated seedlings.

Pst DC3000 was grown at 28°C on King's B (KB) medium (2% (w/v) proteose peptone, 1% (v/v) glycerol, 0,15% (w/v) K_2HPO_4, pH 7,2).

3.6.2 Plasmodiophora infection and disease rating

For *Plasmodiophora brassicae* infection experiments plants grown in soil were inoculated 14 DAS with 2 ml spore suspension (10^7 spores.ml^{-1} in 50 mM KH_2PO_4 pH 5,5) per plant or with 2 ml mock solution (50 mM KH_2PO_4 pH 5,5). For disease rating 27 days after inoculation (DAI) plants were removed from the soil and the progression of the clubroot disease was assessed according to Klewer et al. (2001, [89]) by rating the roots of the infected plants. A disease index (DI) was calculated according to Siemens et al. (2002, [90]) after the formula

$$DI = \frac{(1n_1 + 2n_2 + 3n_3 + 4n_4) \times 100}{4N_{total}}$$

where n_1 to n_4 is the number of plants in the indicated disease class and N_{total} is the total number of plants tested. These class refer to: 0-no symptoms; 1-very small clubs on lateral

roots; 2-small clubs covering main root and few lateral roots; 3-medium to bigger sized clubs including main roots, plant growth can be impaired; 4-severe clubs in lateral, main root or rosette, fine roots destroyed, plant roots impaired. Plants with a DI of ≥90 were termed as susceptible, a DI between 40 and 70 moderately resistant/tolerant and a DI of ≤40 resistant.

Moreover, the shoot index was quantified by dividing the dry weight (DW) of the infected plants by the control plants DW of the same genotype.

3.7 Confocal Laser Scanning Microscopy (CLSM)

For subcellular localisation roots and leaves of plants 15 DAS containing the 35S:AtOXR2-mRFP construct in the *mt-gk* background or 35S:AtOXR5-mRFP in the *pm-gk* background were imaged with a Leica TCS SP8 or a Zeiss LSM880 confocal laser scanning microscope with excitation at 488 nm and detection at 498-531 nm for GFP. The excitation of mRFP was accomplished with the 561-nm laser line, and the emission was detected between 587 and 620 nm. Chlorophyll and the presence of chloroplasts were recorded at 633-nm laser excitation line with emission at 650 to 600 nm.

For NPR1-GFP microscopy detached leaves from two-week-old plants treated for 24h with SA (0,50 mM SA plus 0,025% (v/v) Silwet L-77) or mock solution (0,025% (v/v) Silwet L-77) were imaged with a Leica TCS SP8 or a Zeiss LSM880 confocal laser scanning microscope with excitation at 488 nm and detection at 498-531 nm for GFP and the natural fluorescence of chlorophyll was detected at 600-650 nm.

For TCS::GFP (CK sensor) line imaging CLSM was performed on root tips from 7-10 DAS plants grown on MS medium. The same microscope as before was used with excitation at 488 nm and detection at 498-531 nm for GFP.

3.8 Western blot analysis

Analysis of AtOXR2 mitochondrial localisation by Western blot was performed according to Steinebrunner *et al.* (2011, [91]) with slight modifications. Mitochondria enriched proteins extracts and subcellular fractions were prepared from aerial parts of fully expanded rosette leaves of Arabidopsis plants 20 DAS carrying the 35S:AtOXR2-GFP construct. Briefly, leaf homogenates were first centrifuged at 2500 *g* for 5 min to obtain a fraction enriched in chloroplasts (fraction I). The supernatant was then centrifuged at 15000 *g* for 15 min. The pellet was resuspended and the procedure described above was repeated to obtain a fraction enriched in mitochondria. The supernatant of this centrifugation, containing soluble proteins and small vesicles, is referred to as fraction II. For Western blot (WB) analysis,

protein fractions were loaded in a 15% SDS gels and transferred to a PVDF membrane (GE Healthcare). Blots were incubated with polyclonal rabbit antibodies against GFP (Abcam #ab290) at a dilution of 1:5000, cytochrome *c* oxidase subunit 2 (COX2, Agrisera #AS04 053A), plastocyanin (a gift of Dr. Marinus Pilon, Colorado State University) at a dilution of 1:500, and actin (Agrisera #AS132640) at 1:10000 dilution. Reactions were developed with 1:20000 Goat anti-Rabbit IgG (H&L), HRP conjugated (Agrisera, #AS09 602) using the Agrisera ECL kit (AS16 ECL-SN).

For detection of AOX total protein was extracted from 2-week-old plants of the different genotypes using the protocol described by Martínez-García et al. (1999, [92]). Samples were loaded in a 12% SDS gels and transferred to a PVDF membrane (GE Healthcare). Afterwards, blots were incubated with a 1:1000 dilution of polyclonal rabbit antibodies against AOX1a (Agrisera AS04 054). Reactions were developed with 1:20000 Goat anti-Rabbit IgG (H&L), HRP conjugated (Agrisera, #AS09 602) using the Agrisera ECL kit (AS16 ECL-SN).

3.9 Measurement of photosynthetic parameters

To assess senescence leaf fluorescence parameters were measured using a LiCOR 6400-XT portable photosynthetic system (LI-COR Inc.) with the 6400-40 Leaf Chamber Fluorometer. Analysis was made on the 4th, 5th and 6th leaf pair at different times (from 32 to 49 DAS). Prior to measurements, each leaf was adapted for 10 min to darkness and ten measurements were made using different plants for each genotype. Chlorophyll fluorescence parameters were calculated according to Maxwell and Johnson (2000, [93]) and Baker (2008, [94]).

3.10 Plant mitochondrial respiration determination and mitochondrial membrane potential measurement

Respiration was monitored through oxygen consumption. Plants were kept in darkness for 40 min and then the 4th, 5th and 6th leaves were transferred to 2,5 ml of reaction buffer (300 mM mannitol, 1% (w/v) BSA, 10 mM KH_2PO_4 (pH 7.2), 10 mM KCl, 5 mM $MgCl_2$). Measurements were made at 25°C using a Clark-type oxygen electrode (Hansatech, Norfolk, United Kingdom). The capacity of the CcO pathway was determined as the O_2 uptake sensitive to 1 mM KCN in the presence of 10 mM salicylhydroxamic acid (SHAM). The capacity of the alternative pathway was determined as the O_2 uptake sensitive to 1 mM KCN [95].

Mitochondrial membrane potential was determined using the TMRM dye. Two-week-old whole seedlings were equilibrated in 20 nM TMRM (in MS medium) for 15 min before confocal

imaging of roots. In vivo imaging was performed by CLSM with excitation at 543-nm laser line, and the emission was detected between 560 and 615 nm.

3.11 Detection of ROS

Intracellular ROS levels were determined by 2',7'-dichlorodihydrofluorescein diacetate (H2DCFDA; Molecular Probes) staining. Leaf discs were incubated for 10 min in the dark in a solution containing the probe (1 µM, pH 7.2) and washed tree times with HEPES 20 mM pH 7.2. Discs where placed on a multiwell plate and ROS levels were quantified by measuring the emitted fluorescence (538 nm) using a Thermo Scientific Fluoroskan Ascent$_{TM}$.

Superoxide anion (O_2^-) was measured using nitro-blue tetrazolium (NBT). For this, two-week-old seedling were vacuum infiltrated with a 0,2 ng.ml^{-1} solution of NBT in KH_2PO_4 buffer (10 mM, pH 7,8) and incubated for 2 h. Afterwards the plant tissues were cleared with 70% (v/v) ethanol solution and photographed.

3.12 Free SA identification and quantification by gas chromatography-mass spectrometry (CG-MS)

SA was determined as described in Lovelock et al. (2016 [62]). Briefly, 2-week-old full rosettes were homogenized in a mortar, 500 mg were transferred to homogenization buffer (95% iso-propanol/5% glacial acetic acid) and 100 ng SAD_4 (deuterated compound obtained from Dr. Ehrenstorfer GmbH, Augsburg, Germany) was added as an internal standard. The homogenate was centrifuged and the supernatant was dried under a stream of nitrogen until an aqueous phase was reached. The sample was then twice extracted with equal volumes of ethyl acetate, pooled ethyl acetate fractions were dried under a nitrogen stream and SA was derivatized using trimethylsilyldiazomethane (Sigma) before analysis by GC-MS. The GC-MS analysis was carried out on a Varian Saturn 2100 ion-trap mass spectrometer using electron impact ionization at 70 eV, connected to a Varian CP-3900 gas chromatograph equipped with a CP-8400 autosampler (Varian, Walnut Creek, CA, USA). SA was identified according to the retention time on GC compared with an authentic methylated standard and the amount of SA was calculated using the isotope dilution equation with the ions at m/z 120 (endogenous SA) and m/z 124 (SAD_4).

Isotope dilution equation: $\frac{RI^{120}+RI^{124}}{RI^{124}} - 1 \times \frac{100ngSAD^4}{gfreshweitght} = ng\ SA/g\ freshweight$

where RI_{120} is the relative ion intensity for the 120 m/z ion and RI_{124} is the relative ion intensity for the 124 m/z ion.

3.13 CKs identification and quantification by high performance liquid chromatography (HPLC)

CKs determinations were carried out by the Laboratory of special Analytic Services (Lab FAUBA, Agronomy School, Universidad de Buenos Aires). Extraction was performed using Bieleski solution [96] with small modifications (MeOH-HCO_2H-H_2O; 15/1/4 (v/v/v)). Full rosette leaves of four-week-old plants were freeze-dried and resuspended in extraction buffer and incubated ON at -20ºC. After, homogenates were centrifugated at 13000 *g* for 20 min at 4ºC and pellets were re-extracted with the same buffer for 1 h at -20ºC. Both fractions were pooled and passed through a Sep-Pak Plus C18 column in order to remove pigments and lipids. After samples were vacuum dried at 40ºC. For further purification the method described by Dobrev y Kaminek (2002, [97]) was used. Samples were resuspended in 5 mL formic acid (1 M) and passed through an OASIS MCX column. The column was washed with 5 ml formic acid (1 M) and CKs were eluted using 5 ml of ammonia (0,35 M) and ammonia-methanol (0,35 M in 60% (v/v)). The eluted extracts were dried in a Rotavap at 40ºC. For the subsequent HPLC analysis, the samples were resuspended in 100 µL acetonitrile 50% (v/v) and 5 µL were injected into a HPLC Agilent 1100 series through an Eclipse XDB–C18 column with a 0,5 $ml.min^{-1}$ flow. Separation was achieved using an acetronitrile (B) 0,0005% (v/v) linear gradient with 10% acetic acid. For calibration tZ and tZ-Riboside, commercial standards of were used (Sigma).

3.14 Extraction and determination of chlorophylls and carbohydrates

3.14.1 Ethanolic extraction

For extraction, 20 mg ground fresh weight (FW) tissue from leaf material 20 DAS were incubated 20 min at 80°C with 250 µl 80% ethanol in 10 mM HEPES-KOH pH 7. Afterwards, the samples were centrifuged for 5 min at 14000 rpm, and the supernatant was kept (S1). The pellet was further extracted with 250 µl 50% ethanol in 10 mM HEPES-KOH pH 7 and again incubated for 20 min at 80°C, after centrifugation for 5 min at 14000 rpm the supernatant (S2) was pooled with S1. This second pellet was once more extracted with 150 µl 80% ethanol in 10 mM HEPES-KOH pH 7, incubated for 20 min at 80°C and centrifuged for 5 min at 14000 rpm, S3 fraction was pooled with the previous ones (S1+S2+S3) and the final pellet preserved to determinate starch.

3.14.2 Chlorophyll determination

In a 96-well microplate, 50 µl of ethanolic extract were dispensed in duplicates and 120 µl 98% ethanol (v/v) added. After mixing, the absorbance at 645 (A_{645}) and 665 (A_{665}) nm was measured in a Microplate Reader, taking care of maintaining ODs between 0.3 at 645 nm and 0.6 at 665 nm. Chlorophyll contents were calculated with the following formulas after blank subtraction:

$$ChlA(\mu g/well) = 5{,}21A_{665} - 2{,}07A_{645}$$

$$ChlB(\mu g/well) = 9{,}29A_{645} - 2{,}74A_{665}$$

$$TotalChl(\mu g/well) = ChlA + ChlB$$

3.14.3 Glucose, fructose, sucrose determination

For glucose, fructose and sucrose determinations the following solutions were used:

- Buffer: 100 mM HEPES-KOH pH 7.0 + 3 mM $MgCl_2$
- 60 mg/ml ATP
- 36 mg/ml NADP
- G6PDH grade II from Roche
- Hexokinase from Roche (120 µl suspension dissolved in 400 µl 0.1 M Tris-HCl pH 8 after centrifugation). The enzyme mix is not stable at pH 7.
- Phosphoglucose isomerase from Roche (60 µl suspension dissolved in 400 µl 0.1 M Tris-HCl pH 8 after centrifugation). The enzyme mix is not stable at pH 7.
- Invertase from Sigma (8 mg dissolved in 400 µl buffer)
- Mix for 1 microplate: 15.5 ml buffer, 480 µl ATP, 480 µl NADP, 80 µl G6PDH.

In a 96-well microplate 50 µl of ethanolic extract were dispensed in duplicates adding 160 µl of the mix. The absorbance was read at 340 nm (2 h kinetic, 1 measurement every min), then the following enzymes were added successively once the OD reached a stable value: 2 µl hexokinase, 2 µl phosphoglucose isomerase and finally 2 µl invertase. Standards for each sugar were included for quantification and values were expressed as $\mu mol.g^{-1}$ FW.

3.14.4 Extraction and determination of starch

For starch extraction and determination, the following solutions were used:

- Acetate buffer: 100 mM acetate-NaOH pH 4.9

- 0.5 M HCl

- Amyloglucosidase from Roche (suspension in ammonium sulfate)

- α-amylase from Sigma (suspension in ammonium sulfate)

- HEPES buffer: 100 mM HEPES-KOH pH 7 + 3 mM $MgCl_2$

- 60 mg/ml ATP

- 36 mg/ml NADP

- G6PDH grade II from Roche

- Starch degradation mix: 3 ml amyloglucosidase + 30 µL α-amylase, centrifuge, remove the supernatant and dissolve the pellet in 25 mL of acetate buffer

- Glucose determination mix: 15.5 ml HEPES buffer, 480 µl ATP, 480 µl NADP, 80 µl G6PDH (remove the ammonium sulphate supernatant by centrifugation)

First, 80 µl HCl were added to the pellet (section 3.14.1) previously treated with 400 µl 0.1 M NaOH. One hundred µl of starch degradation mix were added and samples were incubated for 10-16 h at 37°C. After the incubation the samples were centrifuged and 50 µl of the supernatant was dispensed in duplicates in a 96-well microplate adding 160 µl glucose determination mix. The absorbance was read at 340 nm (2 h kinetic, 1 measurement every min), then 2 µl hexokinase were added once the OD was stabilised. Glucose was added as standard for quantification and values were expressed as $\mu mol.g^{-1}$ FW.

3.15 GUS staining and fluorometric activity

ß-Glucuronidase (GUS) activity was analyzed by histochemical staining using the chromogenic substrate 5-Bromo-4-chloro-1H-indol-3-yl ß-D-glucopyranosiduronic acid (X-gluc) as described by Hull and Devic (1995, [98]). Whole plants or separated organs were immersed in a 1 mM X-gluc solution in 100 mM sodium phosphate, pH 7, and 0.1% (v/v) Triton X-100, and, after applying vacuum for 5 min, they were incubated at 37°C until satisfactory staining was observed. Tissues were cleared by immersing them in 70% ethanol. Specific GUS activity in protein extracts was measured using the fluorogenic substrate 4-methylumbelliferyl b-D-glucuronide (MUG) essentially as described by Jefferson et al. (1987, [99]). Total protein extracts were prepared by grinding the tissues in extraction buffer (50 mM NaH_2PO_4, pH 7, 10 mM EDTA, 10 mM β-mercaptoethanol) containing 0.1% (w/v) SDS and 1% (v/v) Triton X-100, followed by centrifugation at 13,000 *g* for 10 min. GUS activity in supernatants was measured in extraction buffer containing 1 mM MUG and 20% methanol. Reactions were stopped with 0.2 M Na_2CO_3 and the amount of 4-methylumbelliferone was calculated by relating relative fluorescence units from the emitted fluorescence (538 nm)

measured with a Thermo Scientific Fluoroskan Ascent™ and expressed relative to the protein concentration. The protein concentration of extracts was determined as described by Sedmak and Grossberg (1977, [100]) using Coomasie G-250 (1 mg.ml^{-1}, 10% phosphoric acid) as protein dye and quantifying by absorbance at 595nm using a standard curve.

3.16 Sequence alignment and phylogenetic tree analysis

Arabidopsis OXR family members were identified using the Blastp tool [101] and human and yeast Oxr1 as query sequences. Sequence similarity was calculated using the Clustal Omega tool [102]. Plant TLDc containing proteins were identified using the Arabidopsis family members AtOXR1 to AtOXR5 as queries. Sequences with an E-value lower than 10^{-5} were downloaded from Phytozome 12 [103] and Gymno PLAZA. Sequence alignment was made using default parameters established in the WebPRANK alignment server [104]. Phylogenetic trees were built using the Seaview 4.5.0 software and the PhyML-aLRT-SH-LIKE algorithm [105] with maximum likelihood tree reconstruction. A model of the amino acid substitution matrix was chosen through the Datamonkey bioinformatic server (www.datamonkey.org; [106]), which showed the WAG model. The resulting tree was represented using iTOL (http://itol.embl.de/itol.cgi, [107]) showing branches with bootstraps higher than 70%.

3.17 Homology modelling

The AtOXR5 TLDc domain homology model was generated using the Swiss-model server [108] using the structure of the zebrafish OXR2 (A9JTH8) TLDc domain as a reference (PDB: 4acj; [5]).

3.18 Statistical analysis

Data were analysed by one-way ANOVA and the means were compared by Tukey or Fisher (LSD) tests. Statistical analysis was performed using InfoStat Version 2013 for Windows (http://www.infostat.com.ar).

4. Results and Discussion

Part I

4.1 Functional characterization of AtOXR2

4.1.1 Identification and evolutionary analysis of OXR family proteins in plants

A survey of sequences in the Arabidopsis genome with similarity to OXR proteins from yeast and humans allowed us to identify five genes coding for OXR family members: *At4g39870*, *At2g05590*, *At5g06260*, *At1g32520* and *At5g39590*, which were arbitrarily named by numbers from one to five: *AtOXR1*, *AtOXR2*, *AtOXR3*, *AtOXR4* and *AtOXR5*, respectively (Fig. 9A). The presence of a TLDc domain in the five proteins was confirmed by searches in the Pfam database [109]. Notably, the TLDc domain of AtOXR4 is shorter and appears to be truncated. Besides, a sixth protein with high identity to AtOXR3, but with a truncated TLDc domain, was identified. This protein is encoded by gene *At4g34070* and was named *AtOXR6*. The TLDc domain is present in the carboxy-terminal half of the identified proteins (Fig. 9A), as previously found in family members from other organisms [110]. AtOXR3 and AtOXR6 contain EF-hand calcium-binding motifs characteristic of the penta-EF hand (EFh) protein family [111]. Using a multiple sequence alignment [102], a percentage identity matrix of the Arabidopsis family members and the yeast and human OXR proteins was obtained (Table 1). The highest sequence identity with the human and yeast proteins was observed for AtOXR1 and AtOXR2 (29-31% for the complete proteins and 40-42% for the TLDc domains, Table 1). AtOXR family members were used to identify OXR protein sequences in different plant species that were used to build a phylogenetic tree (Fig. 9B). The tree shows the presence of three clades (OXR1/2, OXR3/6 and OXR4) containing proteins representative from different lineages, from algae to flowering plants. A fourth clade (OXR5) contains proteins from land plants, but not from algae (Fig. 9B), suggesting that this clade may have originated by a duplication that took place early during land plant evolution. The OXR1 and OXR2 clades probably evolved later, since OXR1 and OXR2 proteins share more similarity among themselves than with the other clades. In addition, the OXR1 and OXR2 clades cannot be recognised in algae, which instead contain a more divergent clade that seems to be the ancestor of OXR1 and OXR2 (Fig. 9B). Since proteins from *P. patens* and *S. moellendorffii* cluster together with OXR1, it is likely that the duplication that was the origin for OXR1and OXR2 took place during land plant evolution (Fig. 9B). OXR proteins from yeast and humans cluster together with the clade containing AtOXR1, AtOXR2 and their ancestors (Fig. 9B), in agreement with the highest similarity found between these proteins. Finally, a very recent duplication probably generated the AtOXR6 family member derived from the AtOXR3 protein only in Arabidopsis.

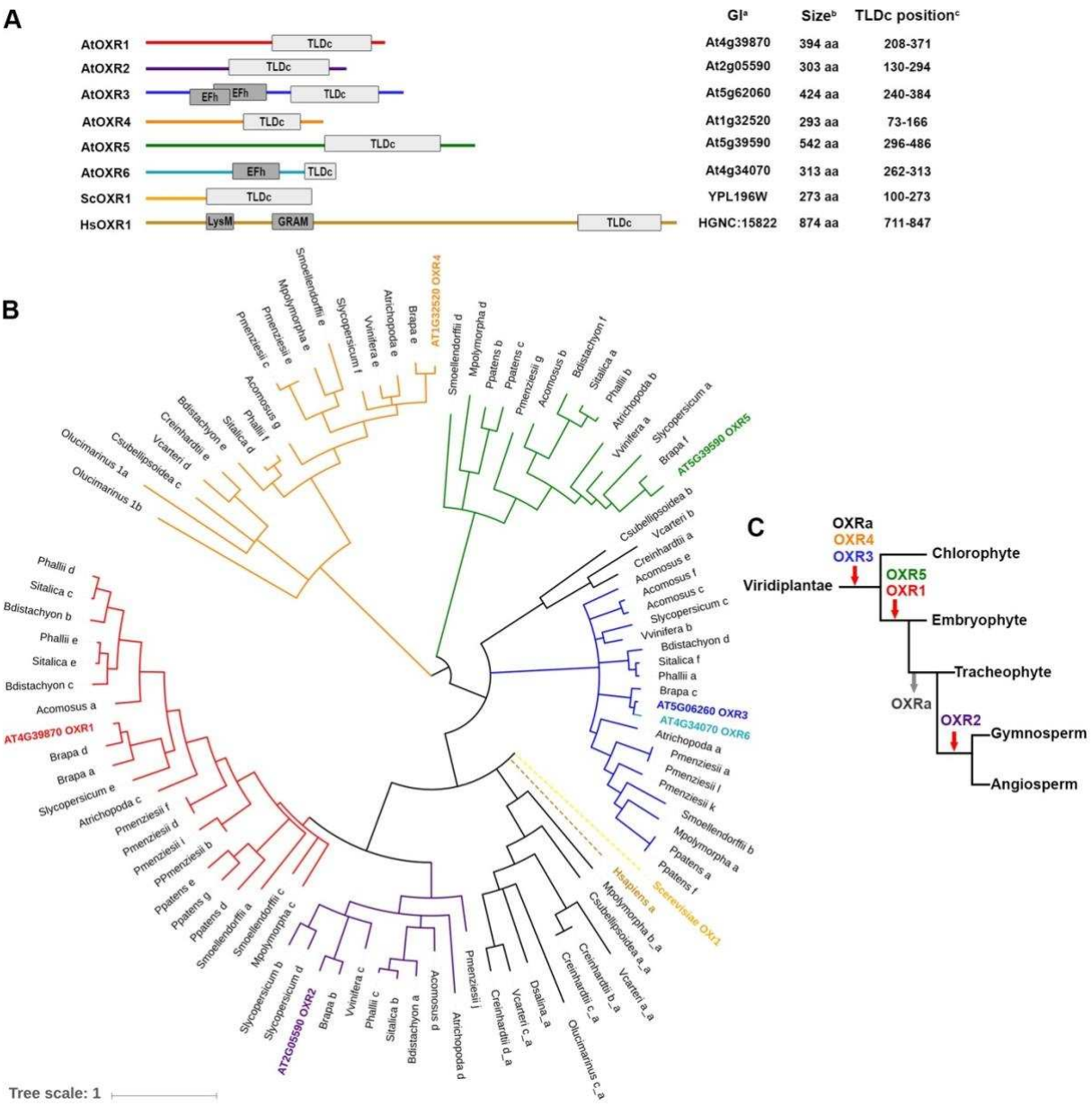

Figure 9: The Oxidation Resistance protein family in plants. (A) Schematic representation of domain architecture of the six members of the Arabidopsis AtOXR protein family (AtOXR1, NP_195697.3; AtOXR2, NP_849938.1; AtOXR3, NP_196244.1; AtOXR4, NP_174530.2; AtOXR5, NP_198775.1; AtOXR6, NP_195133.3), together with OXR1 proteins from yeast (*S. cerevisiae*, ScOXR1, NP_015128.1) and humans (HsOXR1, NP_001185464.1), used for the identification of Arabidopsis members. The gene identification code (GI) corresponds to the AGI (Arabidopsis Genome Initiative) number for Arabidopsis, the Saccharomyces systematic name and the HGNC (HUGO Gene Nomenclature Committee) number for human OXR1. For AtOXR3 and AtOXR6, the EFh domains are shown. For human OXR1, a LysM (Lysin Motif) and GRAM protein domains are drawn. (B) Phylogenetic tree of OXR proteins from selected plant species. An alignment of TLDc-containing protein sequences from 18 members of the *Viridiplantae* was used to construct a phylogenetic tree. Different clades are represented by different colors. OXR1 from *S. cerevisiae* and *H. sapiens* were included. (C) Evolutionary tree of OXR2 proteins.

Table 1: Percent identity matrix of Arabidopsis OXR family members. Sequences were extracted from the UniProt Database (https://www.uniprot.org/) and the percent identity matrix was created using the Multiple sequence alignement tool of Clustal Omega (version2.1) (https://www.ebi.ac.uk/Tools/msa/clustalo/). Yeast and human OXR1 protein sequences were included for comparison.

A) Percent identity between Arabidopsis OXR family members

Name	AtOXR1	AtOXR2	AtOXR3	AtOXR4	AtOXR5	AtOXR6	ScOxr1p	HsOXR1
Gene Identifier	At4g39870.1	At2g05590.2	At5g06260.1	At1g32520.1	At5g39590.1	At4g34070.1	YPL196W	HS_OXR1
UniProt identifier	Q8GUN9	Q9AT60	Q9FNI2	Q682Q6	Q9FKA3	O49497	Q08952	Q8N573
Protein size (AA)	**394**	**303**	**424**	**239**	**542**	**313**	**273**	**874**
AtOXR4	16,18	18,52	14,67	100	13,13	12,33	19,8	14,04
AtOXR2	43,2	100	20,96	18,52	18,85	15,75	25,51	31,45
AtOXR3	20,44	20,96	100	14,67	21,98	89,89	24	21,43
AtOXR1	100	43,2	20,44	16,18	15,76	14,71	30,73	29,61
AtOXR5	15,76	18,85	21,98	13,13	100	23,45	16,97	21,95
AtOXR6	14,71	15,75	89,89	12,33	23,45	100	23,33	18,75
ScOxr1p	30,73	25,51	24	19,8	16,97	23,33	100	27,11
HsOXR1	29,61	31,45	21,43	14,04	21,95	18,75	27,11	100

B) Percent identity within TLDc domain.

Name	AtOXR1	AtOXR2	AtOXR3	AtOXR4	AtOXR5	AtOXR6	ScOxr1p	HsOXR1
Gene Identifier	AT4G39870.1	AT2G05590.2	AT5G06260.1	AT1G32520.1	AT5G39590.1	AT4G34070.1	YPL196W	HS_OXR1
UniProt identifier	Q8GUN9	Q9AT60	Q9FNI2	Q682Q6	Q9FKA3	O49497	Q08952	Q8N573
TLDc Domain size (AA)	**208-371 (164)**	**130-294 (165)**	**240-384 (144)**	**73-166 (94)**	**296-486 (191)**	**262-313 (52)**	**100-273 (174)**	**711-847 (137)**
AtOXR4	18,75	22,5	20,73	100	19,28	16,67	21,59	20
AtOXR2	57,93	100	27,94	22,5	22,15	17,65	32,37	42,22
AtOXR3	28,68	27,94	100	20,73	26,39	67,86	26,09	27,52
AtOXR1	100	57,93	28,68	18,75	17,09	19,61	34,06	40,74
AtOXR5	17,09	22,15	26,39	19,28	100	18	18,98	23,66
AtOXR6	19,61	17,65	67,86	16,67	18	100	21,43	23,53
ScOxr1p	34,06	32,37	26,09	21,59	18,98	21,43	100	32,73
HsOXR1	40,74	42,22	27,52	20	23,66	23,53	32,73	100

4.1.2 AtOXR2 localise in mitochondria

Different OXR proteins have been localised to different cell compartments, notably in humans was found in mitochondria (hOxr1) nucleus and cytoplasm (NCOA7) [2,9]. *In silico* analysis of AtOXR2 shows no N-terminal subcellular targeting sequence [112] and the SUBcellular Arabidopsis consensus algorithm suggests localisation in plastids [113]. The AtOXR2 hydrophobicity profile, according to the ARAMENNON database [114], predicts a consensus transmembrane domain spanning amino acids 236 to 256 and the presence of a putative GPI-anchor attachment signal [115]. To obtain experimental evidence, the coding region of AtOXR2 was tagged with the mRFP coding sequence under the control of a 35SCaMV promoter and expressed in Arabidopsis. AtOXR2-mRFP was observed in dot-shaped structures, most likely reflecting mitochondria (Fig. 10A). To confirm mitochondrial localisation, the construct expressing AtOXR2-mRFP was introduced into the Arabidopsis *mt-gk* line, which expresses GFP in mitochondria (mito-GFP) [116]. Several lines co-expressing AtOXR2-mRFP and mito-GFP were analysed by CLSM showing that GFP fluorescence co-localised with the mRFP fluorescence in root and leaf cells (Fig. 10A), suggesting that AtOXR2 is a mitochondrial protein. In addition, no evidence for co-localisation of the mRFP fluorescence with chlorophyll fluorescence was obtained (Fig. 10A), ruling out a plastid localisation, at least under these conditions. In order to confirm the localisation, Western blot analysis of proteins from different subcellular fractions of rosette leaves from 20- days-old plants expressing AtOXR2-GFP were performed. Using anti-GFP antibodies, AtOXR2-GFP was detected only in the fraction enriched in mitochondria (Fig. 10B). A similar result was obtained with antibodies against the mitochondrial protein COX2 (Fig. 10B). In accordance, the chloroplast protein plastocyanin was present in the non-mitochondrial fraction (Fig. 10B). Finally, actin, a cytosolic protein, was present in both fractions, but clearly enriched in the non-mitochondrial fraction, and the same was observed in the Ponceau staining of the blot for a protein that probably corresponds to the large subunit of Rubisco (Fig. 10B). Altogether, even if plastid or cytosolic localisation in minor amounts cannot be completely ruled out, the results indicate that AtOXR2 is a mitochondrial protein. Its possible presence in other organelles, like peroxisomes, will require additional studies with N-terminal fusions of the fluorescent protein using other compartment specific protein markers as well.

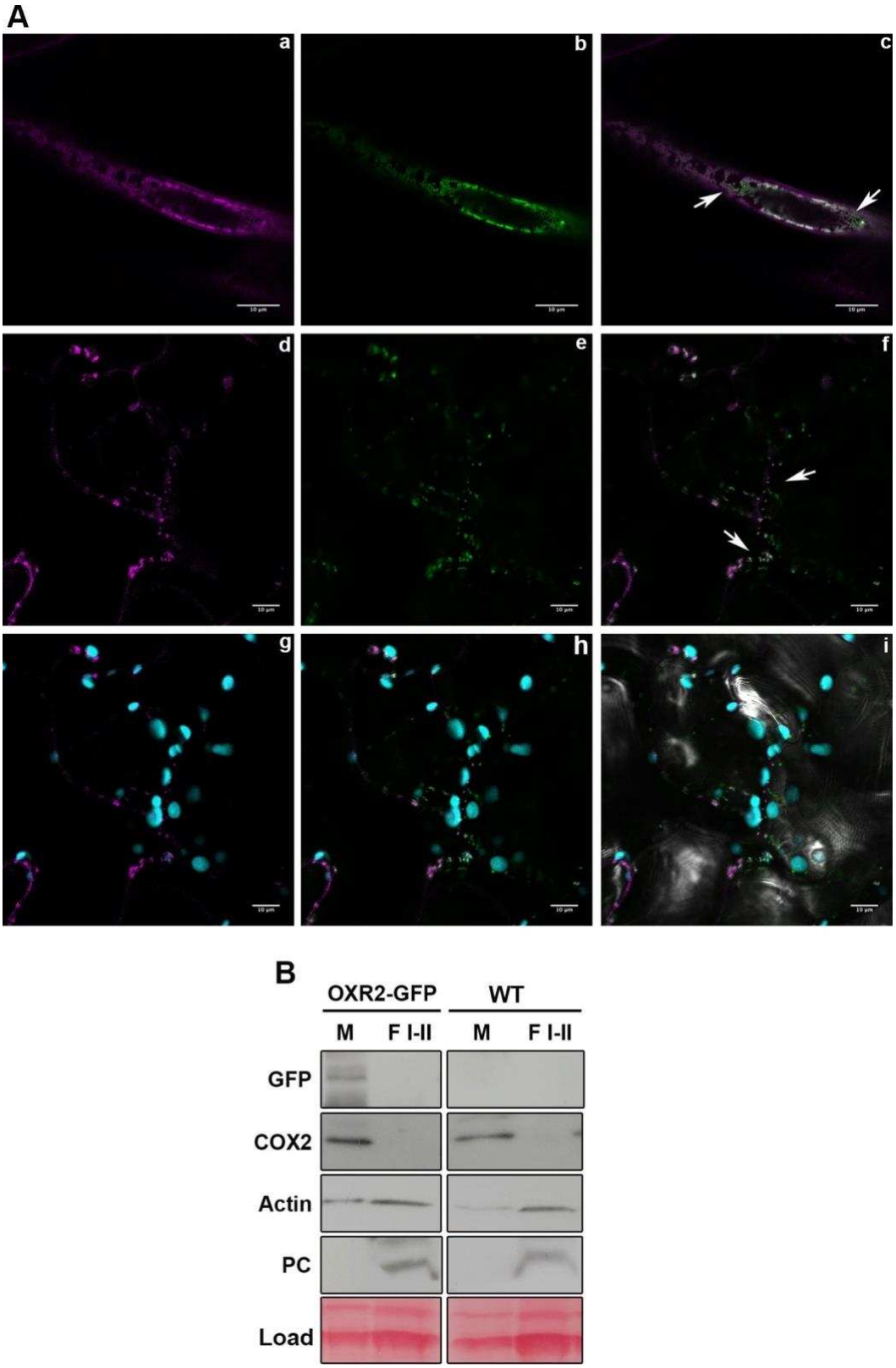

Figure 10: AtOXR2 is localised in mitochondria. (A) Seedlings of transgenic lines 15 DAS co-expressing AtOXR2-mRFP and mito-GFP were imaged by CLSM. Representative cells from roots (a-c) and leaves (d-i) are shown, in which the signals for AtOXR2-mRFP (magenta; panels a and d) and mito-GFP (green; panels b and e) co-localise as merged white dot-signals (c, f). Chlorophyll fluorescence of chloroplasts is observed in cyan in panels g-i. No co-localisation of the AtOXR2-mRFP signals with chloroplasts was observed. A bright field image is shown in i. Scale bars represent 10μm. (B) Subcellular localisation analysis of AtOXR2 by Western blot. Mitochondria enriched extracts (M) and fractions I and II (F I-II; see Materials and methods for details) from fully expanded 20-day-old rosette leaves of a representative transgenic line expressing 35S:AtOXR2-GFP and Wt plants were loaded in a 15% SDS-

PAGE and transferred to a PVDF membrane. Blots were analysed with antibodies against GFP (abcam #ab290; for the fusion protein AtOXR2-GFP), COX2 (mitochondrial marker), plastocyanin (PC; chloroplast marker) and actin (cytosol marker). A Ponceau-staining of the membrane, with a prominent protein band probably corresponding to the large subunit of Rubisco, is shown as loading control.

4.1.3 AtOXR2 modifies plant architecture

To gain more evidence about the function of At*OXR2*, plants with altered expression of this gene were analysed. Two Arabidopsis insertional knockout mutants identified as *oxr2.1* (Flag_510D06) and *oxr2.2* (SK17762) were characterized and several lines overexpressing At*OXR2* under the CaMV *35S* promoter (OXR2) were obtained (Fig. 11). Phenotypic parameters of these plants were characterized through the whole life cycle. No differences in comparison to Wt were observed for *oxr2.2* mutant plants under normal growth conditions (Fig. 12 and 13). In contrast, two independent OXR2 lines (A and B) exhibited increased rosette diameter and area (Fig. 12A, 13A and B), and produced a higher number of leaves and biomass compared to Wt plants (Fig. 13C and H). OXR2 plants also exhibit higher shoots and thicker stem (Fig. 12B, 13D and F). All these parameters may explain the increased biomass observed in At*OXR2* overexpressing lines. Besides, OXR2 plants also exhibited a higher number of lateral shoots (Fig. 13E), resulting in higher seed production at the end of the life cycle in comparison to Wt plants (Fig. 13G).

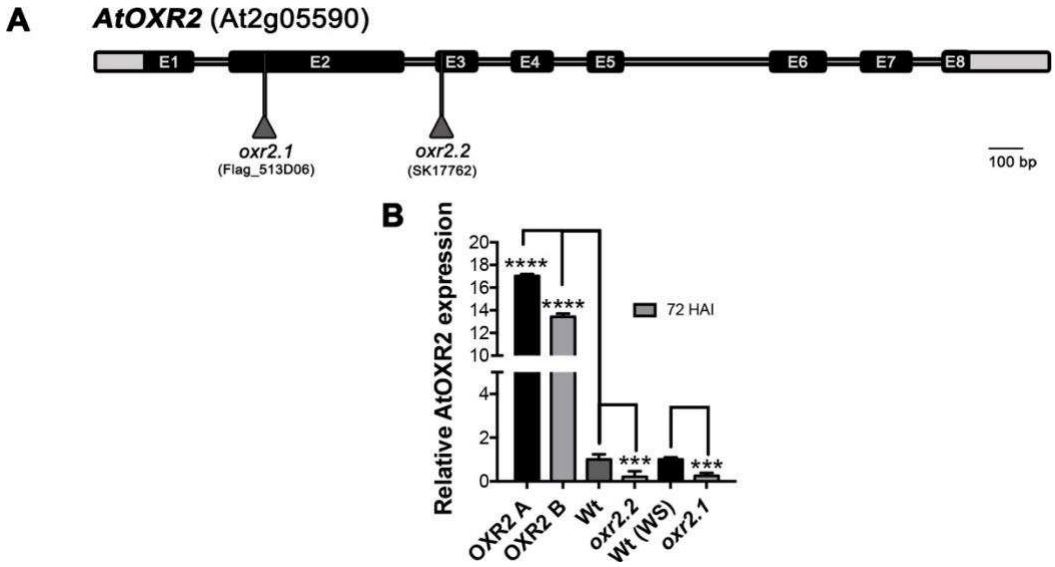

Figure 11: Schematic representation and molecular characterization of the plant lines used in this study. (A) Schematic representation of the AtOXR2 T-DNA insertion mutants used in this study. (B) AtOXR2 transcript levels in overexpressing lines (35S:AtOXR2) and *oxr2* mutants. OXR2 A and OXR2 B are two independent 35S:AtOXR2 lines used in this work. The *oxr2.1* and *oxr2.2* insertional mutants are in Wassilewskija (ws) and Columbia (Col-0) ecotypes, respectively. Transcript levels are referred to those of Wt plants in the same ecotype. Asterisks indicate significant differences at $P<0.05$ (ANOVA, LSD Fisher test).

Figure 12: Representative images of plants grown in LD photoperiod at different times, (A) rosettes and (B) plants after flowering.

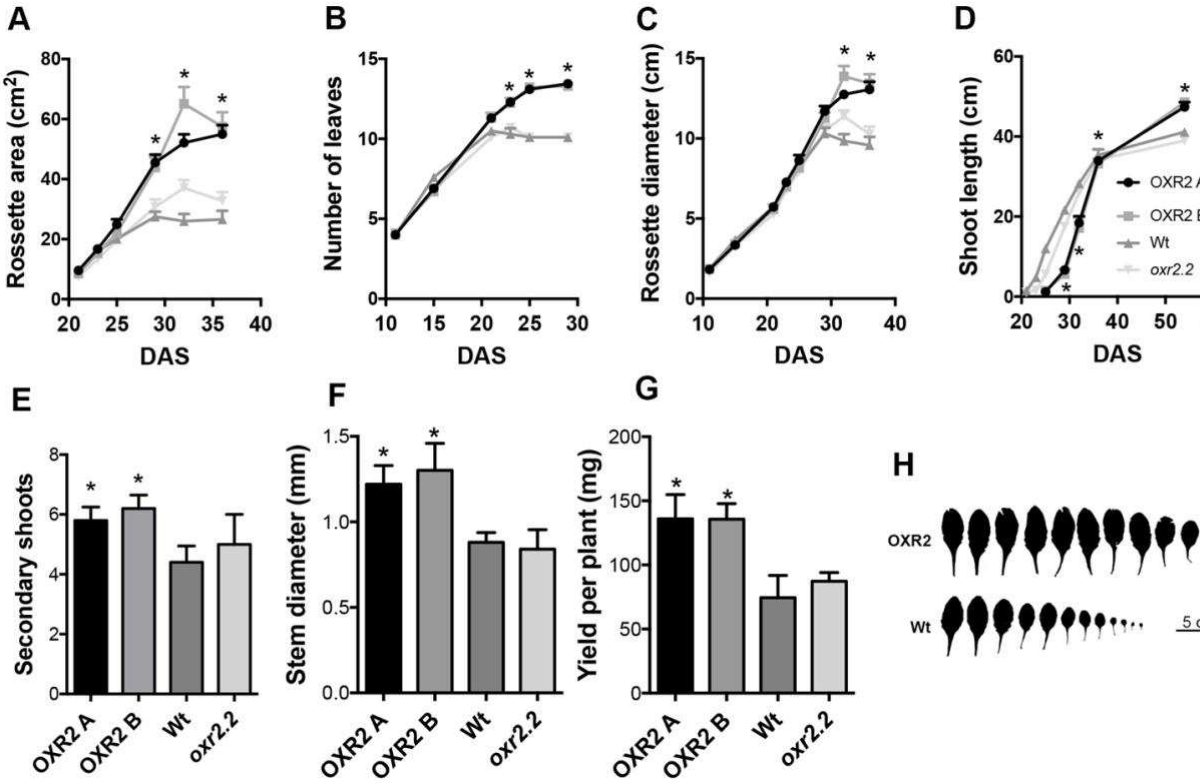

Figure 13: Parameters related to plant growth: (A) rosette area, (B) rosette diameter, (C) number of leaves, (D) shoot length, (E) stem diameter and (F) secondary shoots in Wt, OXR2 and *oxr*2.2 plants grown in LD photoperiod. (G) Yield per plant. (G) Representative images of rosette leaves from OXR2 and Wt plants. Values represent the mean±SEM of five to ten individual plants for each genotype. Asterisks indicate significant differences ($P<0.05$) with Wt plants according to LSD Fisher tests.

4.1.4 AtOXR2 affects the transition between vegetative and reproductive phases and the onset and progression of senescence

Another interesting characteristic exhibited by the OXR2 plants is a slight delay in the transition between vegetative and reproductive phase; flowering occurred approximately four to six days later than in Wt plants (Fig 14A). This delay in days correlates with a higher number of leaves by the time of the reproductive switch (Fig. 14B), as is often seen in plants with altered flowering time [117–119].

Altered *AtOXR2* expression also affects the onset and progression of natural senescence. Measurements of maximum PSII efficiency (Fv/Fm) in different leaves of entire rosettes between days 32 to 49 after sowing indicated that *oxr*2.2 plants age slightly earlier, while OXR2 lines stay green for a longer time (Fig. 15).

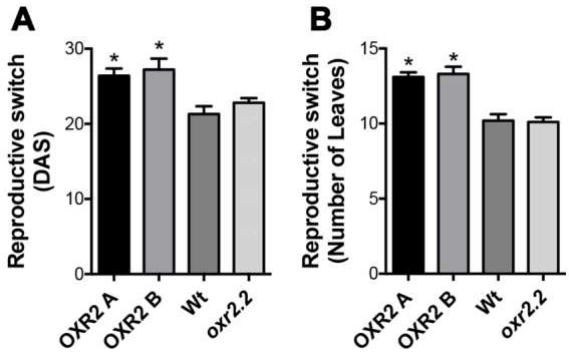

Figure 14: Altered AtOXR2 expression affects the transition between vegetative and reproductive phases. (A) Number of leaves and (B) DAS required to reach the reproductive stage in Wt, OXR2 and *oxr2.2* plants. Values represent the mean±SEM of five to ten individual plants for each genotype. Asterisks indicate significant differences ($P < 0.05$) with Wt plants according to LSD Fisher tests.

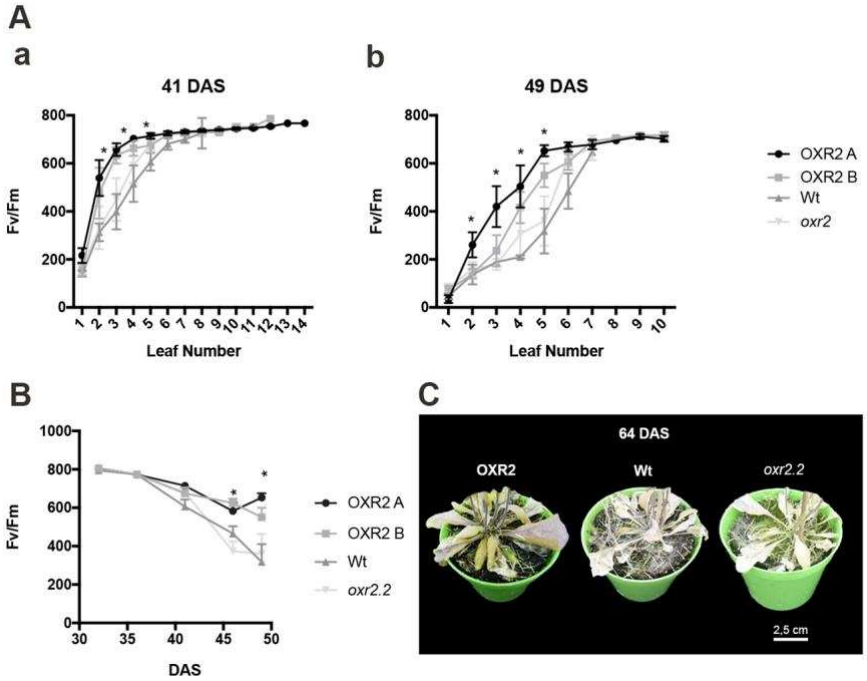

Figure 15: Altered AtOXR2 expression affects the onset and progression of natural senescence. (A) Maximum PSII efficiency (Fv/Fm) measured in different leaves at (a) 41 and (b) 49 DAS. (B) Evolution of the Fv/Fm parameter in the fifth leaf. (C) Representative images of OXR2, *oxr2.2* and Wt plants at 64 DAS. Values represent the mean±SEM of ten plants for each genotype. Asterisks indicate significant differences ($P < 0.05$) with Wt plants of the same age, according to LSD Fisher tests.

Moreover, the response of the plants to dark-induced senescence was analysed. Detached leaves from four-week-old plants grown under LD conditions and incubated them in full darkness for 2 days were used. Chlorophyll content was measured and the values used as marker of senescence progression and expressed it relative to the corresponding mock treatment for each genotype (Fig. 16). Once more, a delay in dark-induce senescence in OXR2 plants was observed. Also an earlier apparition of senescence symptoms in the *oxr2.2* mutants compared to Wt plants was determinate.

Altogether OXR2 plants appear to have a longer lifespan characterised by a delay of 5±2 days in the transition to reproductive phase and the onset and progression of natural and dark-induced senescence.

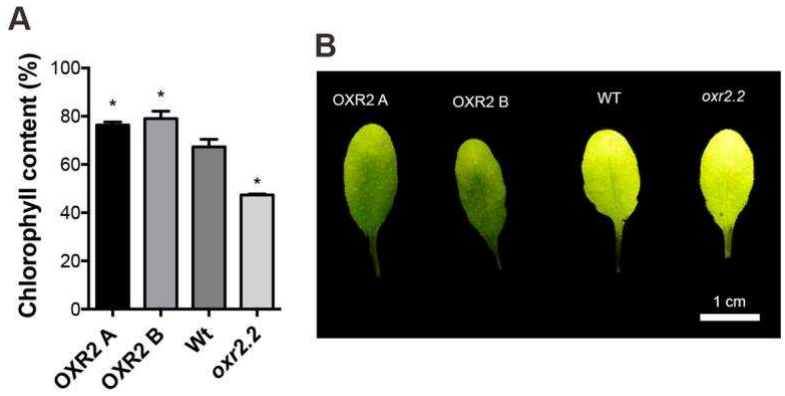

Figure 16: Altered AtOXR2 expression affects the onset and progression of dark-induced senescence. Fully expanded leaves were detached from 3-week-old Wt, OXR2 and *oxr2.2* plants were placed in the dark for 3 days. (A) Chlorophyll content in detached leaves relative to the control for each genotype, and (B) representative images of OXR2, *oxr2.2* and Wt plants after the treatment. Values represent the mean±SEM of ten plants for each genotype. Asterisks indicate significant differences ($P < 0.05$) with Wt plants, according to LSD Fisher tests.

4.1.5 AtOXR2 does not significantly modify the chlorophyll and carbohydrates content in plants

Considering that OXR2 plants exhibit higher biomass and the photosynthetic parameters on these plants are improved [121] we set out to analyse sugar metabolism and chlorophyll content in plants with altered AtOXR2 expression. Soluble sugar content was evaluated, in the form of glucose, fructose, sucrose and starch content at different time points of the diurnal cycle in plants 20 DAS grown under LD photoperiod (Fig. 17). Furthermore, chlorophyll A, chlorophyll B and total chlorophyll content was determined in four-week-old plants grown under LD photoperiod (Fig. 18). All the metabolites measured have been compared between Wt, OXR2 and *oxr2.2* mutant plants.

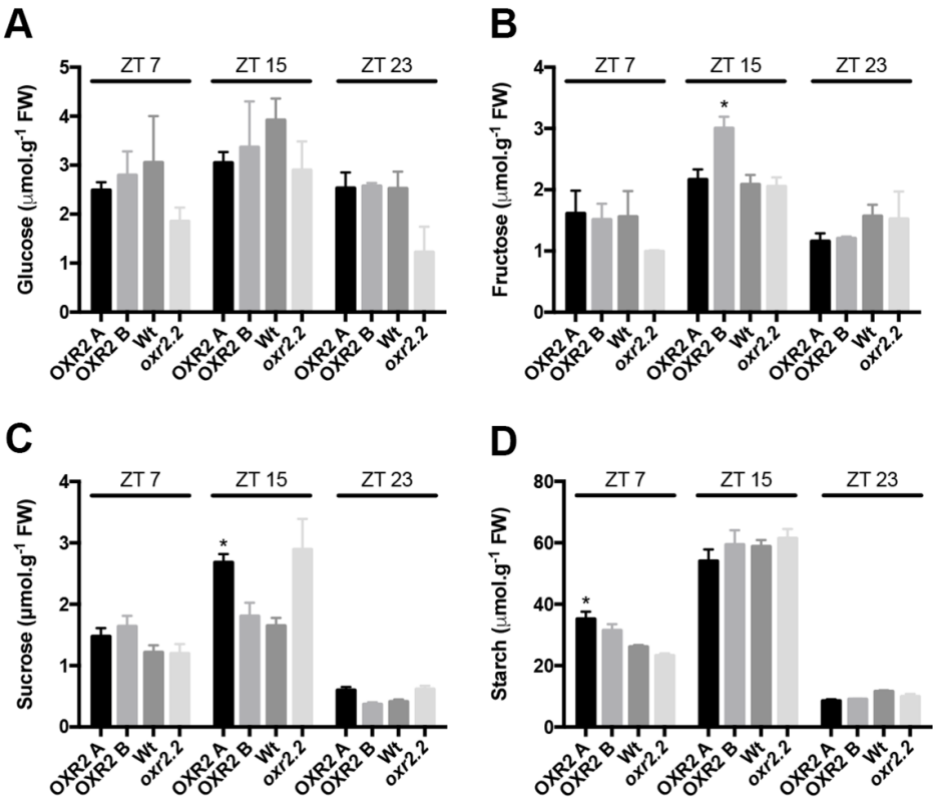

Figure 17: Levels of several metabolites in Wt, OXR2 and oxr2.2 plants 20 DAS grown under LD photoperiod 1 h before (ZT23), 7 and 15 h after (ZT7 and ZT15) the beginning of the illumination period. (A) Glucose, (B) fructose, (C) sucrose and (D) starch content. Values represent the mean±SEM of ten plants for each genotype. Asterisks indicate significant differences ($P < 0.05$) with Wt plants of the same age, according to LSD Fisher tests.

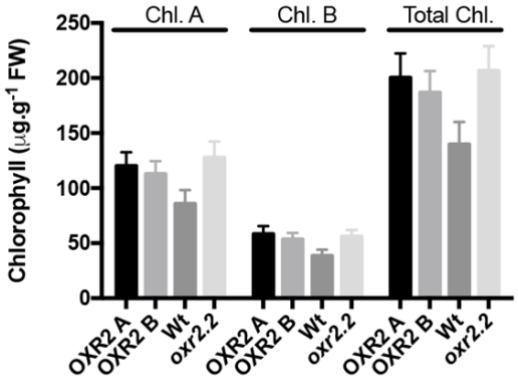

Figure 18: Analysis of chlorophyll content in Wt, OXR2 and *oxr2.2* plants 20 DAS. Values represent the mean±SEM of ten plants for each genotype.

4.1.6 AtOXR2 alters respiration and mitochondrial membrane potential in Arabidopsis

Since AtOXR2 was identified as a mitochondrial protein (section 4.1.2) it was interesting to determine some mitochondrial parameters. Therefore, mitochondrial respiration was evaluated by monitoring O_2 consumption using a Clark electrode, in plants grown under

normal conditions. Total respiration rates were increased in OXR2 plants compared to those measured in Wt and *oxr2.2* plants (Fig. 19A). These values were reached at the expense of an increase in cyanide-sensitive (CcO-dependent) respiration, but no significant differences were seen in alternative or SHAM-sensitive respiration (Fig. 19A).

In parallel, the mitochondrial membrane potential was assessed in living plant cells by CLSM using the cationic lipophilic fluorescent dye tetramethyl rhodamine methyl ester (TMRM). TMRM is capable to accumulate in the mitochondrial matrix in response to the membrane potential of the inner mitochondrial membrane and thus acting as a dynamic reporter of mitochondrial membrane potential [122]. Surprisingly, after analysing several plants roots, a decrease in mitochondrial membrane potential was determinated in both OXR2 and *oxr2.2* compared to Wt (Fig. 19B and C).

Thus, OXR2 plants show higher rates of mitochondrial respiration that is not reflected in turn in an increase in membrane potential. However, the *oxr2.2* showed no difference in respiration rates compared to Wt plants but they also showed a lower membrane potential.

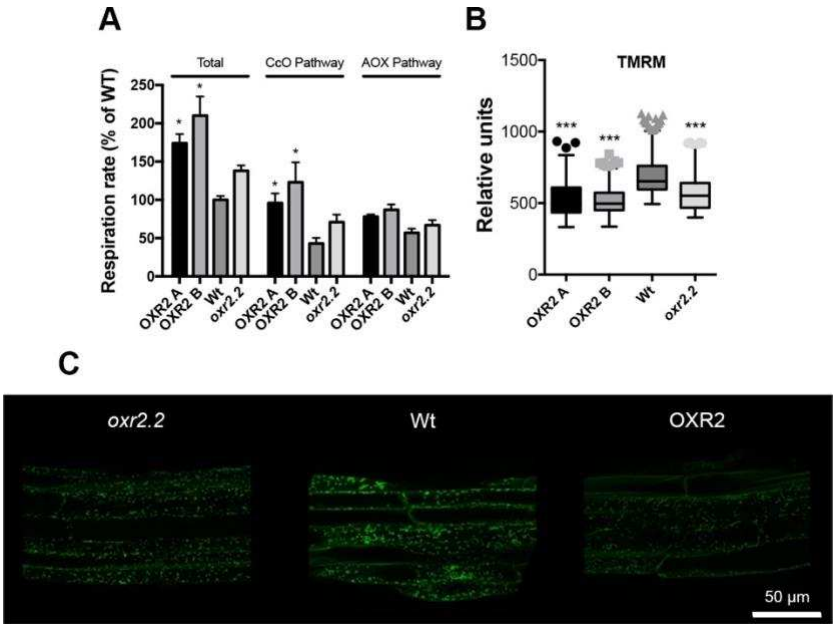

Figure 19: OXR2 plants show increased CcO activity and cyanide-sensitive respiration and decreased mitochondrial membrane potential. (A) Respiration rates (represented as percentage oxygen consumption relative to wild type) were quantified in rosette leaves of four-week-old plants using a Clark-type O_2 electrode. The capacity of the CcO pathway was determined as the O_2 uptake sensitive to 1 mM KCN in the presence of 10 mM SHAM. The alternative pathway capacity was measured as the O_2 uptake after adding 10 mM SHAM in the presence of 1 mM KCN. (B) OXR2 plants exhibit decreased mitochondrial membrane potential measured by TMRM dye (C) CLSM images from OXR2, *oxr2.2* and Wt treated with TMRM. Asterisks indicate significant differences compared with Wt ($P<0.05$).

4.2 AtOXR2 and abiotic stress

4.2.1 Plants with altered levels of AtOXR2 show different sensitivity towards oxidative stressors

It is well known that OXR proteins from several organisms are induced under conditions that promote oxidative stress [13,110]. To evaluate if this also applies to *AtOXR2*, Arabidopsis Wt plants were exposed to different stress treatments. Increased *AtOXR2* transcript levels measured by RT-qPCR in Wt were observed after exposure to UV-B light and treatments with AA and MV, conditions that generate oxidative damage (Fig. 20).

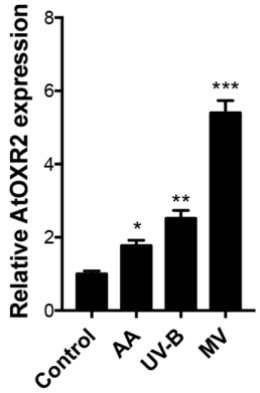

Figure 20: *AtOXR2* is induce by different oxidative stressors. AtOXR2 transcript levels measured in Arabidopsis Wt seedlings grown for 7 DAS in 0.5 x MS medium and then transfer to a solution containing MS (MS, control) or the same medium supplemented with 0.1 µM MV for 3 h, 10 µM AA for 6 h, or exposed to UV-B (5 mW.cm^{-2}; UVP 34-0042-01 lamp) for 1 h. Experiments were carried out with approximately 5 plants per biological replicate. Results are expressed as mean±SEM of three independent experiments. Asterisks represent significantly different values at $P<0.05$ (ANOVA; Tukey test).

Given the transcriptional induction of *AtOXR2* in response to different oxidative stressors, ROS content and the behaviour of plants with altered At*OXR2* expression under oxidative stress was examined. Under normal growth conditions an increase in the intracellular ROS content in OXR2 plants of 20 DAS was observed, measured by using the cell-permeant dye H2DCFDA (Fig 21A). Also increased O_2^- concentration measured by the NBT dye was detected (Fig. 21B). The source of this excess of ROS could be the result of the imbalance between the respiration and the mitochondrial membrane potential that was found in the OXR2 plants (section 4.1.6). On the contrary, and in agreement with the phenotypic parameters described above (section 4.1.3), *oxr2.2* mutants showed no differences in comparison to Wt plants in the level of ROS content under control conditions. This observation could be due to a possible compensatory or redundant effect exerted by other AtOXR family members that could also be localised in the mitochondria.

Next, it was evaluated the behaviour of plants with altered levels of AtOXR2 under stress conditions affecting chloroplast and mitochondrial electron transport [39,123]. MV induces ROS generation in the chloroplast under illumination [123] and AA is a well-known inhibitor of the complex III of the mitochondrial respiratory chain [124] (Fig. 3, Introduction). The effect of MV and AA on plant root growth was tested.

Under normal growth conditions, roots of the different phenotypes did not exhibit differences in length between each other. Under both stress situations, *oxr2* mutants appeared to be more affected exhibiting shorter roots, while roots of OXR2 plants were larger than those of Wt plants (Fig. 21C-F). Our results suggest that lack of AtOXR2 can compromise the tolerance to oxidative stress conditions while higher AtOXR2 levels increase the tolerance to agents perturbing the chloroplast and mitochondrial electron transport chain, in agreement with the induction of *AtOXR2* by these agents.

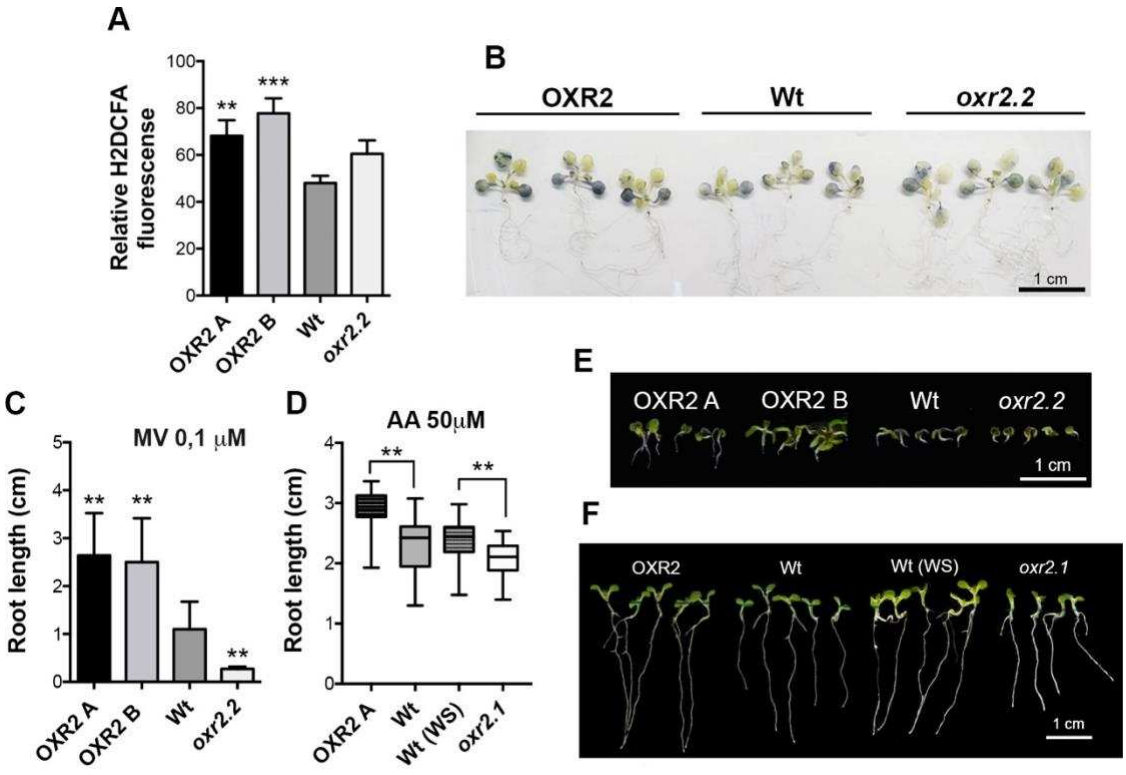

Figure 21: AtOXR2 modifies basal ROS levels and oxidative stress tolerance. (A) Intracellular ROS content in Arabidopsis leaves from OXR2, *oxr2.2* and Wt plants, quantified by the level of fluorescence using the cell permeant dye H2DCFDA measured in fully expanded rosette leaves of 20 DAS plants grown under normal conditions. (B) O_2^- content measured by NBT dye in plants grown 14 days in MS. (C) Root length of OXR2 and *oxr2.2* plants grown in MS medium supplemented with 0,1 µM MV during 10 days. (D) Root length of OXR2 and *oxr2.2* plants grown in MS medium supplemented with 50 µM AA during 7 days. (E) Representative images of the phenotype observed in seedlings grown in 1 µM MV during 6 days. (F) Representative images of the phenotype of seedlings used for quantification of root length shown in (D). Asterisks indicate significant differences at $P<0.05$ (ANOVA, LSD Fisher test), using 20-40 plants of each genotype for the analysis.

4.2.2 AtOXR2 impairs mitochondrial retrograde signalling

Mitochondria play a key role in sensing the environment and modulate their activity to coordinate the provision of energy to the cell according to the external demands [125]. Particularly abiotic stress situations cause accumulation of ROS and induction of stress-response genes, when mitochondrial dysfunction appears MRR genes are induced. It was studied the response of plants with altered levels of AtOXR2 to treatment with AA, which inhibits the complex III of the mitochondrial electron transport chain causing mitochondrial dysfunction. Then, transcript levels of MRR response genes were measured by RT-qPCR in order to identify how sensitive OXR2 plants were at the mitochondrial level. When analysing transcript levels of genes involved in MRR some were basally repressed like *UPOX*, *UGT74E2*, *HSP23.5* and *HRE* in OXR2 plants (Fig. 22B-E). Moreover, the induction of transcript caused by the AA treatment appears to be less intense in OXR2 than in Wt plants. Other characteristic MRR genes like *ANAC013* appear to respond similarly to Wt in the analysed genotypes (Fig. 22A).

However, when transcript levels of the *SAL1* gene were quantified, which is related to chloroplastic retrograde signalling and could be a connection between the two organelles [40], an opposite response in OXR2 and *oxr2.2* plants was observed. In the latter the *SAL1* gene is dramatically induced in *oxr2* mutant upon AA treatment, while in OXR2 transcript levels were not modified with respect to the Wt (Fig. 22F).

AOX is thought to play a potentially crucial role in the maintenance of plant redox homeostasis [37]. AOX catalyses the oxidation of ubiquinol and reduction of oxygen to water, effectively acting as the unique respiratory terminal oxidase whereby electron flow bypasses complex III and IV. Once the electron transport in the cytochrome c pathway is blocked, AOX helps to maintain the electron flux and to reduce mtROS levels [126]. In the AOX family, AOX1a is an important member and often dramatically induced at the transcript level by a variety of oxidative stresses [127]. Based on the previously demonstrated role of AOX1a in stress responses mRNA levels were measured by RT-qPCR and protein content by SDS-PAGE followed by immunodetection with antibodies against AOX1a. Surprisingly, it was observed a decreased amount both in transcript and protein content of AOX1a in OXR2 plants (Fig. 23). Thus, apparently AOX1a is not acting as a retrograde signal to activated stress response in OXR2 plants or a primed state.

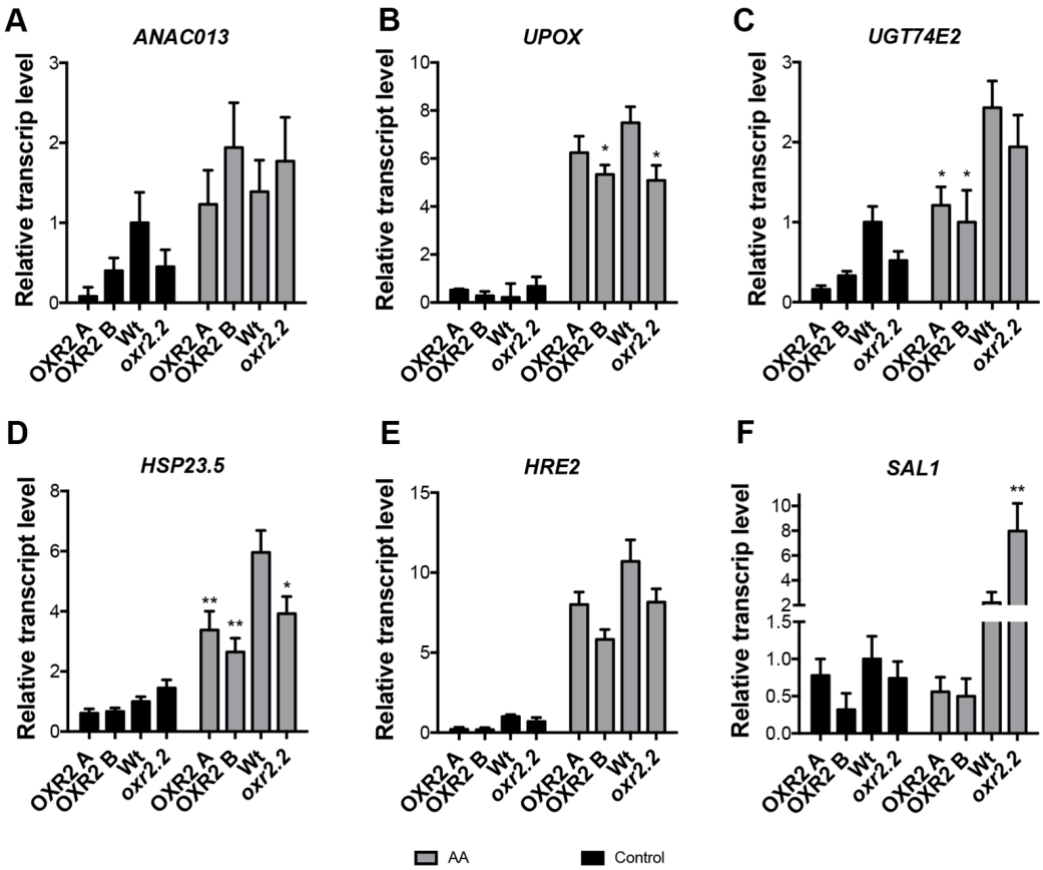

Figure 22: Retrograde signalling response genes fail to induce in OXR2 plants. Wt, OXR2 and *oxr2.2* two-week-old seedlings grown on MS medium were transferred to MS medium supplemented with 50 µM AA and harvested in biological triplicate 6 h after treatment. Relative transcript levels of several genes involve in response to MRR were measured by RT-qPCR. Transcript levels are referred to those of Wt plants in control condition. Asterisks indicate significant differences at P<0.05 (ANOVA, LSD Fisher test).

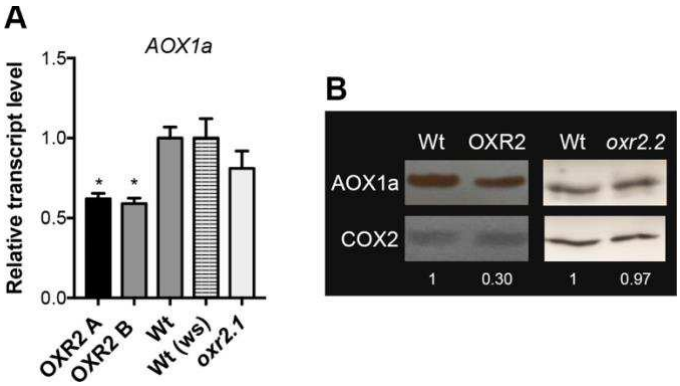

Figure 23: OXR2 plants show lower levels of AtAOX1a in basal conditions. (A) *AtAOX1a* transcript levels measured by RT-qPCR in two-week-old plants from each genotype, transcript levels are referred to those of Wt plants in the same ecotype. Asterisks indicate significant differences at P<0.05 (ANOVA, LSD Fisher test). (B) Protein quantification by Western blot, mitochondria enriched extracts from fully expanded 20-day-old rosette leaves of Wt and OXR2 plants were loaded in a 12% SDS-PAGE and transferred to a PVDF membrane. Blots were analysed with antibodies against AOX1a and COX2 (loading control).

Discussion

In this part, it is showed evidence of a putative role of a single member of the eukaryotic OXR (Oxidation Resistance) protein family in plants. This family was first identified by Volker et al. (2000, [1]) during a screening to identify human genes protective against oxidative stress. These were later studied in several eukaryotic organisms [2,9,13,15,110]. Using the sequences of OXR1 proteins from yeast and humans [128], four family members were identified in Arabidopsis sharing the canonical ~180 amino acid TLDc domain characteristic of OXR proteins [10]. Also two other members were identified: AtOXR4, that is a shorter protein with a truncated version of the TLDc domain, and AtOXR6 that seems to be recent duplication generated from the AtOXR3 family member (Fig. 9A). *AtOXR4* and *AtOXR6* genes are both expressed according to the data present in the transcriptome databases (http://travadb.org/). Whether AtOXR4 and AtOXR6 represent functional OXR proteins remains to be determined. In angiosperms, the OXR protein family is represented by five different clades (Fig. 9B). Duplication in embryophytes, probably from OXR4, resulted in the OXR5 proteins. Later, a duplication that presumably occurred before the appearance of seed plants produced OXR1 and OXR2, which are more similar to yeast and human OXR1 than members from other clades (Fig. 9B).

AtOXR2 was localised in mitochondria (Fig. 10). Oxr1 from yeast and human are also found in mitochondria, and this location is essential for protection against the oxidative stress induced by H_2O_2 or heat treatments [2,13]. Corroborating this observation, some types of human ALS (Amyotrophic Lateral Sclerosis) originated by respiratory dysfunctions and defects in mitochondrial morphology are alleviated by Oxr1 overexpression [13,128]. In agreement, deletion of an Oxr1 isoform present in the mitochondrial outer membrane (OMM) in mice causes neurodegeneration by de-regulation of phospho-Drp1(Ser616), a key mitochondrial fission regulatory factor [15]. Similarly to Oxr1 and Ncoa [7,29], expression of AtOXR2 targeted to mitochondria alleviates the stress sensitivity of a yeast *oxr1* mutant [172]. Our previous observations highlight the conserved function of eukaryotic OXR proteins in the protection against oxidative stress. Previous results proposed a role for the *Ipomoea batatas IbTLD* protein in the induction of antioxidant enzymes during wounding stress [23].

The absence of a canonical cleavable sorting sequence and the predicted structure of ß-barrel domains with α-helices in the N-terminal portion of AtOXR2 [121] suggests a possible localisation at the OMM [129]. OMM localisation was demonstrated for AtVDAC1, AtOM66 and AtPEN2 [130–132] three Arabidopsis mitochondrial proteins involved in oxidative stress responses. Further studies using mitochondrial fractionation or fluorescence microscopy techniques [38] will be required to establish the sub-mitochondrial location of AtOXR2. In

addition, the presence of AtOXR2 in peroxisomes cannot be excluded, considering that several mitochondrial proteins are also targeted to these organelles [133].

AtOXR2 overexpression generates plants with a more significant number of leaves and increased leaf area (Fig. 12 and 13). OXR2 plants have thicker stems, which could indicate a more efficient transport of photoassimilates from source tissues. All these characteristics translate into increased biomass and seed production (Fig. 13). Therefore, several reports are suggesting that higher expression of functionally different mitochondrial proteins has a positive impact on the generation of plant biomass [134,135]. Conversely, loss-of-function mutation of AtOXR2 did not produce significant changes in plant biomass or architecture under normal growth conditions. This may reflect the existence of functional redundancy with other mitochondrial family members.

Furthermore, altering levels of AtOXR2 in plants does not impact on carbohydrates or chlorophyll content (Fig. 17 and 18). In a recent study we show that OXR2 plants showed increased photosynthetic parameters [121], but this is not transduced in increased accumulation of products derived from the photosynthesis nor is traduced into different chlorophyll content [75]. However, increased biomass in OXR2 plants shows the higher capacity of these plants to convert the energy contained in the light into biomass and seed production through more efficient photosynthetic fixation of CO_2.

In addition, mitochondrial respiration was determined by monitoring O_2 consumption and mitochondrial membrane potential using TMRM dye. Notably, OXR2 plants show enhanced O_2 consumption but decreased the membrane potential (Fig. 19). This higher respiration rate is due to an increase in cyanide-sensitive respiration, and not in AOX related respiration, this could mean that plants have a more active carbon metabolism and could produce more energy. In addition, lowering the membrane potential is a common strategy to avoid overproduction of ROS and in consequence the oxidative damage. As an example, mitochondria contain multiple uncoupling proteins (UPCs) which dissipate the membrane electrochemical proton gradient alleviating ROS production [32,136,137]. Thus, it remains unclear how this balance in OXR2 plants is achieved. Further analysis should be carried out to determinate other parameters of mitochondrial respiration such as ATP production and TCA cycle products to have a better understanding.

AtOXR2 is induced by oxidative stress (Fig. 20) and OXR2 plants show tolerance to oxidising conditions imposed by MV or AA (Fig. 21). An interesting question remains how AtOXR2 fulfils its function and alleviates oxidative stress. ROS can transduce signals as mobile messengers by yet unknown mechanisms [138–141]. H_2O_2 can originate “priming effects” by improving plant performance and promoting cellular proliferation and differentiation [142]. ROS are part of the retrograde signalling mechanisms from mitochondria or chloroplasts that activate

the expression of nuclear-encoded stress-responsive genes and coordinate the action of phytohormones [143]. They can also modify the structure and function of target proteins via oxidising their Cys residues [138]. These redox-derived changes in protein function can affect transcription, phosphorylation and other important signalling events [28]. In this sense, Svistunova et al. (2019 [144]) demonstrated that TLDc-containing proteins could modulate protein S-nitrosylation to protect neurons against oxidative stress.

When MRR genes were investigated upon mitochondrial disfunction caused by AA treatment, OXR2 plants reacted to a lesser degree than Wt plants. Mitochondria in OXR2 plants appeared to be less sensible to AA and unable to trigger transcript amplification response in the same degree as Wt plants (Fig. 22). Particularly MRR genes like *UGT74E2* which is considered the linker between mitochondria perturbation responses and the plant growth aspects regulated by auxin [41], behave in the same sense as the lower growth-inhibition upon mitochondrial dysfunction observed in OXR2 plants (e.i. is less induced in OXR2 plants). *UGT674E2* encodes a UDP-glucosyltransferase which preferentially glycosylates indole-3-butyric acid (IBA) thus regulating auxin homeostasis and plant growth [41,145]. This is in agreement with the phenotypic parameters observed, as there is less growth-inhibition upon mitochondrial dysfunction observed in OXR2 plants in comparison to Wt and *oxr2.2* mutant plants.

Another interesting result found in our analysis are the responses of the *SAL1* gene in the background of plants lacking AtOXR2. The *oxr2.2* mutant plants showed marked increased induction of this gene in comparison to Wt, while the opposite result was observed in OXR2 plants. The SAL1 protein is involved in the chloroplastic retrograde response. By the degradation of the PAP metabolite, SAL1 is able to inhibit nuclear activation of genes mostly involved in oxidative stress responses. *SAL1* loss-of-function mutants showed increased resistance to different types of stress response [44,146]. A higher expression of this gene in *oxr2.2* would suggest the inability of these mutant plants to trigger oxidative stress responses. SAL1 is present both in chloroplast and mitochondria but its role in the latter is not yet clear.

Regarding AOX1a, its respective gene appears to be down-regulated in OXR2 plants grown under control conditions (Fig. 23), *AOX1a* expression is induced upon stress conditions, after mitochondrial perturbations, and is also seen to play a role in pathogen responses [34,36,147]. Lower levels of AOX1a could also indicate that OXR2 plants are overall less sensitive towards oxidative stress [148].

Another aspect to elucidate in the future is from where and for what reason or mechanism OXR2 plants produce higher levels of ROS [139]. The lower mitochondrial membrane potential in OXR2 plants could suggest that ROS are not coming from this organelle. Defining

the ROS source would be necessary and could help us to discuss and define the role of AtOXR2 in oxidative stress plant responses.

Anyway, the increased ROS levels observed in OXR2 plants do not seem to be detrimental for plant growth but may be useful to prime plant acclimation responses [28]. It is tempting to speculate that ROS or modifications in the cellular redox state produced by altering the levels of AtOXR2 induce adaptive cellular responses through changes in gene expression and the activity of hormonal pathways. This question will need further studies to be answered.

Part II

4.3 AtOXR2 and biotic stress

4.3.1 AtOXR2 impacts on the accumulation of SA

Since it was show differential responses to abiotic stress in plants expressing different levels of *AtOXR2* (section 4.2), we were interested in studying the plant responses to biotic stress as well. Following previous array data [121] we focus on the study of the SA signalling pathway (see Fig. 6). First, the expression of marker genes of this pathway were measured, related to SA synthesis (*SID2*), accumulation (*EDS1*) and response (*PR1*). All these genes appear to be upregulated in the OXR2 plants and downregulated in *oxr2.2* in relation to Wt plants grown in normal LD conditions (Fig.24A and B). Then SA content was determined in adult rosette tissue grown under LD conditions by GC-MS and it was confirmed that OXR2 accumulate SA in control conditions and on the contrary *oxr2.2* plants appear to have a slightly lower content of the hormone (Fig. 24C).

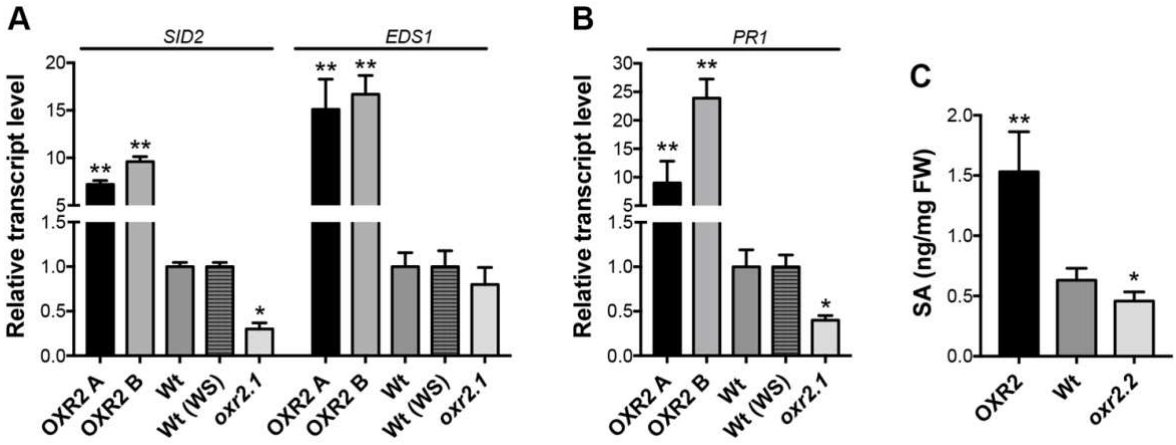

Figure 24: AtOXR2 modifies basal SA levels and several genes related to hormone synthesis and response. (A) Transcript levels of *SID2* and *EDS1*, both involved in hormone synthesis and accumulation. (B) Transcript levels of *PR1* as a SA-response gene. Transcript levels were measured by RT-qPCR in two-week-old plants from each genotype, transcript levels are referred to those of Wt plants of the same ecotype. (C) Gas chromatography-mass spectrometry (GC-MS) measurement of SA in rosette leaves from two-week-old plants for Wt, OXR2 and *oxr2.2* plants. Asterisks indicate significant differences at $P<0.05$ (ANOVA, LSD Fisher test).

Together with the SA accumulation OXR2 plants also showed basal translocation of NPR1 into the nucleus (Fig. 25). Using mutant plants that express different levels of *AtOXR2* and a version of the SA receptor NPR1 fused to GFP the localisation of NPR1 was monitored in different *AtOXR2* backgrounds. Upon pathogen recognition cellular redox changes and SA accumulation leads to the monomer formation of NPR1 in the cytosol and in consequence to its translocation to the nucleus, where it is able to activate defence responses [149] (Fig.6, Introduction). Thus, OXR2 plants showed basal activation of NPR1 by its transport into the

nucleus in comparison to the other analysed plants (Wt or *oxr*2.2 mutants). Treatment with SA for 24 h leads to total translocation of NPR1 into the nucleus in all plants under analysis (Fig. 25).

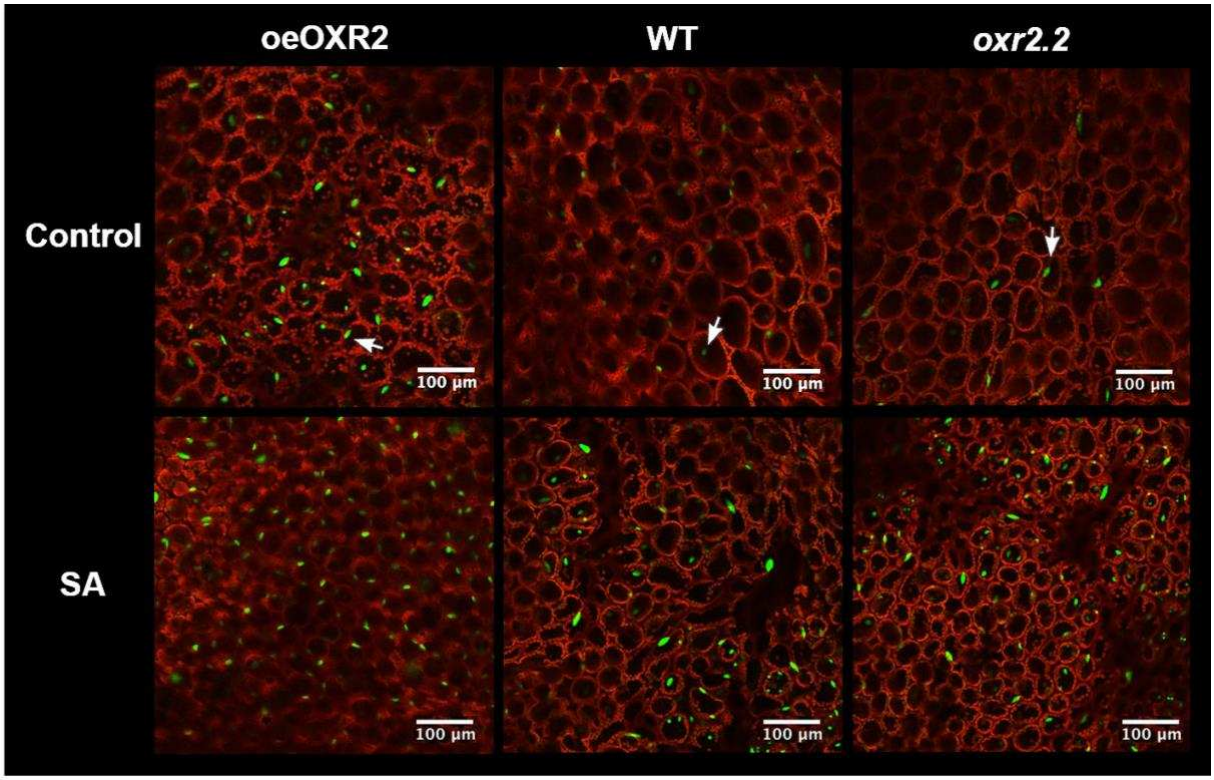

Figure 25: OXR2 shows NPR1 nuclear accumulation when grown in control conditions. OXR2, Wt and oxr2.2 leaves expressing NPR1-GFP were imaged by CLSM. NPR1-GFP signal in green appears into nucleus (marked with arrows) and chlorophyll fluorescence of chloroplast appears in red. OXR2 showed stronger and more GFP signal than Wt or *oxr*2.2 plants. After treatment with 0.5 mM SA all NPR1-GFP signals appears equally in the nucleus of all genotypes.

4.3.2 AtOXR2 alters tolerance to two different pathogens infection

Pseudomonas syringe pv. Tomato Pst DC3000

Continuing with the study of the biotic stress responses, OXR2, *oxr*2.2 and Wt plants were challenged with Pst DC3000. In agreement with the basal levels of SA measured in each genotype (Fig. 22C), OXR2 plants displayed an increased resistance to the pathogen infection, while *oxr*2.2 mutants were more sensitive in comparison to Wt plants (Fig. 26). It was further characterised the infection responses at the molecular level by evaluating transcripts levels of genes related to SA response during the course of infection. As it was expected, an increased induction of these genes before the infection and an even further increased response after the pathogen inoculation was confirmed (Fig. 27). Thus, OXR2 plants appear

to be best prepared for pathogen attack and are able to respond faster by increasing the overall plant resistance.

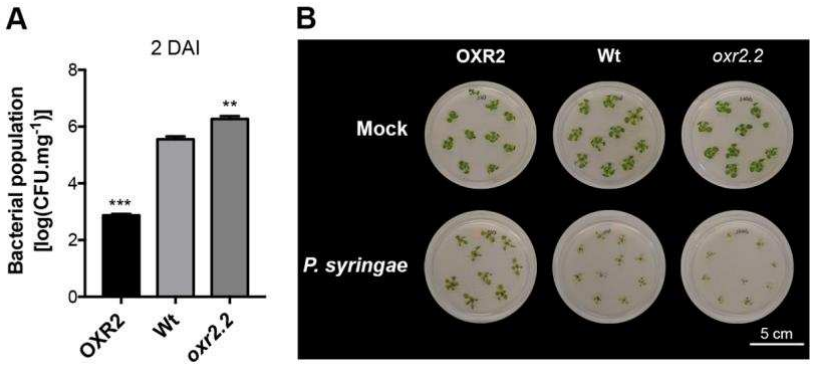

Figure 26: AtOXR2 alters tolerance to Pst DC3000. (A) Bacterial populations of Pst DC300 were quantified at 2 DAI. (B) Disease phenotype of Arabidopsis seedlings flood-inoculated with Pst DC 3000 at a concentration of 5 × 10_8 CFU.ml_{-1}. Mock-inoculated plants were flooded with sterile distilled H_2O containing 0.025% (v/v) Silwet L-77. Photographs were taken 2 DAI. Values represent the mean±SEM from 3 biological replicates. Asterisks indicate significant differences at P<0.05 (ANOVA, LSD Fisher test).

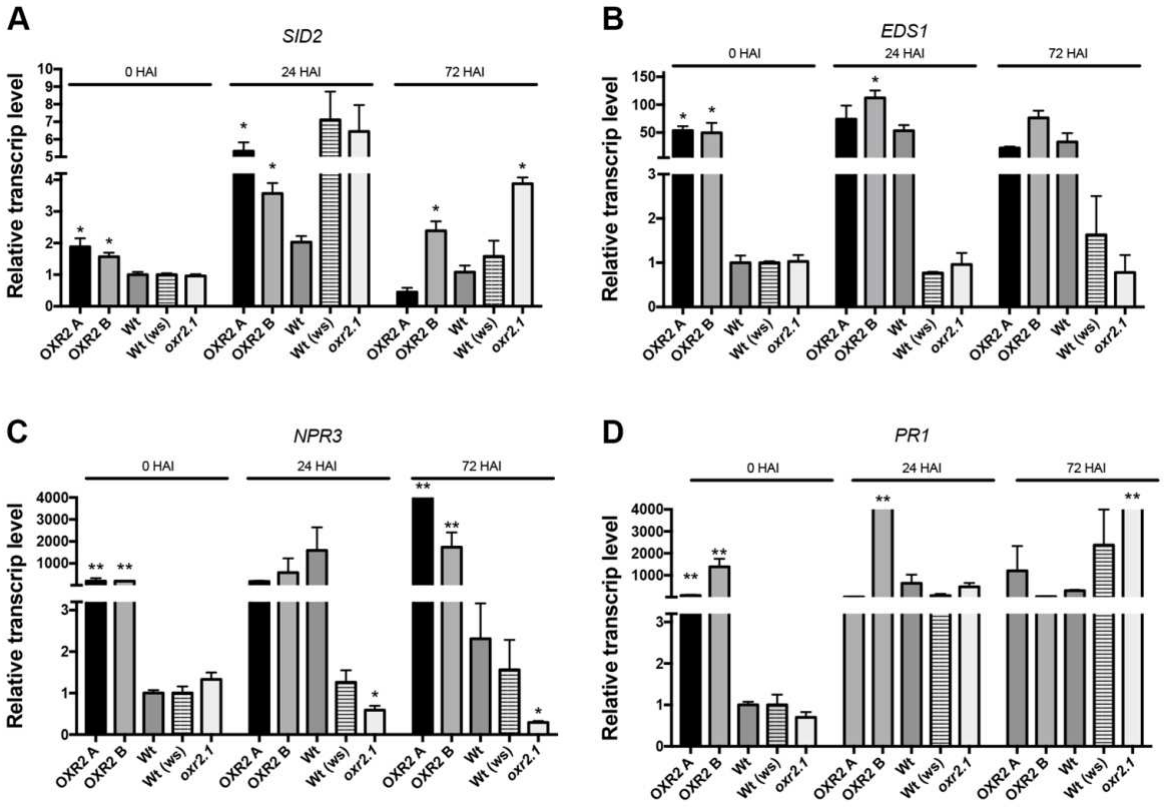

Figure 27: AtOXR2 different tolerance towards Pst DC3000 is partially due to a priming effect. Transcript levels of *SID2* (A) and *EDS1* (B), both involve in hormone synthesis and accumulation. (C)

Transcript levels of *NPR3* and (D) PR1 SA-response genes. Transcript levels were measured by RT-qPCR after different infection times, transcript levels are referred to those of Wt plants of the same ecotype at 0 HAI. Asterisks indicate significant differences at P<0.05 (ANOVA, LSD Fisher test) compared with Wt plants of the same ecotype at the same infection time.

Plasmodiophora brassicae

In addition, the plants expressing different levels of *AtOXR2* were subjected to *Plasmodiophora brassicae*, a pathogen that also activates plant SA responses upon infection. Indeed, OXR2 plants also appear to be resilient to clubroot disease. Some disease parameters were calculated and shown in Fig. 28, according to Siemens et. al. (2002, [90]). Acording to these parameters for disease classification, an increased resistance of the OXR2 and the higher sensitivity of the *oxr2.2* mutants towards the *Plasmodiophora* infection was established, in comparison to Wt plants.

This enhanced resistance to *Plasmodiophora* has a particular biotechnological interest since it is the causal agent of a disease that produces significant economic losses in agriculture [150].

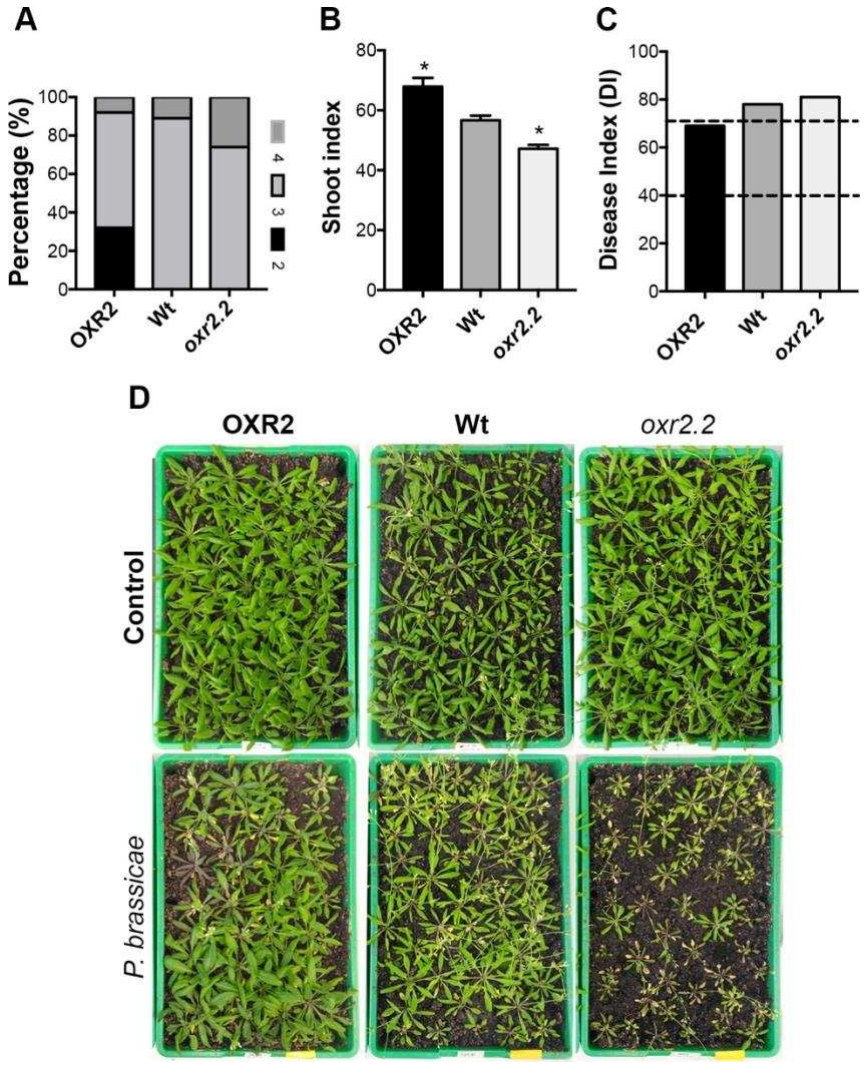

Figure 28: AtOXR2 confers tolerance to *P. brassica* infection. Parameters to evaluate the grade of disease severity in Wt, OXR2 and *oxr2.2* plants. (A) Number of plants in individual disease classes. (B) Shoot Index (shoot index is dry weight of infected plants divided by dry weight of control plants), (C) Disease Index. (D) Plants 27 DAI with *P. brassicae* resting spores. Values represent means±SEM from 20-40 plants. Asterisks indicate significant differences $P \leq 0.05$ (*) and $P \leq 0.01$ (**).

4.3.3 AtOXR2 associated pathogen resistance is dependent on SID2 and NPR1

To elucidate the putative mechanism by which AtOXR2 might be modulating plant-pathogen responses *AtOXR2* was overexpressed in the genetic background of two SA-deficient response mutants. These mutants were: *SALICYLIC ACID INDUCTION DEFICIENT2* (*sid2*/*ics1*) and *NONEXPRESSOR OF PATHOGENESIS-RELATED PROTEINS1* (*npr1*).

When subjecting *sid2*+OXR2 and *npr1*+OXR2 to Pst DC3000 infection, it was observed that the previously demonstrated enhanced resistance conferred by the overexpression of *AtOXR2* in Wt plants was lost in both mutant backgrounds (Fig. 29A). The molecular characterisation of two pathogen response marker genes, *PR1* and *PR5*, also showed a decrease in transcription and are in agreement with the observed phenotype (Fig. 29B and C). In agreement with these results, it was assumed that AtOXR2 could act upstream of SID2 and NPR1 in order to confer SA-dependent defence to the bacterial pathogen Pst DC3000.

Overexpression of AtOXR2 in the *sid2*, but not in the *npr1* mutant, resulted in plants with an increased number of leaves and rosette area (Fig. 29D and E). Furthermore, overexpression of AtOXR2 also reduces the basal content of ROS quantified by NBT dye in *sid2* mutant plants (Fig. 29F). Although OXR2 displays increased basal ROS content (section 4.2.1), it can diminish the ROS content in the *sid2* background.

AtOXR2 expression is induced by treatment with Pst DC3000 and SA (Fig. 30A and B). This data led us to postulate that AtOXR2 could regulate SA accumulation in a positive feedback loop.

Moreover, under control conditions, OXR2 plants appear to have upregulated several *WRKY* genes encoding a specific group of transcription factors (Fig. 30D) associated with the modulation of biotic stress and SA responses [55,151,152].

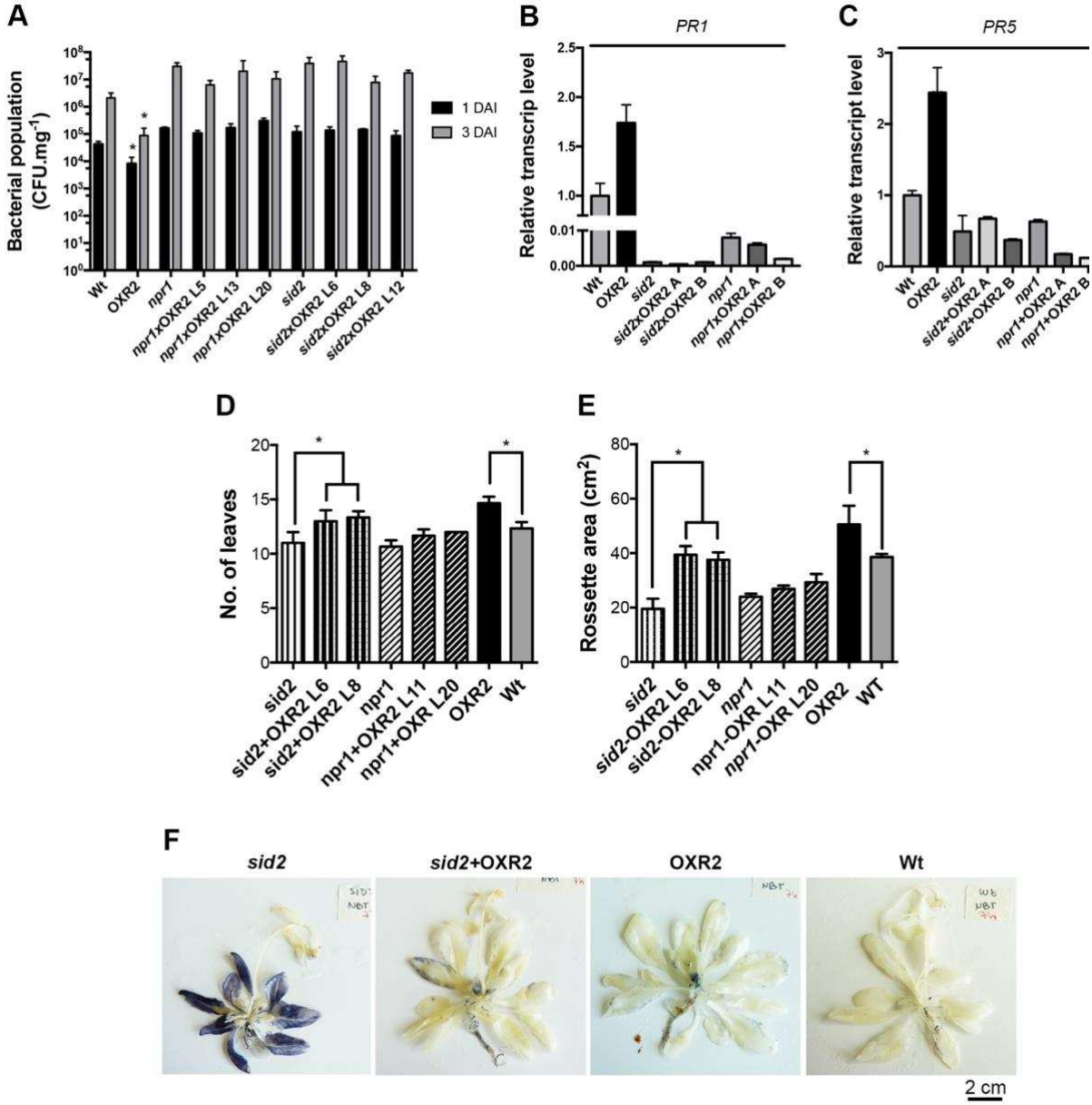

Figure 29: AtOXR2 acts upstream of SID2 and NPR1 in order to confer SA basal defence. (A) The enhanced resistance to Pst DC3000 due to AtOXR2 overexpression is lost in the background of both mutants. (B) and (C) marker genes for pathogen response. AtOXR2 overexpression in *sid2* knockout background (*sid2*+OXR2) show increased number of leaves (D) and rosette area (E). (F) *sid2*+OXR2 plants show lower ROS levels measured by NBT dying similar to OXR2 plants. Asterisks indicate significant differences at $P<0.05$ (ANOVA, LSD Fisher test).

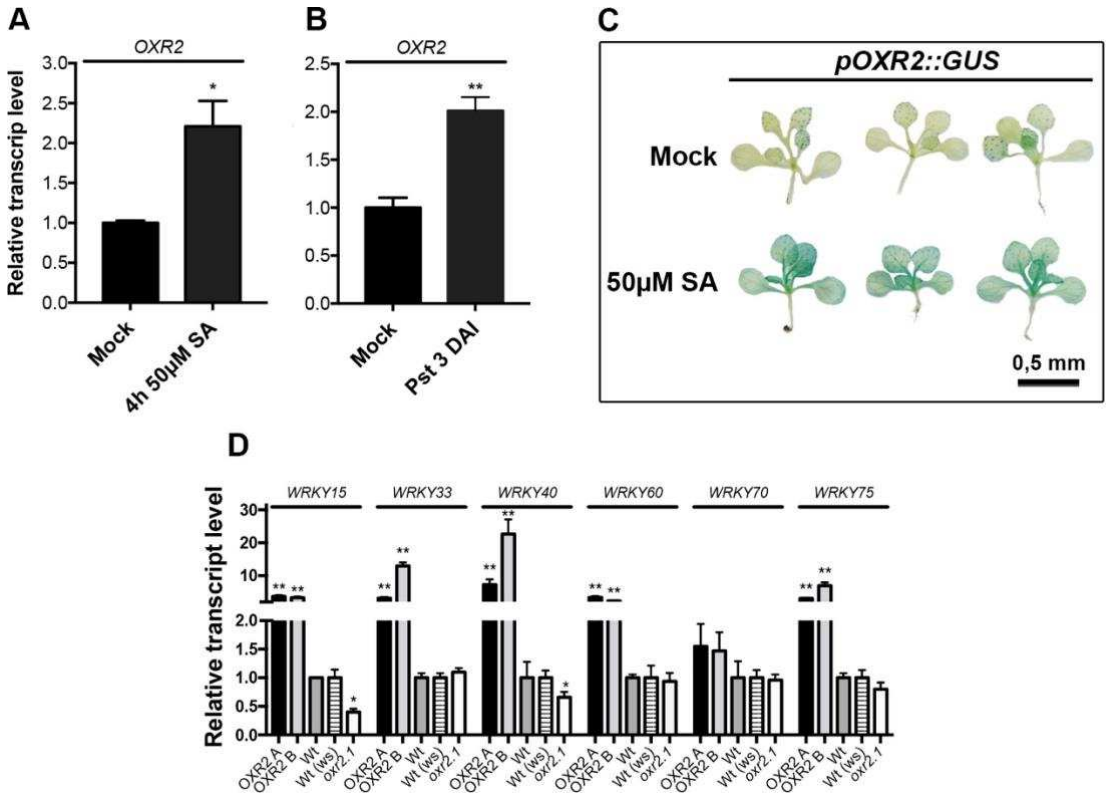

Figure 30: *AtOXR2* is induce both by SA (A) treatment and Pst DC3000 infection (B). AtOXR2 transcript levels were measured in Arabidopsis Wt seedlings grown for 14 DAS in MS medium and then sprayed with a solution containing MS (MS, control) or the same medium supplemented with 50 µM SA and sample were taken after 6 h, pathogen infection was carried out as described before. Treatment with 50 µM SA for 1h leads to induction of *AtOXR2* promoter activity measured by GUS activity (C). AtOXR2 modifies the expression of several *WRKY* genes related to stress response (D). Transcript levels were measured by RT-qPCR in two-week-old plants from each genotype, transcript levels are referred to those of Wt plants of the same ecotype. Results are expressed as mean±SEM of three independent experiments. Asterisks represent significantly different values at $P<0.05$ (ANOVA; Tukey test).

Discussion

In the second part of this thesis its described the possible connection between AtOXR2 and biotic stress responses. In other organisms, many proteins containing a TLDc domain have been implicated in conferring disease resistance. For example, a gain-of-function mutant with an insertion in the same locus renamed *mtd*, showed increased tolerance to oral *Vibrio cholerae* infection mediated by the innate immune response [158]. Consistent with this finding in Drosophila, knockdown of the *A. gambiae* OXR1 homologue produced a significant decrease in the *Plasmodium berghei* proliferation in the mosquitoes [159]. Furthermore, mouse strains expressing higher levels of OXR1 are significantly more resistant to kidney inflammation than strains with lower levels [160]. Based on these pieces of evidences and some preceding transcriptomic data previously obtained by our group [121], we started to study biotic interactions through the SA-related hormonal response pathway. It was quantified the SA content in plants grown under control conditions (i.e. without pathogen challenge) and established that OXR2 plants accumulate SA (Fig. 24). On the opposite, *oxr2.2* plants showed lower levels of the hormone (Fig. 24). In agreement, OXR2 plants upregulated the expression of genes encoding proteins related to SA synthesis and SA-response in control conditions (Fig. 24) and a basal translocation of NPR1 to the nucleus which indicates its activation (Fig. 25). In this context, OXR2 plants appear to be in a priming state [52] and therefore better prepared for future pathogen attack. Constitutive primed plants like *edr1* mutants respond faster to pathogen attack resulting in increased pathogen resistance and also show less growth inhibition caused by pathogen attack and less yield reduction compared to plants that have to generated defence only after being challenged with a pathogen [161].

Then plants were infected with two different plant pathogens that are known to generate a SA based response, *Pseudomonas syringae* and *Plasmodiophora brassicae*. As was expected, OXR2 plants were more tolerant to the pathogens while *oxr2.2* showed increased susceptibility in comparison to Wt plants (Fig. 26 and 28). The molecular characterization during the infection with Pst DC3000 showed basal activation of response genes in OXR2 (0 HAI) that were in some cases achieved in Wt plants during later times after inoculation (24 and 72 HAI). This is the case for *NPR3* and *EDS1* expression. On the contrary, higher expression levels of *SID2* were maintained through all the infection times in OXR2 (Fig. 27). Unfortunately, this molecular analysis fails to explain the increased sensitivity in *oxr2* plants since no particularly relevant difference in defence gene expression was detected during the course of infection. Importantly, for the transcript analysis *oxr2.1* mutants were used and the *oxr2.2* were the plants that showed the most dramatic sensitivity response. Therefore, we might be missing data due to the comparison between two ecotypes Wassilewskija in

oxr2.1 and Columbia in *oxr2.2*, which must be further investigated. It is known that these ecotypes can show different behaviour when facing pathogen attack [174,175].

Also plants overexpressing AtOXR2 and lacking two central proteins in the SA synthesis and signalling pathway were obtained, ICS1 (*sid2* mutant) and NPR1 (*npr1* mutant). When these plants were inoculated with Pst DC3000, the increased pathogen resistance due to the AtOXR2 overexpression was abolished in both genotypes tested (Fig. 29). These results support the idea that the accumulation of SA in OXR2 is due to the action of SID2 *(*ICS1*)*, as was indicated by transcript analysis. It also allows us to conclude that the presence of both proteins are necessary for the OXR2-pathogen resistance and that SA mediates this response (Fig. 31).

Although *sid2*+OXR2 plants did not show enhanced resistance to Pst DC3000 they showed an increased number of leaves and rosette area, similar to OXR2 plants (Fig. 29). Thus, higher biomass in *sid2*+OXR2 due to AtOXR2 overexpression was not affected by the plant's ability to synthesise SA. Also, AtOXR2 overexpression appears to alleviate ROS ($O_2^{\cdot-}$) accumulation in *sid2* [162]. Even though both *sid2*+OXR2 and OXR2 plants present increased accumulation of ROS in comparison to Wt, evidently this do not result in grown-inhibition (Fig. 29). It will be interesting in further studies to test the response of *sid2*+OXR2 plants to abiotic stress to see if this characteristic of OXR2 still remains after the loss-of-function in *ICS1.* SA appears to be implicated in abiotic stress responses, since plants deficient in SA are more sensitive and fail to acclimate to abiotic stress conditions like high light treatment [163].

AtOXR2 its induced by treatment with SA and Pst DC3000 (Fig. 30). Taking all results together, it appears to be a regulation loop in which AtOXR2 induces the accumulation of SA, which further induces expression of *NPR1* and *SID2* [164] and also *AtOXR2* generating a feedback signal (Fig. 31).

An open question is how mitochondrial AtOXR2 is able to trigger all these signals? In previous sections, it was demonstrated that OXR2 plants present increased mitochondrial respiration and ROS levels (Section 4.1 and 4.2). It would be possible that a redox imbalance caused by AtOXR2 could be generating a cellular environment that triggers the priming effect [52]. In accordance, there are several examples of proteins that are activated by redox changes during SA-responses, like NPR1 [56] and many WRKY TFs [47,151].

Several genes encoding WRKY TFs like *WRKY15*, *WRKY33*, *WRKY40*, *WRKY60* and *WRKY75*, which are key regulators in biotic and abiotic responses [47], were upregulated in OXR2 plants and some like *WRKY15* and *WRKY40* repressed in *oxr2.1* plants. These TFs could be the critical connection between AtOXR2 from mitochondria with the SA signalling pathway and stress responses. Further analysis using WRKY loss-of-function mutants will be required to confirm the interplay between AtOXR2 and WRKYs.

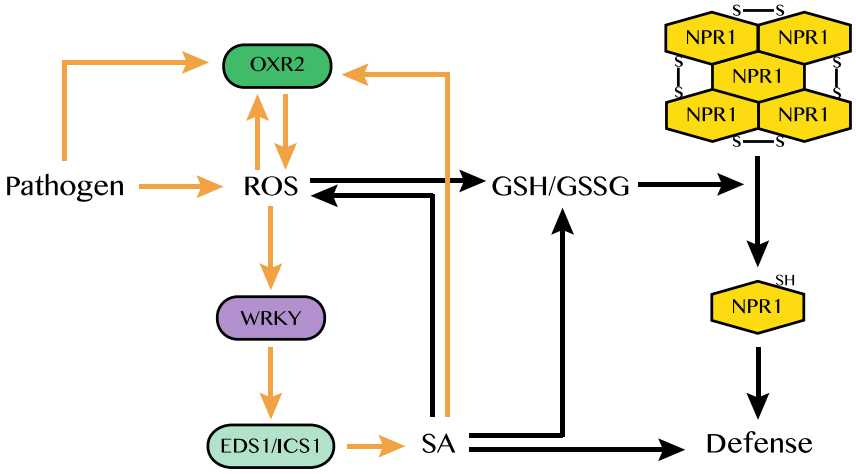

Figure 31: A model of the role of AtOXR2 in plant defense. AtOXR2 is part of a loop for the activation of the SA-mediated plant defense pathway. By increasing ROS levels, AtOXR2 increases the expression of WRKY TFs that induce SA synthesis. In turn, SA, pathogens and oxidative stress (ROS) stimulate the expression of AtOXR2. Altered AtOXR2 expression modifies the intracellular environment and inducing the translocation of NPR1 to the nucleus, thus preparing plants against a potential pathogen attack.

Part III

4.4 AtOXR2 and the crosstalk between growth and pathogen response

4.4.1 AtOXR2 impacts on the accumulation of the phytohormone CKs

Previously it was described the effect of AtOXR2 overexpression on plant architecture (section 4.1) and on promoting resistance to the infection with the pathogen Pst DC3000 and *Plasmodiophora brassicae* (section 4.3). Mainly, the increased pathogen resistance phenotype of OXR2 plants could be due to the higher SA basal content and the increased SA-dependent responses (section 4.3).

To further investigate both characteristics, the larger size and the increased pathogen-resistance, we turned to the analysis of the hormonal pathway represented by the Cytokinins (CKs). CKs are adenine-derived phytohormones involved in various aspects of plant development including cell division, lateral root formation and meristem maintenance [65–67]. Also, CKs mediate plant resistance against many types of pathogens. Several lines of evidence support a role for CKs in plant-pathogen interactions mainly through the regulation of SA-responses [69–72].

Therefore, the content of one of the major forms of CK, tZ and its inactive precursor tZR were determined by HPLC in plants with altered expression of *AtOXR2* (Fig. 32A). Furthermore the TCS::GFP fluorescent sensor was tested, that is a marker for CKs (Fig. 32B) [153]. An increase of CKs in OXR2 plants and lower levels of this hormone in *oxr2.2* plants was observed, in comparison to Wt. The major difference is given by tZR in the overexpressor lines (Fig. 32A).

Molecular analysis of plants reveals that the CKs accumulation in OXR2 plants could be due to the upregulation of synthesis-related genes (*IPT, isopentenyl transferase*; *IPT3*, *IPT5*), of which two are upregulated, namely *IPT3* and *IPT5*. Catabolism genes were not altered in transcript levels. The lower CKs levels present in *oxr2.2* could be explained by downregulation of some of these synthesis-related genes and also upregulation of some genes encoding CKs-catabolic enzymes (*CKX*, Cytokinin oxidase/dehydrogenase; *CKX1-4*), of which two were upregulated (*CKX2*, *CKX4*) (Fig. 33A and B).

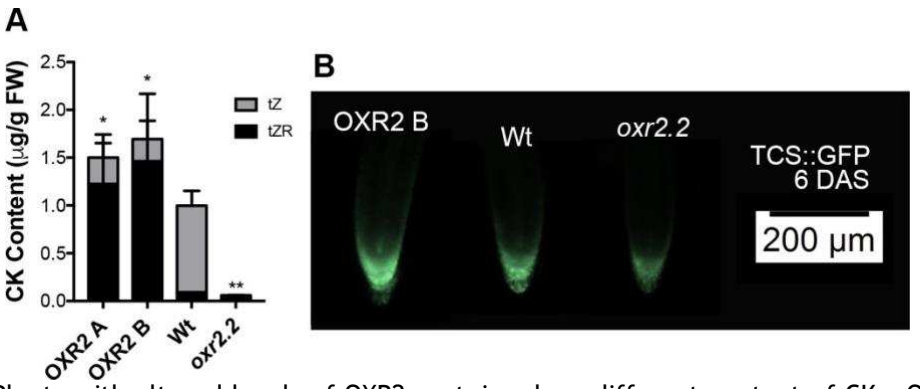

Figure 32: Plants with altered levels of OXR2 proteins show different content of CKs. OXR2 behave opposite to the *oxr2.2* plants. (A) CKs determination by HPLC. (B) Fluorescent signal of the TCS::GFP synthetic sensor [153].

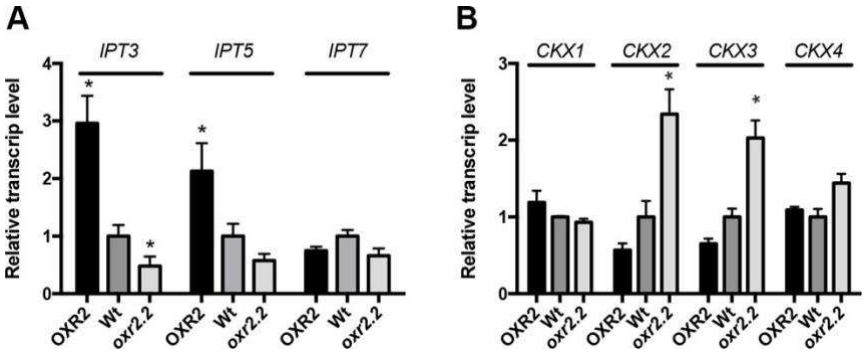

Figure 33: AtOXR2 modifies expression of several genes related to hormone synthesis and metabolism. (A) Transcript levels of *IPT* genes involved in hormone synthesis. (B) Transcript levels of *CKX* genes involved in hormone catalysis. Transcript levels were measured by RT-qPCR in two-week-old plants from each genotype, transcript levels are referred to those of Wt plants. Asterisks indicate significant differences at $P<0.05$ (ANOVA, LSD Fisher test).

Also the transcript levels for several CKs-response genes from the ARR family were analysed. Only the positive regulator encoding *ARR1* transcript levels were induced in OXR2 plants and repressed in *oxr2.2* mutants compared with Wt (Fig. 34A). No significant difference was observed in other CKs-response factors by RT-qPCR. Conversely, the expression of the *GUS* reporter gene driven by the promoter region of two negative response factors, ARR5 and ARR15, expressed in the OXR2 background, resulted in a reduction of GUS activity in comparison to Wt plants (Fig. 34C).

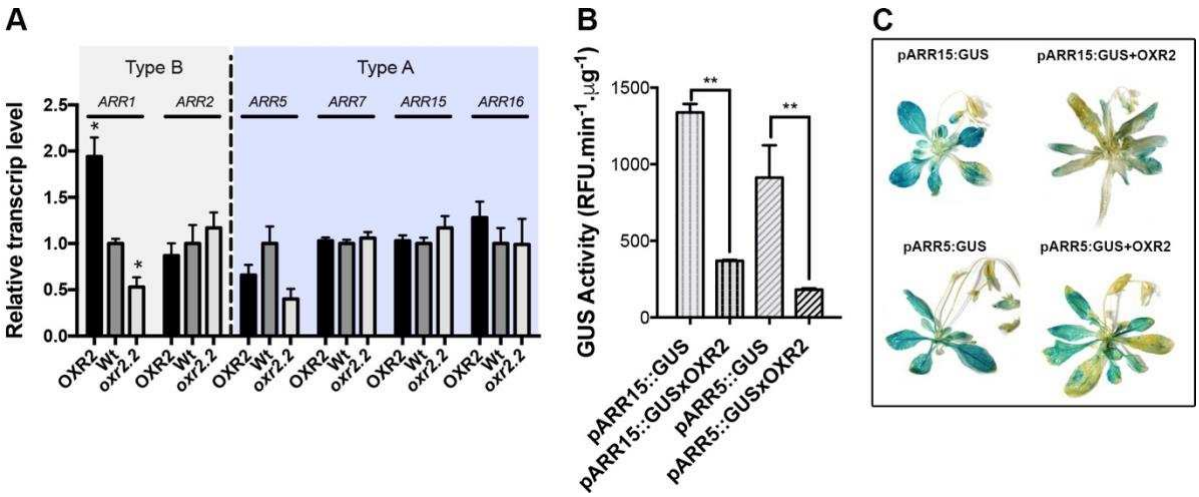

Figure 34: Study of the responsive CKs factor ARRs reveal different expression of the type B factor ARR1 and the type A factors ARR5 and ARR15. (A) Transcript levels of different ARR factors. (B) Fluorescence GUS activity of the promoters of ARR5 and ARR15 in Wt and OXR2 plants. (C) Histochemical analysis of GUS activity of the promoters of ARR5 and ARR15 in Wt and OXR2 plants. Transcript levels were measured by RT-qPCR in two-week-old plants from each genotype, transcript levels are referred to those of Wt plants. Asterisks indicate significant differences at $P<0.05$ (ANOVA, LSD Fisher test).

4.4.2 Accumulation of CKs by AtOXR2 is due to CKX activity modulation and dependent on the presence of *IPT* and *AHP* genes

Additionally, plants expressing higher levels of AtOXR2 in different backgrounds were obtained, corresponding to loss-of-function in *IPT* genes (*ipt1357*, [154]) involved in the synthesis pathway and in *AHP* genes (*ahp1234*, [155]) involved in transfer of the signal to the nucleus (Fig. 8, Introduction). Also AtOXR2 was overexpressed in *CKXs* overexpressors plants (CKX1 and CKX2 [156]). All the plants tested have alterations in the CKs homeostasis or signalling, resulting in an overall lack of hormone response and showing larger roots as a typical phenotype.

Higher levels of AtOXR2 in *ipt1357* (*ipt1357*+OXR2) and *ahp1234* (*ahp1234*xOXR2) backgrounds failed in to revert the original phenotype exhibited by the mutants (Fig. 35).

On the contrary, when AtOXR2 was overexpressed together with higher levels of CKX1 (CKX1xOXR2) and CKX2 catabolic enzymes (CKX2xOXR2), the plants showed a partial reversion of their root phenotype (Fig. 36). Also, the increased sensitivity of CKX1 towards Pst DC3000 was partially reverted by AtOXR2 overexpression (Fig. 37). Thus, the accumulation of CKs in OXR2 could be partially explained by an inhibition of CKX activity.

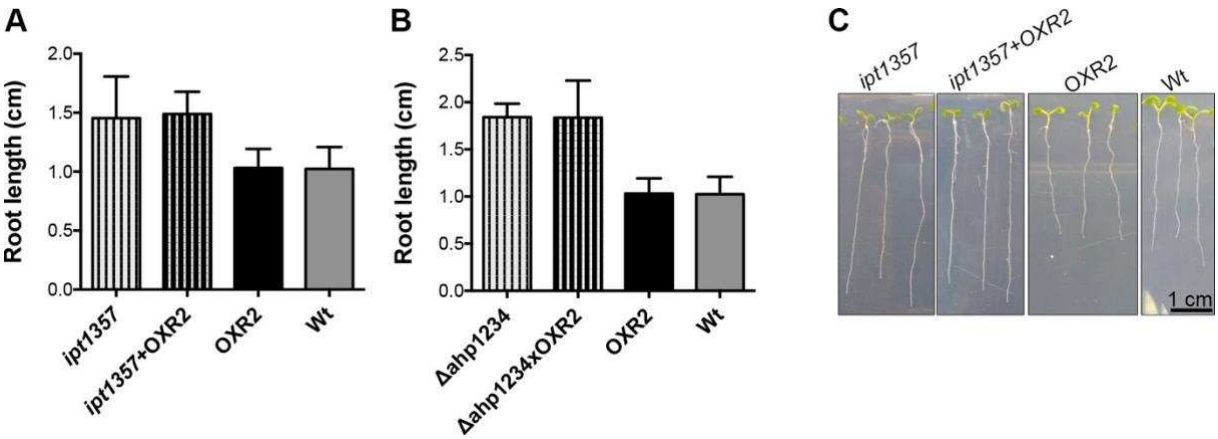

Figure 35: Study of the effect of different OXR protein levels in different CKs pathway-related mutant backgrounds. (A) The over expression of OXR2 does not revert the large root phenotype of *ipt1357*. (B) The overexpression of OXR2 does not succeed to revert the longer root phenotype of *ahp1234*. (C) Representative images of the *ipt1357*, *ipt1357*+OXR2 quantified in (A). Plants were grown on vertical plates with MS medium and main root length measured at 10 DAS. Bars represent mean+SEM using 20-40 plants of each genotype for the analysis.

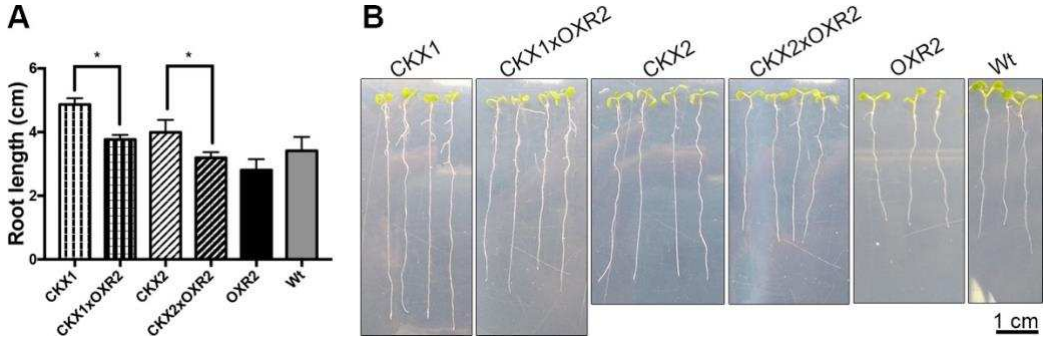

Figure 36: Analysis of the effect of OXR2 in CKX over expressing backgrounds. (A) The overexpression of OXR2 partially reverts the long root phenotypes of CKX1 and CKX2 overexpression. (B) Representative images of the genotypes analysed in (A). Plants were grown on vertical plants on MS medium and main root length measured at 10 DAS. Bars represent mean+SEM using 20-40 plants of each genotype for the analysis. Asterisks indicate significant differences at $P<0.05$ (ANOVA, LSD Fisher test), using 20-40 plants of each genotype for the analysis.

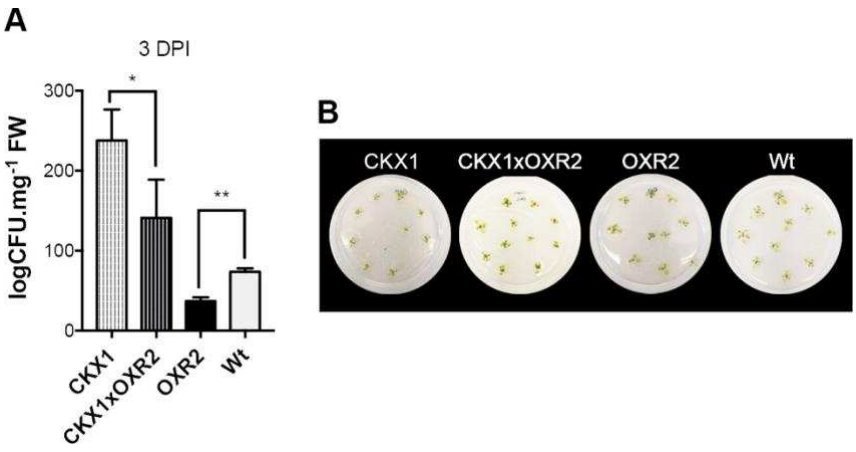

Figure 37: Analysis of the effect of OXR2 in CKX overexpressing backgrounds to Pst DC3000 inoculation. (A) The increased sensitivity of CKX1 to Pst DC3000 colonization is reduced when AtOXR2 is overexpressed as well, the pathogen experiment was carried out as describe before. (B) Disease phenotype of Arabidopsis seedlings flood-inoculated with Pst DC 3000 at a concentration of 5 × 108 CFU.ml-1. Asterisks indicate significant differences at $P<0.05$ (ANOVA, LSD Fisher test), using 10-15 plants of each genotype for the analysis.

Discussion

The observation that OXR2 plants exhibit increased biomass and pathogen resistance simultaneously is peculiar since increased pathogen resistance is often associated with a penalty in growth [79,80]. To investigate this phenotype further, we turned our attention to another class of plant hormones: the CKs. Many groups have previously described the role of CKs, a classical grown hormone [66], in pathogen response, particularly by the modulation of the SA pathway [72,80,165]. When first quantified the hormone content by HPLC, it was saw that OXR2 accumulated resulted in higher levels of CKs while *oxr2.2* displayed a lower amount. The main difference was given by the accumulation of the non-active precursor tZR, expression levels of *LOGs* genes, which are the main enzyme in charge of transforming the ribosides into active CKs, should be analysed [182]. Also, it will be interesting to measured other CKs as well as their conjugated forms. Further, the CKs accumulation was confirmed by using the CKs fluorescent reporter TCS::GFP (Fig. 29). In agreement, transcriptional analysis of plants with altered expression of *AtOXR2* revealed upregulation of syntheses genes (*IPTs*) and downregulation of catabolic-pathway related genes (*CKXs*) (Fig. 30). Besides, transcript levels of CKs response regulators (*ARRs*) were measured. In this analysis, differential expression of the positive regulator *ARR1* was identified, that was induced in OXR2 and repressed in *oxr2.2* plants *(*Fig. 31). Similarly, it was showed different GUS activity in two plants carrying negative regulators ARR5 and ARR15 promoter region regulating *GUS* expression. When *AtOXR2* was overexpress in these lines the GUS activity was decreased (Fig. 31).

Overall, OXR2 plants accumulate CKs and show different expression of genes in a similar manner. OXR2 plants also display some characteristics reported for plants that either accumulate CKs or are treated exogenous with the hormone [166], like thicker stem, higher yield, enhanced stem length and delayed senescence (Section 4.1).

We continued the study on CKs using the same approach as for SA, namely plants overexpressing AtOXR2 in backgrounds with loss-of-function in several proteins related to syntheses (*ipt1357*+OXR2) and signalling (*ahp1234*+OXR2) were obtained. There was no reversion of the root length phenotype caused by the lack of CKs (Fig. 32), therefore, it is assumed that accumulation of CKs in OXR2 plants is dependent on the presence of *IPT* and *AHP* genes. When it was observed the effect of AtOXR2 in plants with gain-of-function in catabolic enzymes (CKX1+OXR2 and CKX2+OXR2), a partial reversion of the root length phenotype was detected (Fig. 33) and also the increased sensitivity towards Pst DC3000 (Fig. 34).

It seems likely that the accumulation of CKs in OXR2 plants could be partially due to a decrease in CKX activity. Further measurements of CKX activity should be carried out to

confirm this possibility. It has been reported that CKX1 activity depends on its homodimerization form and its attachment to the ER membrane, other CKX protein activities are regulated by its glycosylation, substrate availability, electron acceptor identity and other hormones like auxin which enhance CKX activity [167–169].

In the overall hormonal balance, AtOXR2 overexpression appears to generate cellular conditions that allow the accumulation of two major plant hormones, SA (Part II) and CKs. This scenario enables the OXR2 plants to be better prepared for pathogen attack and resist to abiotic stress without a penalty in growth. Elucidating the mechanism by which AtOXR2 can achieve this is interesting for scientific purposes and its biotechnological value since this could be eventually taken to obtain GMOs with increased pathogen resistance and increased biomass.

Part IV

4.5 Functional characterization of AtOXR5

In this last part of the work, another member of the OXR family in Arabidopsis was characterized: the AtOXR5 protein. This protein is the largest of the family (Fig. 8). For an in depth characterization of AtOXR5, plants with altered expression of this TLDc protein were obtained, characterized their phenotype and subjected them to different stresses analysing their behaviour. Comparable responses as in plants overexpressing *AtOXR2* were identified, supporting the idea that different TLDc containing proteins have shared functions and act redundantly in the presence of similar stresses in different subcellular positions as it was demonstrated below. However, it cannot be excluded the existence of unique functions for each family member, strictly connected with their subcellular localisation.

4.5.1 Structural analysis of AtOXR5

As it was shown in section 4.1, AtOXR5 is one member of the OXR family in Arabidopsis. It is the largest family member with 542 aa in length and is encoded on chromosome 5 in the *At5g39590* gene locus. In the phylogenetic tree, AtOXR5 appears in a fourth clade containing proteins from land plants, but not from algae, suggesting that this clade may have originated by a duplication that took place early during land plant evolution (Fig. 8).

Data taken from Blaise et al. (2012, [5]) related to the crystal structure of the TLDc domain of OXR2 from *Danio rerio* (DreOXR2; Uniprot: A9JTH8) was used to deduce the structure of the AtOXR5 TLDc domain. The DreOXR2 domain is composed of four α-helices that surround a globular core conformed by a ß-sandwich. The three-dimensional structure of the AtOXR5 TLDc domain is similar but lacks an α-helix. The ß-sandwich structure at the centre matches perfectly with the previously reported structure of DreOXR2 (Fig. 38A).

The relevant amino acid residues Gly-93, Gly-174 and Glu-216 (numbering based on the human Nuclear receptor coactivator 7 (Ncoa7B) TLDc-containing protein sequence, [11]) are conserved in AtOXR5 and AtOXR2 (outlined in Fig. 35C). The Gly-93 and Gly-174 residues would be necessary for maintaining the structural integrity of the TLDc domain, while Glu-216 is essential for the neuroprotective function of HsOXR1 [110].

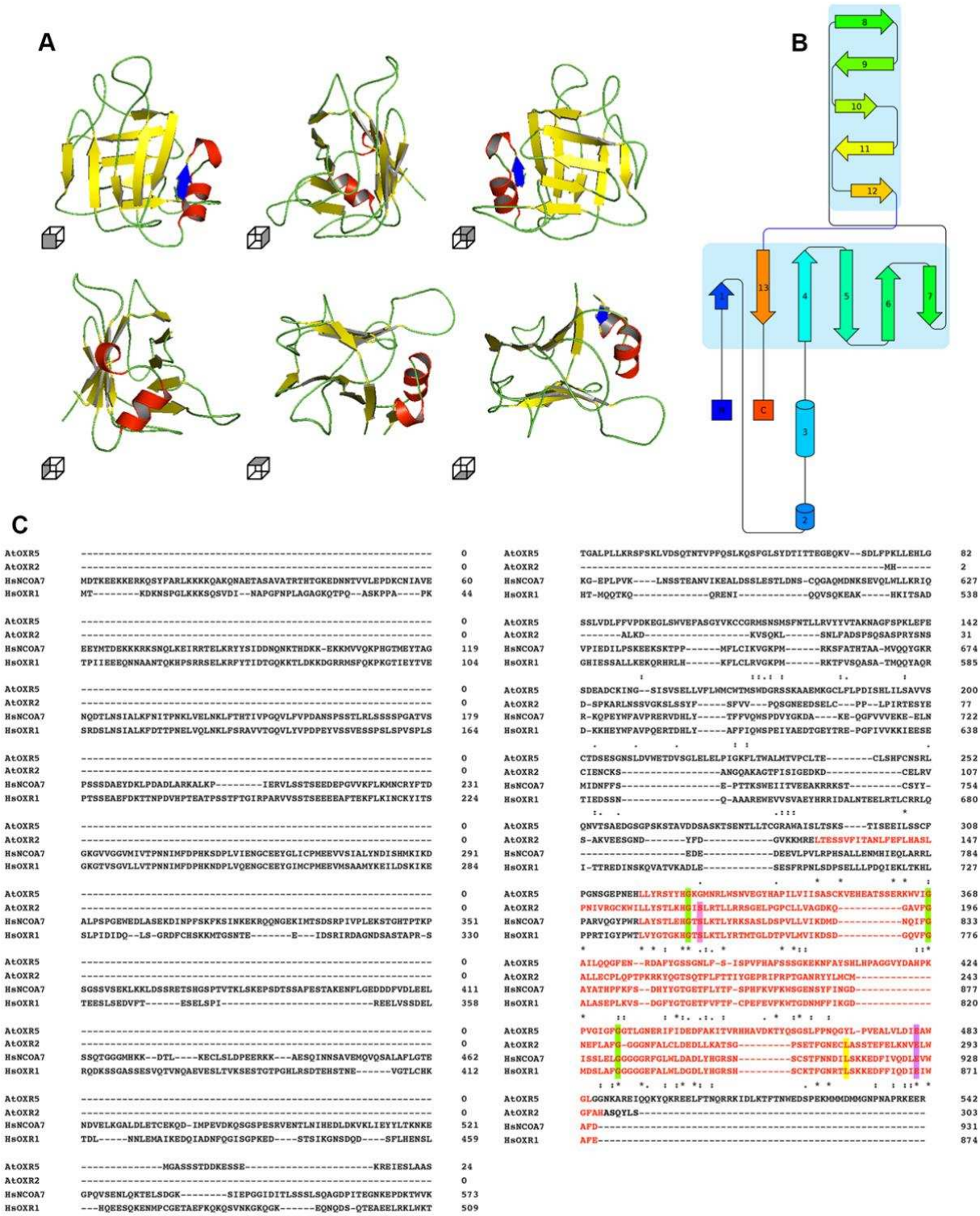

Figure 38: Structural analysis of AtOXR5. (A) Structure of the AtOXR5 TLDc domain based on the DreOXR2 crystal structure [5]. The structure consists of a ß-sandwich surrounded by an α-helix. The helices and the strands are shown in red and yellow, respectively. (B) secondary structure topology of the AtOXR5 TLDc domain. (C) Sequence alignment of the AtOXR2 and AtOXR5 proteins, the TLDc domain appears in red, key aa residues appear outlined in color. The alignment was created using the MView tool of CLUSTAL OMEGA (https://www.ebi.ac.uk/Tools/msa/clustalo/).

4.5.2 AtOXR5 is localised in the apoplast

Different OXR proteins have been localised into different cellular compartments. As it was previously demonstrated, AtOXR2 localised in mitochondria. The *in silico* analysis of AtOXR5 analysis show no N-terminal subcellular targeting sequence (MitoFates [112]), and the SUBcellular Arabidopsis consensus (SUBAcon) database locates it in the Golgi apparatus [113]. To obtain experimental evidences, the coding region of AtOXR5 was tagged with the coding sequence of mRFP and was stably expressed in Arabidopsis. AtOXR5-mRFP was observed surrounding cell borders as a strong continuous signal, apparently coming from the apoplast (Fig. 36A). To confirm this, the construct expressing AtOXR5-mRFP was introduced into an Arabidopsis transgenic line, expressing GFP as a marker for the plasma membrane (*pm-gk*, [116]). Several lines expressing both constructions in roots (AtOXR5-mRFP and membrane marker GFP) were analysed by CLSM. The GFP fluorescence due to the plasma membrane marker did not co-localised with the AtOXR5-mRFP fluorescence, which allowed us to obtain a clear image of the signal coming from the apoplastic compartment (Fig. 39C), suggesting that AtOXR5 would be expressed in the apoplast as a secreted protein. It will need a further characterisation in other plant tissue to discard the possible localisation in other cellular compartments. Also, it would be useful to perform a Westerm blot analysis of proteins from different subcellular fractions to confirm apoplastic localisation by plasmolysis experiment [170].

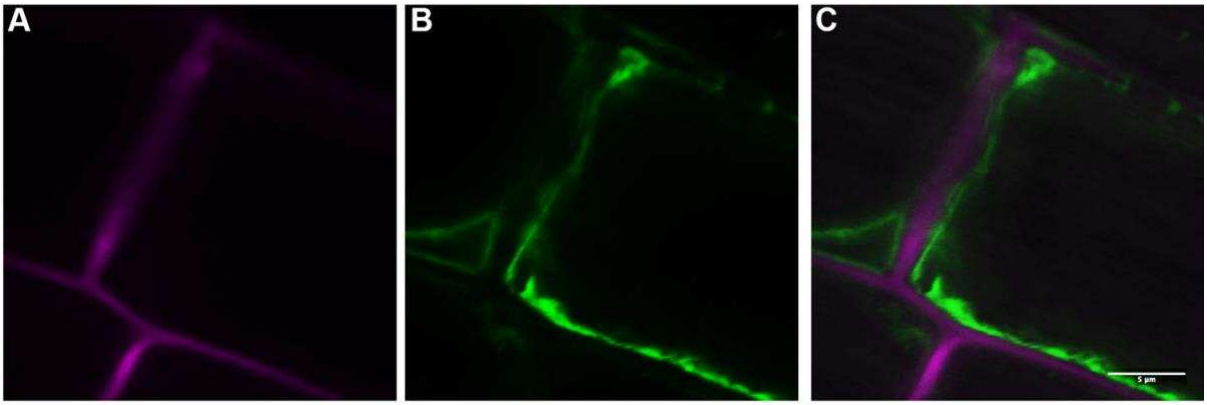

Figure 39: AtOXR5 is localised in the apoplast. (A) Seedlings of transgenic lines 15 DAS co-expressing AtOXR5-mRFP and plasma membrane-GFP were imaged by CLSM. Representative cells from roots are shown in which the signals for AtOXR5-mRFP (magenta; panel A) and cell membrane-GFP (*pm-gk*, green; panel B) do not co-localise (C). Scale bar represents 5µm.

4.5.3 Characterization of plants with altered levels of AtOXR5

To gain more evidence about the function of *AtOXR5*, plants with altered levels of this protein were analysed. An Arabidopsis insertional knockout mutant *oxr5.1* (SAIL_205_E11.V1)

was characterized and several lines overexpressing *AtOXR5* under the CaMV *35S* promoter (OXR5) were obtained (Fig. 40).

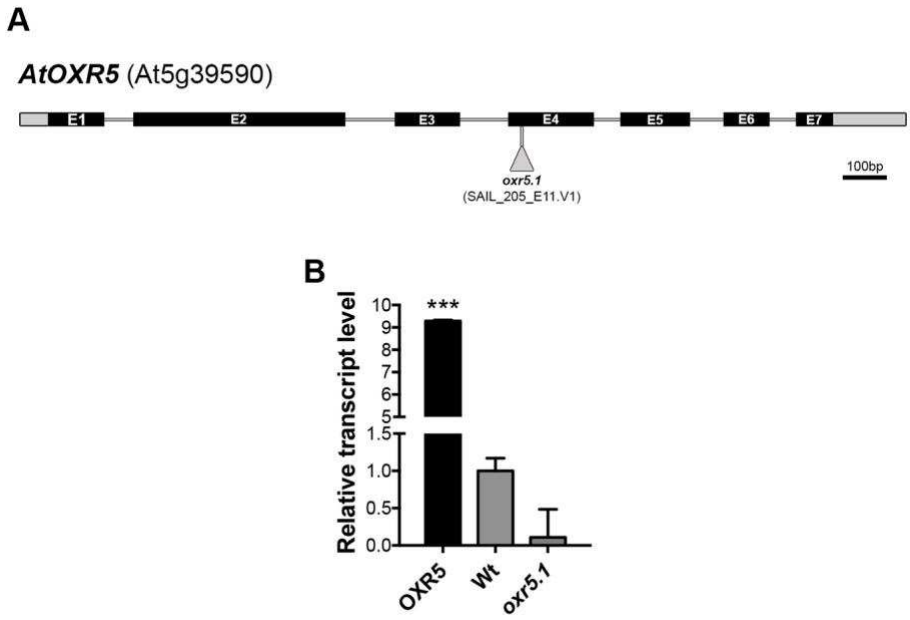

Figure 40: Schematic representation and molecular characterization of the plant lines. (A) Schematic representation of the AtOXR5 T-DNA insertion mutant used in this study. (B) AtOXR5 transcript levels in overexpressing lines (OXR5) and *oxr5* mutants. Transcript levels are referred to those of Wt plants. Asterisks indicate significant differences at $P<0.05$ (ANOVA, LSD Fisher test).

It was evaluated phenotypic parameters of these plants through the whole life cycle. No dramatic differences in comparison to Wt were observed for OXR5 plants under normal growth conditions (Fig. 41), just an increase in the stem diameter was detected. In contrast, the knockout mutant showed higher number of rosette leaves (Fig. 41B), but no significant increase in rosette diameter and no changes in the other parameters determined.

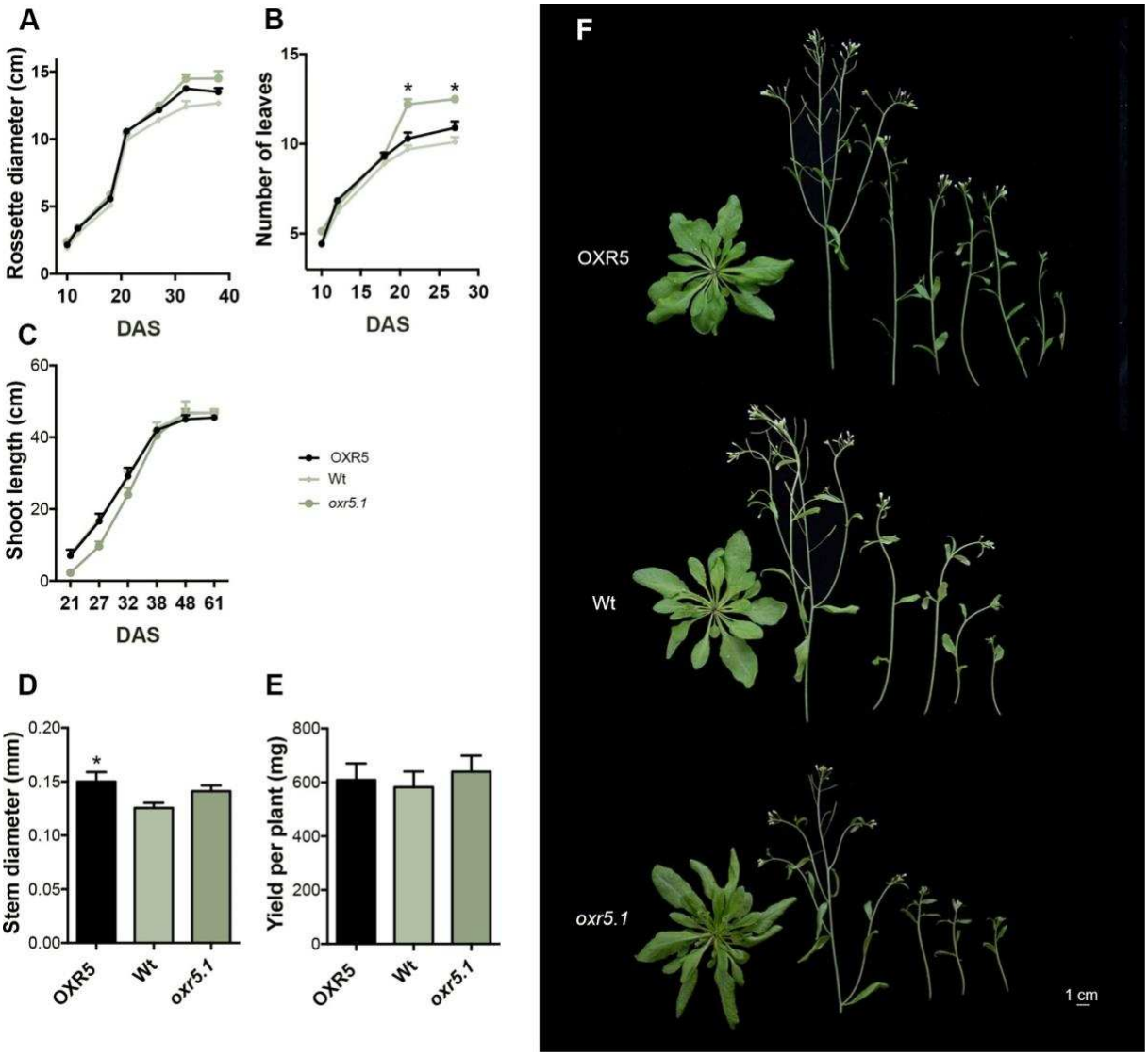

Figure 41: Parameters related to plant growth: (A) rosette diameter, (B) number of leaves, (C) shoot length, (D) stem diameter and € yield per plant in Wt, OXR2 and *oxr5.1* plants grown under a LD photoperiod. (F) Representative images of OXR5 Wt and *oxr5.1* plants grown under a LD photoperiod at 32 DAS. Values represent the mean±SEM of five to ten individual plants for each genotype. Asterisks indicate significant differences ($P < 0.05$) with Wt plants according to LSD Fisher tests.

4.5.4 AtOXR5 affects the transition between vegetative and reproductive phases and the onset and progression of senescence

Another interesting characteristic exhibited by the *oxr5.1* plants is a marked delay in the transition between vegetative and reproductive phase, since flowering occurs approximately four to six days later than in Wt plants (Fig 42A). The delay in days correlates with a higher number of leaves by the time of the reproductive switch (Fig. 42B). This phenotype in the *oxr5.1* mutants is, however, the same phenotype that it was saw when overexpressing *AtOXR2*. On the contrary, OXR5 plants flower a little early with the same number of leaves as Wt plants (Fig. 42).

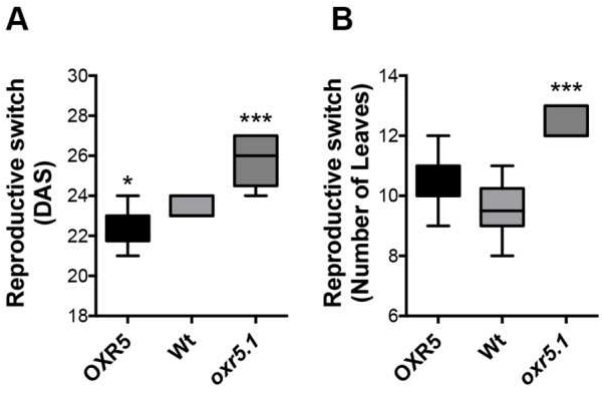

Figure 42: (A) Number of leaves and (B) DAS required to reach the reproductive stage in Wt, OXR5 and *oxr5.1* plants. Values represent the mean±SEM of five to ten individual plants for each genotype. Asterisks indicate significant differences (P < 0.05) with Wt plants according to LSD Fisher tests.

Altered *AtOXR5* expression also affects the onset and progression of natural senescence. Measurements of maximum PSII efficiency (Fv/Fm) in different leaves of entire rosettes between 32 to 49 DAS indicated that OXR5 plants stay green for a more extended time (Fig. 43). However, there was no difference between *oxr5.1* plants and Wt.

Altogether OXR5 plants appear to have a longer lifespan characterised by an early entrance to reproductive phase and a delay in the onset of senescence. On the contrary *oxr5.1* appears to have a shorter reproductive phase.

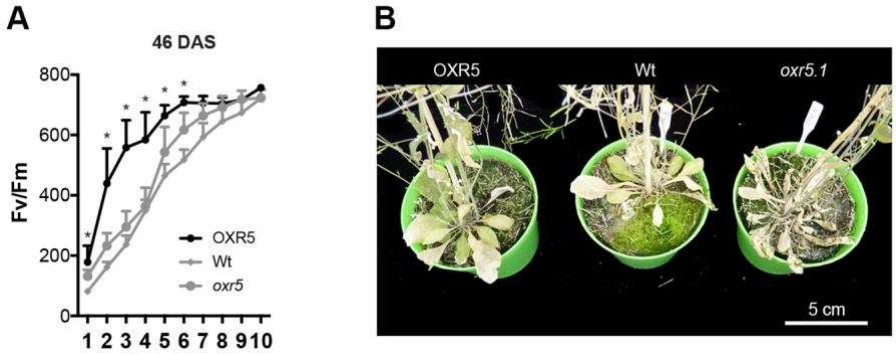

Figure 43: Altered AtOXR5 expression affects the onset and progression of natural senescence. (A) Maximum PSII efficiency (Fv/Fm) measured in different leaves at 46 DAS. (B) Representative images of OXR5, *oxr5.1* and Wt plants at 64 DAS. Values represent the mean±SEM of ten plants for each genotype. Asterisks indicate significant differences (P < 0.05) with Wt plants of the same age, according to LSD Fisher tests.

4.5.5 AtOXR5 does not significantly alters chlorophyll and carbohydrates content in plants

To continue the analysis sugar metabolism and chlorophyll content was measured. Soluble carbohydrates and starch content were analysed at different points during the diurnal cycle

in plants grown under LD photoperiod (Fig. 44B and C). There was no difference for the carbohydrate content measured between the genotypes.

Also, it was determined chlorophyll A, chlorophyll B and total chlorophyll using four-week-old plants grown under LD photoperiod (Fig. 44A). An increase in the accumulation of total chlorophyll in *oxr5.1* plants was observed. It will be interesting to perform a complete analysis of photosynthesis in these plants to see if the accumulation of chlorophyll generates an improvement in the photosynthetic plant performance.

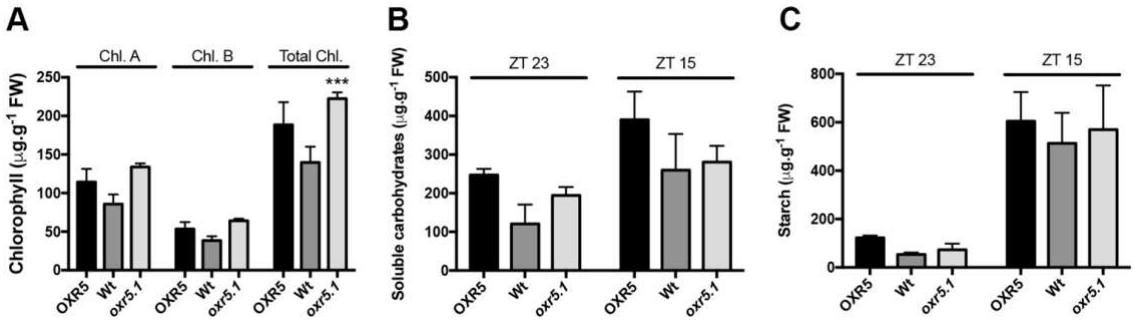

Figure 44: (A) Analysis of chlorophyll content in Wt, OXR5 and *oxr5.1* plants. (B, C) Levels of carbohydrates in Wt, OXR5 and *oxr5* plants grown under LD photoperiod 1 h before (ZT23) and 15 h after (ZT1) the beginning of the illumination period. (B) Soluble carbohydrates, and (C) starch content. Values represent the mean±SEM of ten plants for each genotype. Asterisks indicate significant differences ($P < 0.05$) with Wt plants according to LSD Fisher tests.

4.5.6 AtOXR5 and stress responses

Since it was described earlier that lack of AtOXR2 (Section 4.2 and 4.3) causes increased sensitivity to stress conditions, it was interesting to evaluate the responses of knock-out plants in *AtOXR5* and double mutants of both *OXR* genes (*oxr2xoxr5*). Furthermore, a double mutant *oxr5xoxr2* was obtained by crossing *oxr5.1* with *oxr2.2* (Section 4.1) plants. With this double mutant is possible to analyse functional redundancy and the possible effect of lacking two OXR family members located in two different cell compartments, mitochondria and apoplast, in Arabidopsis plants.

When the effect of MV on all mutant plants lacking AtOXR2 and/or AtOXR5 proteins was tested, plants showed a higher sensitivity to the stress situation (Fig. 45). Interestingly double mutants do not appear to be more sensitive than single mutants, therefore it was concluded that the two proteins did not act synergistically.

In addition, infection assays with Pst DC3000 were performed and observed again that *oxr5.1* mutants have enhanced susceptibility towards the pathogen in comparison to Wt plants (Fig. 46). The double mutant did not show differences in comparison to any single mutant (Fig. 46).

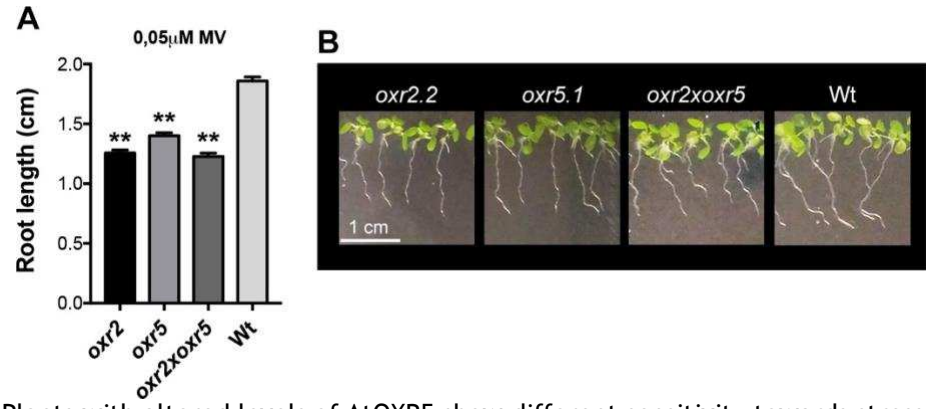

Figure 45: Plants with altered levels of AtOXR5 show different sensitivity towards stressors. (A) Root length of *oxr5.1*, *oxr2.2 a*nd *oxr2xoxr5* plants grown on MS medium supplemented with 0,1 µM MV during 10 days. (B) Representative images of the phenotype of seedlings used for quantification of root length shown in (A). Asterisks indicate significant differences at P<0.05 (ANOVA, LSD Fisher test), using 20-40 plants of each genotype for the analysis.

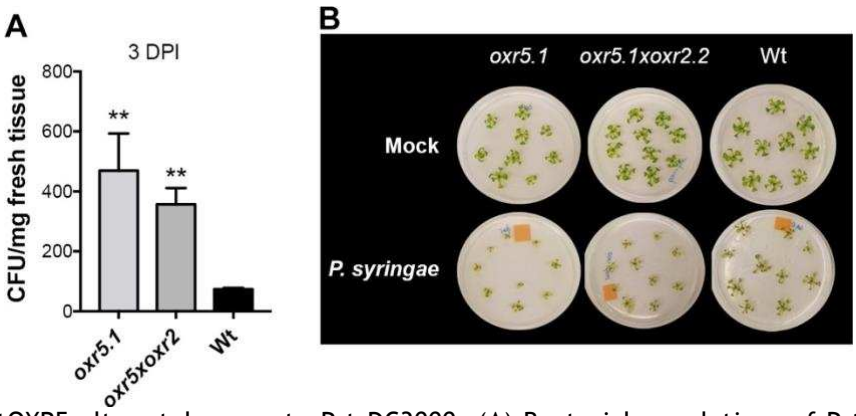

Figure 46: AtOXR5 alters tolerance to Pst DC3000. (A) Bacterial populations of Pst DC300 were quantified at 3 days after being flood-inoculated with Pst DC 3000 at a concentration of 5 × 10^8 CFU/ml. Mock-inoculated plants were flooded with sterile distilled H_2O containing 0,025% (v/v) Silwet L-77. Values represent the mean±SEM from 3 biological replicates. (B) Disease phenotype of Arabidopsis seedlings flood-inoculated with Pst DC 3000 at a concentration of 5 × 10^8 CFU.ml^{-1}. Asterisks indicate significant differences at P<0.05 (ANOVA, LSD Fisher test), using 10-15 plants of each genotype for the analysis.

Discussion

In this last part it is described the first functional characterization of the Arabidopsis protein AtOXR5. This is the largest family member, with 542 aa in length and contains a TLDc domain at the C-terminal portion with a 23,66% identity to the HsOXR1 domain. Essential aa described in other OXR proteins, involved in maintaining the structure, are also conserved in the AtOXR5-TLDc domain (Gly-93 and Gly-174 in NCOA7), and a Glu residue (Glu-216 in NCOA7) which appears to be essential for the neuroprotective function of HsOXR1 [11,110] (Fig 35). A homology-based modelling of the AtOXR5-TLDc domain was performed based on the crystal structure available for another TLDc protein from *Danio rerio* [5]. The model resulted in a ß-sandwich with an α-helix at one flank, very similar to the structure resolved for *Danio rerio* (Fig. 35).

In addition, the subcellular localisation of AtOXR5 was determined by CLSM using a fusion protein between AtOXR5 and mRFP. It was determined that AtOXR5 localise in apoplast, at least in root cell at the conditions of the assay (Fig. 36). This analysis should be performed in other tissues and with a specific apoplast marker to confirm the subcellular location. Apoplastic localisation has been reported to various stress response proteins, in this space takes places the initial recognition and response of multiple types of stresses [176-179].

To continue with the analysis plants that overexpress AtOXR5 (OXR5) and knockout mutant (*oxr5.1*) were obtained. The OXR5 did not show particular biotechnological interesting phenotype, as it was previously observed in OXR2 plants. OXR5 plants reached the reproductive stage early than Wt and showed a delay in senescence (Fig. 40 and 41). Unexpectedly *oxr5.1* showed some characteristic similar to OXR2 plants, like an increased number of leaves and a delayed transition to reproductive phase (Fig. 38 and 40). It will be needed to analyse these aspects of the plant phenotype into another independent knockout mutant, to confirm that our observations were definitively due to the lack of AtOXR5.

Neither overexpression, nor mutation of AtOXR5 resulted in a different accumulation of carbohydrate metabolites compared to Wt (Fig. 42). Although *oxr5.1* showed an increased amount of chlorophyll (Fig. 42). It will be interesting to analyse the photosynthetic efficiency in mutants and AtOXR5 overexpressing plants to evaluate if it is improved [180, 181].

Furthermore, the response of the plants lacking AtOXR5 to different stresses was tested, and it was also included a double knockout mutant lacking AtOXR5 and also AtOXR2. For both of two stress-conditions analysed, MV and Pst DC3000 infection, *oxr5.1* was similar susceptible as the *oxr2.2* plants (Fig. 43 and Fig.44). It was intriguing that double mutants did not show a higher sensitivity toward stress compared to both single mutants, the effect was not additive (Fig. 43 and Fig.44). The different subcellular localisation of both proteins and the presence of other OXR family members could explain the non-additive response that

was observed in double mutants. The mechanism by which the stress responses are triggered might differ for each protein and the other four members could act redundantly to fulfil the response upon the lack of one or two members.

Summarising AtOXR5 appears to perform the same role as AtOXR2 during stress responses since both loss-of-function mutants behaved in a similar manner. It is needed to perform more experiments and include another independent loss-of-function mutant for AtOXR5 to explain a putative general mechanism for OXRs proteins in Arabidopsis.

5. Overall conclusion and future perspectives

In this thesis work, it was studied two members belonging to the new protein family OXR in *Arabidopsis thaliana*. OXR proteins are characterized by the presence of a TLDc domain at the C-terminal end, which is highly conserved among eukaryotes. Six members of the OXR family in Arabidopsis were identified, and centre the work on two of them: AtOXR2 and AtOXR5.

Both proteins conserve essential amino acid residues having relevant functions in TLDc proteins from other organisms. The 3D structure of the TLDc domain present in AtOXR2 and AtOXR5 that was obtained by homology modelling, resulted in the similar structure previously documented for the OXR2 protein from *D. rerio* (sections 4.1 and 4.5).

By CLSM and marker lines for different OXR genes and cellular compartments, it was observed AtOXR2 in the mitochondria and AtOXR5 in the apoplastic compartment (sections 4.1 and 4.5) in plants grown under normal conditions. It cannot be discarded a possible change in the subcellular localisation in the presence of stress or any differential growth condition.

To start with the functional characterization of our proteins of interest, plants that overexpress AtOXR2 or AtOXR5 (named: OXR2 and OXR5) were obtained and different loss-of-function insertional mutants (*oxr2.1*, *oxr2.2* and *oxr5.1*) were characterized. The plant phenotype and behaviour were characterized during the whole life cycle and established different characteristics associated with the overexpression or the lack of these proteins. Mainly, OXR2 plants showed an increased number of leaves, thicker stems, increased yield and biomass. The *oxr2* mutants and OXR5 plants did not show any different characteristic compared to Wt, in plants grown under control conditions. However, *oxr5* single mutant exhibited an increased number of leaves (sections 4.2 and 4.5).

OXR2 and *oxr5* displayed a delay in the transition to the reproductive stage, reaching the flowering time with higher number of leaves in comparison to Wt. Also, OXR2 and OXR5 exhibited a delay in senescence.

None of the plant lines exhibited differences in carbohydrate accumulation. In the case of chlorophyll measurement, *oxr5* plants accumulated higher levels of the photosynthetic pigment (section 4.2 and 4.5).

Interestingly, OXR2 plants exhibited an increased respiratory rate, decreased mitochondrial membrane potential an also accumulate higher level of ROS; *oxr2.2* had, however, a decreased mitochondrial membrane potential (section 4.2).

Under stress conditions, OXR2 plants showed increased resistant to both abiotic and biotic stresses. With the opposite behaviour, *oxr2* and *oxr5* displayed higher sensitivity towards the stressors. A double mutant (*oxr2xoxr5*) was tested, but this line behaved similarly to the single mutants (sections 4.3, 4.4 and 4.5).

AtOXR2 appears to influence the SA and CKs hormonal pathways. OXR2 plants accumulated higher levels of both hormones while *oxr2.2* exhibits lower amounts of SA and CKs when compared with Wt plants. They also show altered expression of different marker genes regulated by these hormones, which supports the data about the accumulation of different hormones.

By complementing different mutants with impaired SA and CKs-responses (*sid2, nrp1, ipt1357*, *ahp1234*, CKX1 and CKX2) they were identified key proteins that allow the apparition of the different characteristic in OXR2 related to the hormonal pathways. Then the necessity of the presence of ICS1 and NPR1 for the enhanced pathogen resistance in OXR2 plants was determinated, and the necessity of IPT and AHPs for the apparition of CKs-related responses in OXR2. Furthermore, it was described a partial reversion of the phenotypes related to the lower CKs content in CKX plants that should have lower CKs when overexpressing OXR2. Thus, AtOXR2 could be able to modulate CKX activity (section 4.4).

Overall, it is provided new evidence for the role of OXR proteins in Arabidopsis, further work would be needed to describe a specific mechanism of action.

The capacity to overcome different stresses without a penalty in growing (Fig. 47) makes OXR proteins a tempting target for future crop improvement strategies. It will be interesting to study OXRs proteins in agronomical relevant crops, GMOs could be designed focusing in stress tolerance and yield aspects. Current climate change crisis makes even more important to focus scientific effort into optimizing crops in order to ensure food provisions for the human population and livestock.

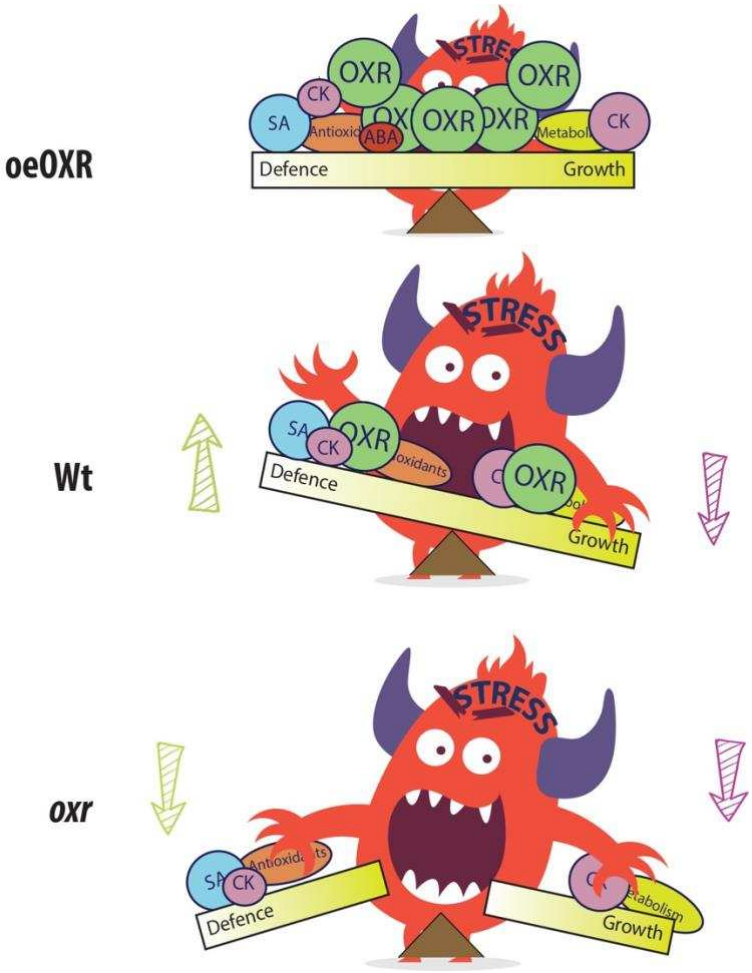

Figure 47: Overexpression of OXR2 protein allows the plant to maintain equilibrium between defence responses and growth upon different types of stress situations (A). In Wt plants, growth is suppressed upon stress situations in order to use more energy in the activation of defence responses (B). In loss-of-function mutants for OXR proteins plants become more sensitive to different types of stress situations, losing the ability to equilibrate the defence responses and growth (C).

6. References

[1] Volkert, M.R., Elliott, N.A. and Housman, D.E. (2000) Functional genomics reveals a family of eukaryotic oxidation protection genes. *Proceedings of the National Academy of Sciences*, **97**, 14530–5. https://doi.org/10.1073/pnas.260495897

[2] Elliott, N.A. and Volkert, M.R. (2004) Stress Induction and Mitochondrial Localization of Oxr1 Proteins in Yeast and Humans. *Molecular and Cellular Biology*, **24**, 3180–7. https://doi.org/10.1128/mcb.24.8.3180-3187.2004

[3] Fischer, H., Zhang, X.U., O'Brien, K.P., Kylsten, P. and Engvall, E. (2001) C7, a novel nucleolar protein, is the mouse homologue of the Drosophila late puff product l82 and an isoform of human OXR1. *Biochemical and Biophysical Research Communications*, **281**, 795–803. https://doi.org/10.1006/bbrc.2001.4345

[4] Jaramillo-Gutierrez, G., Molina-Cruz, A., Kumar, S. and Barillas-Mury, C. (2010) The Anopheles gambiae oxidation resistance 1 (OXR1) gene regulates expression of enzymes that detoxify reactive oxygen species. *PLoS ONE*, **5**, 1–9. https://doi.org/10.1371/journal.pone.0011168

[5] Blaise, M., Alsarraf, H.M.A.B., Wong, J.E.M.M., Midtgaard, S.R., Laroche, F., Schack, L. et al. (2012) Crystal structure of the TLDc domain of oxidation resistance protein 2 from zebrafish. *Proteins: Structure, Function and Bioinformatics*, **80**, 1694–8. https://doi.org/10.1002/prot.24050

[6] Sanada, Y., Asai, S., Ikemoto, A., Moriwaki, T., Nakamura, N., Miyaji, M. et al. (2014) Oxidation resistance 1 is essential for protection against oxidative stress and participates in the regulation of aging in Caenorhabditis elegans. *Free Radical Research*, **48**, 919–28. https://doi.org/10.3109/10715762.2014.927063

[7] Natoli, R., Provis, J., Valter, K. and Stone, J. (2008) Expression and role of the early-response gene Oxr1 in the hyperoxia-challenged mouse retina. *Investigative Ophthalmology and Visual Science*, **49**, 4561–7. https://doi.org/10.1167/iovs.08-1722

[8] Zhang, R., Miao, J., Song, Y., Zhang, W., Xu, L., Chen, Y. et al. (2019) Genome-wide association study identifies the PLAG1-OXR1 region on BTA14 for carcass meat yield in cattle. *Physiological Genomics*, **51**, 137–44. https://doi.org/10.1152/physiolgenomics.00112.2018

[9] Durand, M., Kolpak, A., Farrell, T., Elliott, N.A., Shao, W., Brown, M. et al. (2007) The OXR domain defines a conserved family of eukaryotic oxidation resistance proteins. *BMC Cell Biology*, **8**, 13. https://doi.org/10.1186/1471-2121-8-13

[10] Doerks, T., Copley, R.R., Schultz, J., Ponting, C.P. and Bork, P. (2002) Systematic identification of novel protein domain families associated with nuclear functions. *Genome Research*, **12**, 47–56. https://doi.org/10.1101/

[11] Finelli, M.J., Sanchez-Pulido, L., Liu, K.X., Davies, K.E. and Oliver, P.L. (2016) The evolutionarily conserved Tre2/Bub2/Cdc16 (TBC), lysin motif (LysM), domain catalytic (TLDc) domain is neuroprotective against oxidative stress. *Journal of Biological Chemistry*, **291**, 2751–63. https://doi.org/10.1074/jbc.M115.685222

[12] Falace, A., Filipello, F., La Padula, V., Vanni, N., Madia, F., De Pietri Tonelli, D. et al. (2010) TBC1D24, an ARF6-interacting protein, is mutated in familial infantile

myoclonic epilepsy. *American Journal of Human Genetics*, **87**, 365–70. https://doi.org/10.1016/j.ajhg.2010.07.020

[13] Oliver, P.L., Finelli, M.J., Edwards, B., Bitoun, E., Butts, D.L., Becker, E.B.E. et al. (2011) Oxr1 is essential for protection against oxidative stress-induced neurodegeneration. *PLoS Genetics*, **7**. https://doi.org/10.1371/journal.pgen.1002338

[14] Liu, K.X., Edwards, B., Lee, S., Finelli, M.J., Davies, B., Davies, K.E. et al. (2015) Neuron-specific antioxidant OXR1 extends survival of a mouse model of amyotrophic lateral sclerosis. *Brain*, **138**, 1167–81. https://doi.org/10.1093/brain/awv039

[15] Wu, Y., Davies, K.E. and Oliver, P.L. (2016) The antioxidant protein Oxr1 influences aspects of mitochondrial morphology. *Free Radical Biology and Medicine*, **95**, 255–67. https://doi.org/10.1016/j.freeradbiomed.2016.03.029

[16] Pires-Luís, A.S., Costa-Pinheiro, P., Ferreira, M.J., Antunes, L., Lobo, F., Oliveira, J. et al. (2017) Identification of clear cell renal cell carcinoma and oncocytoma using a three-gene promoter methylation panel. *Journal of Translational Medicine*, **15**, 1–9. https://doi.org/10.1186/s12967-017-1248-y

[17] Mo, J.L., Pan, Z.G., Chen, X., Lei, Y., Lv, L.L., Qian, C. et al. (2019) MicroRNA-365 Knockdown Prevents Ischemic Neuronal Injury by Activating Oxidation Resistance 1-Mediated Antioxidant Signals. *Neuroscience Bulletin*, https://doi.org/10.1007/s12264-019-00371-y

[18] Wang, L., Wang, L., Chang, W., Li, Y. and Wang, L. (2019) MicroRNA-373 promotes the development of esophageal squamous cell carcinoma by targeting LATS2 and OXR1. *The International Journal of Biological Markers*, 1-8. https://doi.org/10.1177/1724600819827964

[19] Kobayashi, N., Takahashi, M., Kihara, S., Niimi, T., Yamashita, O. and Yaginuma, T. (2014) Cloning of cDNA encoding a Bombyx mori homolog of human oxidation resistance 1 (OXR1) protein from diapause eggs, and analyses of its expression and function. *Journal of Insect Physiology*, **68**, 58–68. https://doi.org/10.1016/j.jinsphys.2014.06.020

[20] Yang, M., Lin, X., Rowe, A., Rognes, T., Eide, L. and Bjørås, M. (2015) Transcriptome analysis of human OXR1 depleted cells reveals its role in regulating the p53 signaling pathway. *Scientific Reports*, **5**, 1–12. https://doi.org/10.1038/srep17409

[21] Yang, M., Luna, L., Sørbø, J.G., Alseth, I., Johansen, R.F., Backe, P.H. et al. (2014) Human OXR1 maintains mitochondrial DNA integrity and counteracts hydrogen peroxide-induced oxidative stress by regulating antioxidant pathways involving p21. *Free Radical Biology and Medicine*, **77**, 41–8. https://doi.org/10.1016/j.freeradbiomed.2014.09.003

[22] Pomatto, L.C.D., Sun, P.Y., Yu, K., Gullapalli, S., Bwiza, C.P., Sisliyan, C. et al. (2019) Limitations to adaptive homeostasis in an hyperoxia-induced model of accelerated ageing. *Redox Biology*, **24**, 101194. https://doi.org/10.1016/j.redox.2019.101194

[23] Lin, J.S., Lin, C.C., Lin, H.H., Chen, Y.C. and Jeng, S.T. (2012) MicroR828 regulates lignin and h2O2 accumulation in sweet potato on wounding. *New Phytologist*, **196**, 427–40. https://doi.org/10.1111/j.1469-8137.2012.04277.x

[24] Krämer, U. (2015) Planting molecular functions in an ecological context with Arabidopsis thaliana. *ELife*, **4**, 1–13. https://doi.org/10.7554/elife.06100

[25] Noctor, G., Reichheld, J.P. and Foyer, C.H. (2017) ROS-related redox regulation and signaling in plants. *Semin. Cell Dev. Biol.* https://doi.org/10.1016/j.semcdb.2017.07.013

[26] Szymańska, R., Ślesak, I., Orzechowska, A. and Kruk, J. (2017) Physiological and biochemical responses to high light and temperature stress in plants. *Environmental and Experimental Botany*, **139**, 165–77. https://doi.org/10.1016/j.envexpbot.2017.05.002

[27] Foyer, C.H., Ruban, A. V. and Noctor, G. (2017) Viewing oxidative stress through the lens of oxidative signalling rather than damage. *Biochemical Journal*, **474**, 877–83. https://doi.org/10.1042/bcj20160814

[28] Mittler, R. (2017) ROS Are Good. *Trends in Plant Science*, **22**, 11–9. https://doi.org/10.1016/j.tplants.2016.08.002

[29] Gleason, C., Huang, S., Thatcher, L.F., Foley, R.C., Anderson, C.R., Carroll, A.J. et al. (2011) Mitochondrial complex II has a key role in mitochondrial-derived reactive oxygen species influence on plant stress gene regulation and defense. *Proceedings of the National Academy of Sciences*, **108**, 10768–73. https://doi.org/10.1073/pnas.1016060108

[30] Jardim-Messeder, D., Caverzan, A., Rauber, R., de Souza Ferreira, E., Margis-Pinheiro, M. and Galina, A. (2015) Succinate dehydrogenase (mitochondrial complex II) is a source of reactive oxygen species in plants and regulates development and stress responses. *New Phytologist*, **208**, 776–89. https://doi.org/10.1111/nph.13515

[31] Vanlerberghe, G.C. (2002) Induction of Mitochondrial Alternative Oxidase in Response to a Cell Signal Pathway Down-Regulating the Cytochrome Pathway Prevents Programmed Cell Death. *Plant Physiology*, **129**, 1829–42. https://doi.org/10.1104/pp.002691

[32] Vercesi, A.E., Borecký, J., Maia, I. de G., Arruda, P., Cuccovia, I.M. and Chaimovich, H. (2006) Plant Uncoupling Mitochondrial Proteins. *Annual Review of Plant Biology*, **57**, 383–404. https://doi.org/10.1146/annurev.arplant.57.032905.105335

[33] Nowicka, B., Ciura, J., Szymańska, R. and Kruk, J. (2018) Improving photosynthesis, plant productivity and abiotic stress tolerance – current trends and future perspectives. *Journal of Plant Physiology*, **231**, 415–33. https://doi.org/10.1016/j.jplph.2018.10.022

[34] Cvetkovska, M. and Vanlerberghe, G.C. (2013) Alternative oxidase impacts the plant response to biotic stress by influencing the mitochondrial generation of reactive oxygen species. *Plant, Cell and Environment*, **36**, 721–32. https://doi.org/10.1111/pce.12009

[35] De Clercq, I., Vermeirssen, V., Van Aken, O., Vandepoele, K., Murcha, M.W., Law, S.R. et al. (2013) The Membrane-Bound NAC Transcription Factor ANAC013 Functions in Mitochondrial Retrograde Regulation of the Oxidative Stress Response in Arabidopsis. *The Plant Cell*, **25**, 3472–90. https://doi.org/10.1105/tpc.113.117168

[36] Selinski, J., Scheibe, R., Day, D.A. and Whelan, J. (2018) Alternative Oxidase Is Positive for Plant Performance. *Trends in Plant Science*, **23**, 588–97. https://doi.org/10.1016/j.tplants.2018.03.012

[37] Noctor, G., De Paepe, R. and Foyer, C.H. (2007) Mitochondrial redox biology and homeostasis in plants. *Trends in Plant Science*, **12**, 125–34. https://doi.org/10.1016/j.tplants.2007.01.005

[38] Wagner, S., Behera, S., De Bortoli, S., Logan, D.C., Fuchs, P., Carraretto, L. et al. (2015) The EF-Hand Ca 2+ Binding Protein MICU Choreographs Mitochondrial Ca 2+ Dynamics in Arabidopsis. *The Plant Cell*, **27**, 3190–212. https://doi.org/10.1105/tpc.15.00509

[39] Schwarzlander, M., Logan, D.C., Johnston, I.G., Jones, N.S., Meyer, A.J., Fricker, M.D. et al. (2012) Pulsing of Membrane Potential in Individual Mitochondria: A Stress-Induced Mechanism to Regulate Respiratory Bioenergetics in Arabidopsis. *The Plant Cell*, **24**, 1188–201. https://doi.org/10.1105/tpc.112.096438

[40] Xu, Y., Whelan, J., Berkowitz, O., Hartmann, A., Wang, Y. and Selinski, J. (2018) Stress responsive mitochondrial proteins in Arabidopsis thaliana. *Free Radical Biology and Medicine*, **122**, 28–39. https://doi.org/10.1016/j.freeradbiomed.2018.03.031

[41] Kerchev, P.I., De Clercq, I., Denecker, J., Mühlenbock, P., Kumpf, R., Nguyen, L. et al. (2014) Mitochondrial perturbation negatively affects auxin signaling. *Molecular Plant*, **7**, 1138–50. https://doi.org/10.1093/mp/ssu071

[42] Van Aken, O., Pečenková, T., Van De Cotte, B., De Rycke, R., Eeckhout, D., Fromm, H. et al. (2007) Mitochondrial type-I prohibitins of Arabidopsis thaliana are required for supporting proficient meristem development. *Plant Journal*, **52**, 850–64. https://doi.org/10.1111/j.1365-313X.2007.03276.x

[43] Skirycz, A., De Bodt, S., Obata, T., De Clercq, I., Claeys, H., De Rycke, R. et al. (2010) Developmental Stage Specificity and the Role of Mitochondrial Metabolism in the Response of Arabidopsis Leaves to Prolonged Mild Osmotic Stress. *Plant Physiology*, **152**, 226–44. https://doi.org/10.1104/pp.109.148965

[44] Van Aken, O. and Whelan, J. (2012) Comparison of Transcriptional Changes to Chloroplast and Mitochondrial Perturbations Reveals Common and Specific Responses in Arabidopsis. *Frontiers in Plant Science*, **3**, 1–18. https://doi.org/10.3389/fpls.2012.00281

[45] Zhang, S., Li, C., Wang, R., Chen, Y., Shu, S., Huang, R. et al. (2017) The Arabidopsis Mitochondrial Protease FtSH4 Is Involved in Leaf Senescence via Regulation of WRKY-Dependent Salicylic Acid Accumulation and Signaling. *Plant Physiol*. https://doi.org/10.1104/pp.16.00008

[46] Schwarzländer, M., König, A.C., Sweetlove, L.J. and Finkemeier, I. (2012) The impact of impaired mitochondrial function on retrograde signalling: A meta-analysis of transcriptomic responses. *Journal of Experimental Botany*, **63**, 1735–50. https://doi.org/10.1093/jxb/err374

[47] Bakshi, M. and Oelmüller, R. (2014) Wrky transcription factors jack of many trades in plants. *Plant Signaling and Behavior*, **9**, 1–18. https://doi.org/10.4161/psb.27700

[48] Bary, A. De. (2012) Fighting for their lives: Plants and pathogens. *The Plant Cell*, **24**. https://doi.org/10.1105/tpc.112.tt0612

[49] Jones, J.D.G. and Dangl, J.L. (2006) The plant immune system. *Nature*, **444**, 323–9. https://doi.org/10.1038/nature05286

[50] Torres, M.A. (2010) ROS in biotic interactions. *Physiologia Plantarum*, **138**, 414–29. https://doi.org/10.1111/j.1399-3054.2009.01326.x

[51] Ádám, A.L., Nagy, Z., Kátay, G., Mergenthaler, E. and Viczián, O. (2018) Signals of systemic immunity in plants: Progress and open questions. *International Journal of Molecular Sciences*, **19**, 1–21. https://doi.org/10.3390/ijms19041146

[52] Conrath, U. (2011) Molecular aspects of defence priming. *Trends in Plant Science*, **16**, 524–31. https://doi.org/10.1016/j.tplants.2011.06.004

[53] Wildermuth, M.C., Dewdney, J., Wu, G. and Ausubel, F.M. (2001) Isochorismate synthase is required to synthesize salicylic acid for plant defence. *Nature*, **414**, 562–5. https://doi.org/10.1038/35107108

[54] Shah, J. (2003) The salicylic acid loop in plant defense. *Current Opinion in Plant Biology*, **6**, 365–71. https://doi.org/10.1016/S1369-5266(03)00058-X

[55] Dong, X. (2004) NPR1, all things considered. *Current Opinion in Plant Biology*, **7**, 547–52. https://doi.org/10.1016/j.pbi.2004.07.005

[56] Tada, Y., Spoel, S.H., Pajerowska-Mukhtar, K., Mou, Z., Song, J., Wang, C. et al. (2008) Plant immunity requires conformational charges of NPR1 via S-nitrosylation and thioredoxins. *Science*, **321**, 952–6. https://doi.org/10.1126/science.1156970

[57] Wu, Y., Zhang, D., Chu, J.Y., Boyle, P., Wang, Y., Brindle, I.D. et al. (2012) The Arabidopsis NPR1 Protein Is a Receptor for the Plant Defense Hormone Salicylic Acid. *Cell Reports*, **1**, 639–47. https://doi.org/10.1016/j.celrep.2012.05.008

[58] Kumar, D. (2014) Salicylic acid signaling in disease resistance. *Plant Science*, **228**, 127–34. https://doi.org/10.1016/j.plantsci.2014.04.014

[59] Xin, X.-F. and He, S.Y. (2013) Pseudomonas syringae pv. tomato DC3000: A Model Pathogen for Probing Disease Susceptibility and Hormone Signaling in Plants. *Annual Review of Phytopathology*, **51**, 473–98. https://doi.org/10.1146/annurev-phyto-082712-102321

[60] Schwelm, A., Fogelqvist, J., Knaust, A., Jülke, S., Lilja, T., Bonilla-Rosso, G. et al. (2015) The Plasmodiophora brassicae genome reveals insights in its life cycle and ancestry of chitin synthases. *Scientific Reports*, **5**, 1–12. https://doi.org/10.1038/srep11153

[61] Ludwig-Müller, J., Jülke, S., Geiß, K., Richter, F., Mithöfer, A., Šola, I. et al. (2015) A novel methyltransferase from the intracellular pathogen Plasmodiophora brassicae methylates salicylic acid. *Molecular Plant Pathology*, **16**, 349–64. https://doi.org/10.1111/mpp.12185

[62] Lovelock, D.A., Šola, I., Marschollek, S., Donald, C.E., Rusak, G., van Pée, K.H. et al. (2016) Analysis of salicylic acid-dependent pathways in Arabidopsis thaliana following infection with Plasmodiophora brassicae and the influence of salicylic acid on disease. *Molecular Plant Pathology*, **17**, 1237–51. https://doi.org/10.1111/mpp.12361

[63] Chen, T., Bi, K., He, Z., Gao, Z., Zhao, Y., Fu, Y. et al. (2016) Arabidopsis Mutant bik1 Exhibits Strong Resistance to Plasmodiophora brassicae. *Frontiers in Physiology*, **7**, 1–13. https://doi.org/10.3389/fphys.2016.00402

[64] Miller, C.O. (1961) a Kinetin-Like Compound in Maize. *Proceedings of the National Academy of Sciences*, **47**, 170–4. https://doi.org/10.1073/pnas.47.2.170

[65] Mok, D.W.S. and Mok, M.C. (2001) Etabolism and. *Annu Rev Plant Physiol Plant Mol Bio*, **52**, 89–118.

[66] Bartrina, I., Otto, E., Strnad, M., Werner, T. and Schmülling, T. (2011) Cytokinin Regulates the Activity of Reproductive Meristems, Flower Organ Size, Ovule Formation, and Thus Seed Yield in Arabidopsis thaliana . *The Plant Cell*, **23**, 69–80. https://doi.org/10.1105/tpc.110.079079

[67] Werner, T. and Schmülling, T. (2009) Cytokinin action in plant development. *Current Opinion in Plant Biology*, **12**, 527–38. https://doi.org/10.1016/j.pbi.2009.07.002

[68] Higuchi, M., Pischke, M.S., Mahonen, A.P., Miyawaki, K., Hashimoto, Y., Seki, M. et al. (2004) In planta functions of the Arabidopsis cytokinin receptor family. *Proceedings of the National Academy of Sciences*, **101**, 8821–6. https://doi.org/10.1073/pnas.0402887101

[69] Kojima, M., Hwang, I., Paek, K.-H., Choi, J., Huh, S.U. and Sakakibara, H. (2010) The Cytokinin-Activated Transcription Factor ARR2 Promotes Plant Immunity via TGA3/NPR1-Dependent Salicylic Acid Signaling in Arabidopsis. *Developmental Cell*, **19**, 284–95. https://doi.org/10.1016/j.devcel.2010.07.011

[70] Argueso, C.T., Ferreira, F.J., Epple, P., To, J.P.C., Hutchison, C.E., Schaller, G.E. et al. (2012) Two-component elements mediate interactions between cytokinin and salicylic acid in plant immunity. *PLoS Genetics*, **8**. https://doi.org/10.1371/journal.pgen.1002448

[71] Naseem, M., Kaltdorf, M., Hussain, A. and Dandekar, T. (2013) The impact of cytokinin on jasmonate-salicylate antagonism in Arabidopsis immunity against infection with Pst DC3000. *Plant Signaling and Behavior*, **8**. https://doi.org/10.4161/psb.26791

[72] Arnaud, D., Lee, S., Takebayashi, Y., Choi, D., Choi, J., Sakakibara, H. et al. (2017) Cytokinin-Mediated Regulation of Reactive Oxygen Species Homeostasis Modulates Stomatal Immunity in Arabidopsis. *The Plant Cell*, **29**, 543–59. https://doi.org/10.1105/tpc.16.00583

[73] Collette, L., Hodgkin, T., Kassam, A., Kenmore, P., Lipper, L., Nolte, C. et al. (2001) Save and grow. FAO 2011.

[74] Global, T.H.E., For, D. and Increasing, I.S. (2009) Why Study Plants? *The Plant Cell*, **21**. https://doi.org/10.1105/tpc.109.tt1009

[75] Demmig-Adams, B., Stewart, J.J., Baker, C.R. and Adams, W.W. (2018) Optimization of photosynthetic productivity in contrasting environments by regulons controlling plant form and function. *International Journal of Molecular Sciences*, **19**. https://doi.org/10.3390/ijms19030872

[76] Huner, N.P.A., Öquist, G. and Sarhan, F. (1998) Energy balance and acclimation to light and cold. *Trends in Plant Science*, **3** (6), 224-230.

[77] Noctor, G., Arisi, A.C.M., Jouanin, L., Kunert, K.J., Rennenberg, H. and Foyer, C.H. (1998) Glutathione: Biosynthesis, metabolism and relationship to stress tolerance explored in transformed plants. *Journal of Experimental Botany*, **49**, 623–47. https://doi.org/10.1093/jxb/49.321.623

[78] Gómez, R., Vicino, P., Carrillo, N., Lodeyro, A.F., Gómez, R., Vicino, P. et al. (2019) Critical Reviews in Biotechnology Manipulation of oxidative stress responses as a strategy to generate stress-tolerant crops . From damage to signaling to tolerance stress-tolerant crops. From damage to signaling to tolerance. *Critical Reviews in Biotechnology*, **0**, 1–16. https://doi.org/10.1080/07388551.2019.1597829

[79] Domínguez-Ferreras, A., Kiss-Papp, M., Jehle, A.K., Felix, G. and Chinchilla, D. (2015) An Overdose of the Arabidopsis Coreceptor BRASSINOSTEROID INSENSITIVE1-ASSOCIATED RECEPTOR KINASE1 or Its Ectodomain Causes Autoimmunity in a SUPPRESSOR OF BIR1-1-Dependent Manner. *Plant Physiology*, **168**, 1106–21. https://doi.org/10.1104/pp.15.00537

[80] Albrecht, T. and Argueso, C.T. (2017) Should I fight or should I grow now? The role of cytokinins in plant growth and immunity and in the growth-defence trade-off. *Annals of Botany*, **119**, 725–35. https://doi.org/10.1093/aob/mcw211

[81] Vyska, M., Cunniffe, N., Gilligan, C. and Vyska, M. (2016) Trade-off between disease resistance and crop yield: a landscape-scale mathematical modelling perspective. *J. R. Soc. Interface*, **13**, 1-9.

[82] Jones, J.D.G. (2011) Why genetically modified crops? *Philosophical Transactions of the Royal Society A: Mathematical, Physical and Engineering Sciences*, **369**, 1807–16. https://doi.org/10.1098/rsta.2010.0345

[83] Boyes, D.C., Zayed, A.M., Ascenzi, R., McCaskill, A.J., Hoffman, N.E., Davis, K.R. et al. (2001) Growth stage-based phenotypic analysis of Arabidopsis: a model for high throughput functional genomics in plants. *The Plant Cell*, **13**, 1499–510.

[84] Nakagawa, T., Suzuki, T., Murata, S., Nakamura, S., Hino, T., Maeo, K. et al. (2007) Improved gateway binary vectors: High-performance vectors for creation of fusion constructs in transgenic analysis of plants. *Bioscience, Biotechnology and Biochemistry*, **71**, 2095–100. https://doi.org/10.1271/bbb.70216

[85] Clough, S.J. and Bent, A.F. (1999) Floral dip: a simplified method for Agrobacterium-mediated transformation of Arabidopsis thaliana. *The Plant Journal* **16**, 735–43.

[86] O'Connell, J. The Basics of RT-PCR: Some Practical Considerations. *RT-PCR Protocols*, Humana Press, New Jersey. p 019–25. https://doi.org/10.1385/1-59259-283-X:019

[87] Czechowski, T., Stitt, M., Altmann, T. and Udvardi, M.K. (2005) Genome-Wide Identification and Testing of Superior Reference Genes for Transcript Normalization. *Plant Physiol.***139**, 5–17. https://doi.org/10.1104/pp.105.063743.1

[88] Ishiga, Y., Ishiga, T., Uppalapati, S.R. and Mysore, K.S. (2011) Arabidopsis seedling flood-inoculation technique: a rapid and reliable assay for studying plant-bacterial interactions. *Plant Methods*, **7**, 32. https://doi.org/10.1186/1746-4811-7-32

[89] Klewer, Luerssen, Graf and Siemens. (2001) Restriction Fragment Length Polymorphism Markers to Characterize Plasmodiophora brassicae Single-spore Isolates with Different Virulence Patterns. *Journal of Phytopathology*, **149**, 121–7. https://doi.org/10.1046/j.1439-0434.2001.00595.x

[90] Siemens, J., Nagel, M., Ludwig-Müller, J. and Sacristán, M.D. (2002) The interaction of Plasmodiophora brassicae and Arabidopsis thaliana: Parameters for disease quantification and screening of mutant lines. *Journal of Phytopathology*, **150**, 592–605. https://doi.org/10.1046/j.1439-0434.2002.00818.x

[91] Steinebrunner, I., Landschreiber, M., Krause-buchholz, U., Teichmann, J. and Ro, G. (2011) HCC1, the Arabidopsis homologue of the yeast mitochondrial copper chaperone SCO1, is essential for embryonic development. *J. Exp. Bot*, **62**, 319–30. https://doi.org/10.1093/jxb/erq269

[92] Martínez-García, J.F., Monte, E. and Quail, P.H. (1999) A simple, rapid and quantitative method for preparing Arabidopsis protein extracts for immunoblot analysis. *The Plant Journal*, **20**, 251–7. https://doi.org/10.1046/j.1365-313x.1999.00579.x

[93] Maxwell, K. and Johnson, G.N. (2000) Chlorophyll fluorescence—a practical guide. *J. Exp. Bot*, **51**, 659–68.

[94] Baker, N.R. (2008) Chlorophyll Fluorescence: A Probe of Photosynthesis In Vivo. *Annu. Rev. Plant Biol.*, **59**, 89-113. https://doi.org/10.1146/annurev.arplant.59.032607.092759

[95] Welchen, E., Hildebrandt, T.M., Lewejohann, D., Gonzalez, D.H. and Braun, H. (2012) Biochimica et Biophysica Acta Lack of cytochrome c in Arabidopsis decreases stability of Complex IV and modi fi es redox metabolism without affecting Complexes I and III. *Biochim. Biophys. Acta*, **1817**, 990–1001. https://doi.org/10.1016/j.bbabio.2012.04.008

[96] Hoyerova, K., Gaudinova, A., Malbeck, J., Dobrev, P., Kocabek, T., Solcova, B. et al. (2006) Efficiency of different methods of extraction and purification of cytokinins. *Phytochemistry*, **67**, 1151–9. https://doi.org/10.1016/j.phytochem.2006.03.010

[97] Dobrev, P.I. (2002) Fast and efficient separation of cytokinins from auxin and abscisic acid and their purification using mixed-mode solid-phase. *J. Chromatogr. A,* **950**, 21–9.

[98] Hull, G.A. and Devic, M. (1987) The ß-Glucuronidase (gus) Reporter Gene System Gene: Fusions; Spectrophotometric, Fluorometric, and Histochemical Detection. *Plant Gene Transfer and Expression Protocols*, Humana Press, New Jersey. p. 125–42. https://doi.org/10.1385/0-89603-321-X:125

[99] Jefferson, R.A., Kavanagh, T.A. and Bevan, M.W. (1987) GUS fusions: ,B-glucuronidase as a sensitive and versatile gene fusion marker in higher plants. *The EMBO Journal,* **6** (13), 3901–7.

[100] Sedmakand, J.J. and Grossberg, S.E. (1977) A Rapid, Sensitive , and Versatile Assay for Protein Using Coomassie Brilliant Blue G250. *Analytical Biochemistry,* **79**, 544–52.

[101] Boratyn, G.M., Camacho, C., Cooper, P.S., Coulouris, G., Fong, A., Ma, N. et al. (2013) BLAST: a more efficient report with usability improvements. *Nucleic Acids Research*, **41**, 29–33. https://doi.org/10.1093/nar/gkt282

[102] Sievers, F., Wilm, A., Dineen, D., Gibson, T.J., Karplus, K., Li, W. et al. (2011) Fast, scalable generation of high-quality protein multiple sequence alignments using Clustal Omega. *Molecular Systems Biology*, **7**. https://doi.org/10.1038/msb.2011.75

[103] Goodstein, D.M., Shu, S., Howson, R., Neupane, R., Hayes, R.D., Fazo, J. et al. (2012) Phytozome: a comparative platform for green plant genomics. *Nucleic Acids Research*, **40**, 1178–86. https://doi.org/10.1093/nar/gkr944

[104] Löytynoja, A. and Goldman, N. (2010) webPRANK : a phylogeny-aware multiple sequence aligner with interactive alignment browser webPRANK : a phylogeny-aware multiple sequence aligner with interactive alignment browser. *BMC Bioinformatics,* **11**, 1-7.

[105] Gouy, M., Guindon, S. and Gascuel, O. (2010) SeaView Version 4: A Multiplatform Graphical User Interface for Sequence Alignment and Phylogenetic Tree Building. *Molecular Biology and Evolution*, **27**, 221–4. https://doi.org/10.1093/molbev/msp259

[106] Delport, W., Poon, A.F.Y., Frost, S.D.W. and Pond, S.L.K. (2010) Datamonkey 2010: a suite of phylogenetic analysis tools for evolutionary biology. *Bioinformatics*, **26**, 2455–7. https://doi.org/10.1093/bioinformatics/btq429

[107] Letunic, I. and Bork, P. (2016) Interactive tree of life (iTOL) v3 : an online tool for the display and annotation of phylogenetic and other trees. *Nucleic Acids Research*, **44**, 242–5. https://doi.org/10.1093/nar/gkw290

[108] Kiefer, F., Arnold, K. and Ku, M. (2009) The SWISS-MODEL Repository and associated resources. *Nucleic Acids Research*, **37**, 387–92. https://doi.org/10.1093/nar/gkn750

[109] El-Gebali, S., Mistry, J., Bateman, A., Eddy, S.R., Luciani, A., Potter, S.C. et al. (2019) The Pfam protein families database in 2019. *Nucleic Acids Research*, **47**, D427–32. https://doi.org/10.1093/nar/gky995

[110] Finelli, M.J. and Oliver, P.L. (2017) TLDc proteins: new players in the oxidative stress response and neurological disease. *Mammalian Genome*, **28**, 395–406. https://doi.org/10.1007/s00335-017-9706-7

[111] Maki, M., Kitaura, Y., Satoh, H., Ohkouchi, S. and Shibata, H. (2002) Structures, functions and molecular evolution of the penta-EF-hand Ca 2+-binding proteins. *Biochimica et Biophysica Acta - Proteins and Proteomics*, **1600**, 51–60. https://doi.org/10.1016/S1570-9639(02)00444-2

[112] Fukasawa, Y., Tsuji, J., Fu, S.-C., Tomii, K., Horton, P. and Imai, K. (2015) MitoFates: Improved Prediction of Mitochondrial Targeting Sequences and Their Cleavage Sites. *Molecular & Cellular Proteomics*, **14**, 1113–26. https://doi.org/10.1074/mcp.m114.043083

[113] Hooper, C.M., Castleden, I.R., Tanz, S.K., Aryamanesh, N. and Millar, A.H. (2017) SUBA4: The interactive data analysis centre for Arabidopsis subcellular protein locations. *Nucleic Acids Research*, **45**, D1064–74. https://doi.org/10.1093/nar/gkw1041

[114] Schwacke, R. (2003) ARAMEMNON, a Novel Database for Arabidopsis Integral Membrane Proteins. *Plant Physiology*, **131**, 16–26. https://doi.org/10.1104/pp.011577

[115] Fankhauser, N. and Mäser, P. (2005) Identification of GPI anchor attachment signals by a Kohonen self-organizing map. *Bioinformatics*, **21**, 1846–52. https://doi.org/10.1093/bioinformatics/bti299

[116] Nelson, B.K., Cai, X. and Nebenführ, A. (2007) A multicolored set of in vivo organelle markers for co-localization studies in Arabidopsis and other plants. *Plant Journal*, **51**, 1126–36. https://doi.org/10.1111/j.1365-313X.2007.03212.x

[117] Onouchi, H., Igeño, M.I., Périlleux, C., Graves, K. and Coupland, G. (2000) Mutagenesis of plants overexpressing CONSTANS demonstrates novel interactions among Arabidopsis flowering-time genes. *The Plant Cell*, **12**, 885–900.

[118] Gómez-Mena, C., Piñeiro, M., Franco-Zorrilla, J.M., Salinas, J., Coupland, G. and Martínez-Zapater, J.M. (2001) early bolting in short days: an Arabidopsis mutation that causes early flowering and partially suppresses the floral phenotype of leafy. *The Plant Cell*, **13**, 1011–24.

[119] Steffen, A., Elgner, M. and Staiger, D. (2019) Regulation Of Flowering Time By The RNA-binding Proteins AtGRP7 And AtGRP8 *Plant Cell Physiol*, **60** (9), 2040-2050, https://doi.org/10.1093/pcp/pcz124

[120] Wei, B., Zhang, W., Chao, J., Zhang, T., Zhao, T., Noctor, G. et al. (2017) Functional analysis of the role of hydrogen sulfide in the regulation of dark-induced leaf senescence in Arabidopsis. *Scientific Reports*, **7**, 1–16. https://doi.org/10.1038/s41598-017-02872-0

[121] Colombatti, F., Mencia, R., Garcia, L., Mansilla, N., Alemano, S., Andrade, A.M. et al. (2019) The mitochondrial oxidation resistance protein AtOXR2 increases plant biomass and tolerance to oxidative stress. *Journal of Experimental Botany*, **70**, 3177–95. https://doi.org/10.1093/jxb/erz147

[122] Brand, M.D. and Nicholls, D.G. (2015) Assessing mitochondrial dysfunction in cells. *Biochemical Journal*, **437**, 575.1-575. https://doi.org/10.1042/bj4370575u

[123] Cui, F., Brosché, M., Shapiguzov, A., He, X.Q., Vainonen, J.P., Leppälä, J. et al. (2019) Interaction of methyl viologen-induced chloroplast and mitochondrial signalling in Arabidopsis. *Free Radical Biology and Medicine*, **134**, 555–66. https://doi.org/10.1016/j.freeradbiomed.2019.02.006

[124] Alexandre, A. and Lehninger, A.L. (1984) Bypasses of the antimycin A block of mitochondrial electron transport in relation to ubisemiquinone function. *Biochimica et Biophysica Acta (BBA) - Bioenergetics*, **767**, 120–9. https://doi.org/10.1016/0005-2728(84)90086-0

[125] Van Aken, O., Zhang, B., Carrie, C., Uggalla, V., Paynter, E., Giraud, E. et al. (2009) Defining the mitochondrial stress response in arabidopsis thaliana. *Molecular Plant*, **2**, 1310–24. https://doi.org/10.1093/mp/ssp053

[126] Plaxton, W.C. and Podestá, F.E. (2006) The functional organization and control of plant respiration. *Critical Reviews in Plant Sciences*, **25**, 159–98. https://doi.org/10.1080/07352680600563876

[127] Millenaar, F.F. and Lambers, H. (2002) The Alternative Oxidase: in vivo Regulation and Function. *Plant Biology*, **5**, 2–15.

[128] Finelli, M.J., Liu, K.X., Wu, Y., Oliver, P.L. and Davies, K.E. (2015) Oxr1 improves pathogenic cellular features of ALS-associated FUS and TDP-43 mutations. *Human Molecular Genetics*, **24**, 3529–44. https://doi.org/10.1093/hmg/ddv104

[129] Wiedemann, N. and Pfanner, N. (2017) Mitochondrial Machineries for Protein Import and Assembly. *Annual Review of Biochemistry*, **86**, 685–714. https://doi.org/10.1146/annurev-biochem-060815-014352

[130] Tateda, C., Watanabe, K., Kusano, T. and Takahashi, Y. (2011) Molecular and genetic characterization of the gene family encoding the voltage-dependent anion channel in Arabidopsis. *Journal of Experimental Botany*, **62**, 4773–85. https://doi.org/10.1093/jxb/err113

[131] Zhang, B., Van Aken, O., Thatcher, L., De Clercq, I., Duncan, O., Law, S.R. et al. (2014) The mitochondrial outer membrane AAA ATPase AtOM66 affects cell death and pathogen resistance in Arabidopsis thaliana. *Plant Journal*, **80**, 709–27. https://doi.org/10.1111/tpj.12665

[132] Fuchs, R., Kopischke, M., Klapprodt, C., Hause, G., Meyer, A.J., Schwarzländer, M. et al. (2016) Immobilized subpopulations of leaf epidermal mitochondria mediate PEN2-dependent pathogen entry control in Arabidopsis. *The Plant Cell*, **28**, TPC2015-00887-RA. https://doi.org/10.1105/tpc.15.00887

[133] Chris, C. and Whelan, J. (2013) Widespread dual targeting of proteins in land plants. Plant Signaling & Behavior, **8**, 1–13.

[134] Racca, S., Welchen, E., Gras, D.E., Tarkowská, D., Turečková, V., Maurino, V.G. et al. (2018) Interplay between cytochrome c and gibberellins during Arabidopsis vegetative development. *Plant Journal*, **94**, 105–21. https://doi.org/10.1111/tpj.13845

[135] Jiang, C., Tholen, D., Xu, J.M., Xin, C., Zhang, H., Zhu, X. et al. (2014) Increased expression of mitochondria-localized carbonic anhydrase activity resulted in an increased biomass accumulation in Arabidopsis thaliana. *Journal of Plant Biology*, **57**, 366–74. https://doi.org/10.1007/s12374-014-0330-8

[136] Lee, C.P., Grigory Maksaev, Jensen, G.S., Murcha, M.W., Wilson, M.E., Fricker, M. et al. (2017) MSL1 is a mechanosensitive ion channel that dissipates mitochondrial

membrane potential and maintains redox homeostasis in mitochondria during abiotic stress. *J Autism Dev Disord*, **47**, 549–62. https://doi.org/10.1097/CCM.0b013e31823da96d.Hydrogen

[137] Smith, A.M.O., Ratcliffe, R.G. and Sweetlove, L.J. (2004) Activation and Function of Mitochondrial Uncoupling Protein in Plants. *J Bio. Chem*, **279**, 51944–52. https://doi.org/10.1074/jbc.M408920200

[138] Akter, S., Huang, J., Waszczak, C., Jacques, S., Gevaert, K., Van Breusegem, F. et al. (2015) Cysteines under ROS attack in plants: A proteomics view. *Journal of Experimental Botany*, **66**, 2935–44. https://doi.org/10.1093/jxb/erv044

[139] Vaahtera, L., Brosché, M., Wrzaczek, M. and Kangasjärvi, J. (2013) Specificity in ROS Signaling and Transcript Signatures. *Antioxidants & Redox Signaling*, **21**, 1422–41. https://doi.org/10.1089/ars.2013.5662

[140] Mittler, R., Vanderauwera, S., Suzuki, N., Miller, G., Tognetti, V.B., Vandepoele, K. et al. (2011) ROS signaling: The new wave? *Trends in Plant Science*, **16**, 300–9. https://doi.org/10.1016/j.tplants.2011.03.007

[141] Mullineaux, P.M., Exposito-Rodriguez, M., Laissue, P.P. and Smirnoff, N. (2018) ROS-dependent signalling pathways in plants and algae exposed to high light: Comparisons with other eukaryotes. *Free Radical Biology and Medicine*, **122**, 52–64. https://doi.org/10.1016/j.freeradbiomed.2018.01.033

[142] Hossain, M.A., Bhattacharjee, S., Armin, S.-M., Qian, P., Xin, W., Li, H.-Y. et al. (2015) Hydrogen peroxide priming modulates abiotic oxidative stress tolerance: insights from ROS detoxification and scavenging. *Frontiers in Plant Science*, **6**, 1–19. https://doi.org/10.3389/fpls.2015.00420

[143] Crawford, T., Lehotai, N. and Strand, Å. (2018) The role of retrograde signals during plant stress responses. *Journal of Experimental Botany*, **69**, 2783–95. https://doi.org/10.1093/jxb/erx481

[144] Svistunova, D.M., Simon, J.N., Rembeza, E., Crabtree, M., Yue, W.W., Oliver, P.L. et al. (2019) Oxidation resistance 1 regulates post-translational modifications of peroxiredoxin 2 in the cerebellum. *Free Radical Biology and Medicine*, **130**, 151–62. https://doi.org/10.1016/j.freeradbiomed.2018.10.447

[145] Tognetti, V.B., Van Aken, O., Morreel, K., Vandenbroucke, K., van de Cotte, B., De Clercq, I. et al. (2010) Perturbation of Indole-3-Butyric Acid Homeostasis by the UDP-Glucosyltransferase UGT74E2 Modulates Arabidopsis Architecture and Water Stress Tolerance. *The Plant Cell*, **22**, 2660–79. https://doi.org/10.1105/tpc.109.071316

[146] Xun, K., Mabbitt, P.D., Yin, S., Mueller, J.W., Nisar, N. and Gigolashvili, T. (2016) Sensing and signaling of oxidative stress in chloroplasts by inactivation of the SAL1 phosphoadenosine phosphatase. *PNAS*, 4567–76. https://doi.org/10.1073/pnas.1604936113

[147] Zhang, L., Oh, Y., Li, H., Baldwin, I.T. and Galis, I. (2012) Alternative Oxidase in Resistance to Biotic Stresses: Nicotiana attenuata AOX Contributes to Resistance to a Pathogen and a Piercing-Sucking Insect But Not Manduca sexta Larvae. *Plant Physiology*, **160**, 1453–67. https://doi.org/10.1104/pp.112.200865

[148] Vanlerberghe, G.C. (2013) Alternative oxidase: A mitochondrial respiratory pathway to maintain metabolic and signaling homeostasis during abiotic and biotic stress in plants. *International Journal of Molecular Sciences*, **14**, 6805–47. https://doi.org/10.3390/ijms14046805

[149] Mou, Z., Fan, W. and Dong, X. (2003) Inducers of Plant Systemic Acquired Resistance Regulate NPR1 Function through Redox Changes. *Cell*, **113**, 935–44. https://doi.org/10.1016/S0092-8674(03)00429-X

[150] Diederichsen, E., Frauen, M. and Ludwig-Müller, J. (2014) Special Issue: Clubroot disease management challenges from a German perspective. *Canadian Journal of Plant Pathology*, **36**, 85–98. https://doi.org/10.1080/07060661.2013.861871

[151] Gibala, M., Kicia, M., Sakamoto, W., Gola, E.M., Kubrakiewicz, J., Smakowska, E. et al. (2009) The lack of mitochondrial AtFtsH4 protease alters Arabidopsis leaf morphology at the late stage of rosette development under short-day photoperiod. *Plant Journal*, **59**, 685–99. https://doi.org/10.1111/j.1365-313X.2009.03907.x

[152] Van Aken, O., Zhang, B., Law, S., Narsai, R. and Whelan, J. (2013) AtWRKY40 and AtWRKY63 Modulate the Expression of Stress-Responsive Nuclear Genes Encoding Mitochondrial and Chloroplast Proteins. *Plant Physiology*, **162**, 254–71. https://doi.org/10.1104/pp.113.215996

[153] Zurcher, E., Tavor-Deslex, D., Lituiev, D., Enkerli, K., Tarr, P.T. and Muller, B. (2013) A Robust and Sensitive Synthetic Sensor to Monitor the Transcriptional Output of the Cytokinin Signaling Network in Planta. *Plant Physiology*, **161**, 1066–75. https://doi.org/10.1104/pp.112.211763

[154] Miyawaki, K., Tarkowski, P., Matsumoto-Kitano, M., Kato, T., Sato, S., Tarkowska, D. et al. (2006) Roles of Arabidopsis ATP/ADP isopentenyltransferases and tRNA isopentenyltransferases in cytokinin biosynthesis. *Proceedings of the National Academy of Sciences*, **103**, 16598–603. https://doi.org/10.1073/pnas.0603522103

[155] Hutchison, C.E., Li, J., Argueso, C., Gonzalez, M., Lee, E., Lewis, M.W. et al. (2006) The Arabidopsis Histidine Phosphotransfer Proteins Are Redundant Positive Regulators of Cytokinin Signaling. *The Plant Cell Online*, **18**, 3073–87. https://doi.org/10.1105/tpc.106.045674

[156] Werner, T. (2003) Cytokinin-Deficient Transgenic Arabidopsis Plants Show Multiple Developmental Alterations Indicating Opposite Functions of Cytokinins in the Regulation of Shoot and Root Meristem Activity. *The Plant Cell Online*, **15**, 2532–50. https://doi.org/10.1105/tpc.014928

[157] Brandt, S.M., Jaramillo-Gutierrez, G., Kumar, S., Barillas-Mury, C. and Schneider, D.S. (2008) Use of a Drosophila model to identify genes regulating plasmodium growth in the mosquito. *Genetics*, **180**, 1671–8. https://doi.org/10.1534/genetics.108.089748

[158] Wang, Z., Berkey, C.D. and Watnick, P.I. (2012) The Drosophila Protein Mustard Tailors the Innate Immune Response Activated by the Immune Deficiency Pathway. *The Journal of Immunology*, **188**, 3993–4000. https://doi.org/10.4049/jimmunol.1103301

[159] Jaramillo-Gutierrez, G., Rodrigues, J., Ndikuyeze, G., Povelones, M., Molina-Cruz, A. and Barillas-Mury, C. (2009) Mosquito immune responses and compatibility between

Plasmodium parasites and anopheline mosquitoes. *BMC Microbiology*, **9**, 1–11. https://doi.org/10.1186/1471-2180-9-154

[160] Mei Yan, C.L. (2014) Delivering Oxidation Resistance-1 (OXR1) to Mouse Kidney by Genetic Modified Mesenchymal Stem Cells Exhibited Enhanced Protection against Nephrotoxic Serum Induced Renal Injury and Lupus Nephritis. *Journal of Stem Cell Research & Therapy*, **04**. https://doi.org/10.4172/2157-7633.1000231

[161] van Hulten, M., Pelser, M., van Loon, L.C., Pieterse, C.M.J. and Ton, J. (2006) Costs and benefits of priming for defense in Arabidopsis. *Proceedings of the National Academy of Sciences*, **103**, 5602–7. https://doi.org/10.1073/pnas.0510213103

[162] Straus, M.R., Rietz, S., Ver Loren Van Themaat, E., Bartsch, M. and Parker, J.E. (2010) Salicylic acid antagonism of EDS1-driven cell death is important for immune and oxidative stress responses in Arabidopsis. *Plant Journal*, **62**, 628–40. https://doi.org/10.1111/j.1365-313X.2010.04178.x

[163] Rivas-San Vicente, M. and Plasencia, J. (2011) Salicylic acid beyond defence: Its role in plant growth and development. *Journal of Experimental Botany*, **62**, 3321–38. https://doi.org/10.1093/jxb/err031

[164] Lu, H., Greenberg, J.T. and Holuigue, L. (2016) Salicylic Acid Signaling Networks. *Front. Plant Science*. https://doi.org/10.3389/978-2-88919-827-6

[165] Ha, S., Vankova, R., Yamaguchi-Shinozaki, K., Shinozaki, K. and Tran, L.S.P. (2012) Cytokinins: Metabolism and function in plant adaptation to environmental stresses. *Trends in Plant Science*, **17**, 172–9. https://doi.org/10.1016/j.tplants.2011.12.005

[166] Bartrina, I., Jensen, H., Novák, O., Strnad, M., Werner, T. and Schmülling, T. (2017) Gain-of-Function Mutants of the Cytokinin Receptors AHK2 and AHK3 Regulate Plant Organ Size, Flowering Time and Plant Longevity. *Plant Physiology*, **173**, 1783–97. https://doi.org/10.1104/pp.16.01903

[167] Schmülling, T., Werner, T., Riefler, M., Krupková, E. and Bartrina Y Manns, I. (2003) Structure and function of cytokinin oxidase/dehydrogenase genes of maize, rice, Arabidopsis and other species. *Journal of Plant Research*, **116**, 241–52. https://doi.org/10.1007/s10265-003-0096-4

[168] Niemann, M.C.E., Weber, H., Hluska, T., Leonte, G., Anderson, S.M., Novák, O. et al. (2018) The Cytokinin Oxidase/Dehydrogenase CKX1 Is a Membrane-Bound Protein Requiring Homooligomerization in the Endoplasmic Reticulum for Its Cellular Activity. *Plant Physiology*, **176**, 2024–39. https://doi.org/10.1104/pp.17.00925

[169] Frébort, I., Kowalska, M., Hluska, T., Frébortová, J. and Galuszka, P. (2011) Evolution of cytokinin biosynthesis and degradation. *Journal of Experimental Botany*, **62**, 2431–52. https://doi.org/10.1093/jxb/err004

[170] Gagne, J.M. and Clark, S.E. (2010) The Arabidopsis Stem Cell Factor POLTERGEIST Is Membrane Localized and Phospholipid Stimulated. *The Plant Cell*, **22**, 729–43. https://doi.org/10.1105/tpc.109.068734

[171] Charrier, B., Champion, A., Henry, Y. and Kreis, M. (2002) Expression Profiling of the Whole Arabidopsis Shaggy-Like Kinase Multigene Family by Real-Time Reverse

Transcriptase-Polymerase Chain Reaction. *Plant Physiology*, **130**, 577–90. https://doi.org/10.1104/pp.009175

[172] Colombatti, F. (2016) Estudios funcionales de proteínas mitocondriales de arabidopsis relacionadas con los mecanismos de defensa generados por estrés biótico y abiótico. Phd Thesis, FBCB-UNL. URI: http://hdl.handle.net/11185/1037

[173] Ha, S., Vankova, R., Yamaguchi-Shinozaki, K., Shinozaki, K., Tran, L. (2012) Cytokinins: metabolism and function in plant adaptation to environmental stresses. *Trends in Plant Sci.*, **17** (3), 172-179. https://doi.org/10.1016/j.tplants.2011.12.005

[174] Forsyth, A., Mansfield, J.W., Grabov, N., Torres, M. De, Sinapidou, E. and Grant, M.R. (2010) Genetic dissection of basal resistance to Pseudomonas syringae pv. phaseolicola in accessions of Arabidopsis. *Molecular Plant-Microbe Interactions*, **23**, 1545–52. https://doi.org/10.1094/MPMI-02-10-0047

[175] Traw, M.B., Kim, J., Enright, S., Cipollini, D.F. and Bergelson, J. (2003) Negative cross-talk between salicylate- and jasmonate-mediated pathways in the Wassilewskija ecotype of Arabidopsis thaliana. *Molecular Ecology*, **12**, 1125–35. https://doi.org/10.1046/j.1365-294X.2003.01815.x

[176] Rutter, B.D. and Innes, R.W. (2017) Extracellular vesicles isolated from the leaf apoplast carry stress-response proteins. *Plant Physiology*, **173**, 728–41. https://doi.org/10.1104/pp.16.01253

[177] Kimura, S., Waszczak, C., Hunter, K. and Wrzaczek, M. (2017) Bound by Fate: The Role of Reactive Oxygen Species in Receptor-Like Kinase Signaling. *The Plant Cell*, **29**, 638–54. https://doi.org/10.1105/tpc.16.00947

[178] Trentin, A.R., Pivato, M., Mehdi, S.M.M., Barnabas, L.E., Giaretta, S., Fabrega-Prats, M. et al. (2015) Proteome readjustments in the apoplastic space of arabidopsis thaliana ggt1 mutant leaves exposed to UV-B radiation. *Frontiers in Plant Science*, **6**, 1–12. https://doi.org/10.3389/fpls.2015.00128

[180] Zhang, H., Xie, X., Kim, M.S., Kornyeyev, D.A., Holaday, S. and Paré, P.W. (2008) Soil bacteria augment Arabidopsis photosynthesis by decreasing glucose sensing and abscisic acid levels in planta. *Plant Journal*, **56**, 264–73. https://doi.org/10.1111/j.1365-313X.2008.03593.x

[181] Van Tol, N., Rolloos, M., Augustijn, D., Alia, A., De Groot, H.J., Hooykaas, P.J.J. et al. (2017) An Arabidopsis mutant with high operating efficiency of Photosystem II and low chlorophyll fluorescence. *Scientific Reports*, Springer US. **7**, 1–15. https://doi.org/10.1038/s41598-017-03611-1

[182] Kuroha, T., Tokunaga, H., Kojima, M., Ueda, N., Ishida, T., Nagawa, S. et al. (2009) Functional Analyses of LONELY GUY Cytokinin-Activating Enzymes Reveal the Importance of the Direct Activation Pathway in Arabidopsis. *The Plant Cell*, **21**, 3152–69. https://doi.org/10.1105/tpc.109.068676

7. Appendix

7.1 Plants lines used in this study

Table A1: List of Arabidopsis mutants and overexpression lines used in this study. Lines obtained during this thesis are signalled as Agrobacterium transformation or crosses.

Name	Characteristic	ABRC* code	Source
OXR2	Line overexpressing *AtOXR2*		Agrobacterium transformation [121]
Wt	Wild type ecotype Columbia		ABRC
oxr2.2	T-DNA mutant in AtOXR2	SK17762	ABRC
oxr2.1	T-DNA mutant in *AtOXR2*, ecotype Wassilewskija	Flag_510D06	ABRC
Wt (ws)	Wild type ecotype Wassilewskija		ABRC
mito-GFP	Contains mitochondria targeted with GFP		ABRC [116]
AtOXR2-mRFP	Line overexpressing *AtOXR2* fused to mRFP		Agrobacterium transformation
AtOXR2-mRFP+mito-GFP	Line overexpressing *AtOXR2* fused to mRFP in background with GFP-marked mitochondria		Agrobacterium transformation
AtOXR1-GFP	Line overexpressing *AtOXR2* fused to GPF		Agrobacterium transformation
NPR1-GFP	Line overexpressing *NPR1* fused to GFP		Agrobacterium transformation
NPR1-GFP+OXR2	Line overexpressing *AtOXR2* and *NPR1* fused to GFP		Agrobacterium transformation
NPR1-GFP+*oxr2.2*	T-DNA mutant for *AtOXR2* overexpressing and NPR1 fused to GFP		Agrobacterium transformation
sid2	Loss of function in *ICS1*, fails in SA syntheses		ABRC
npr1	Loss of function in *NPR1*, fails in SA signalling		ABRC
*sid2*xOXR2	Line overexpressing *AtOXR2* and loss of function in *ICS1*		Crossing
*npr1*xOXR2	Line overexpressing AtOXR2 and loss of function in *NPR1*		Crossing
TCS::GFP	CKs fluorescent sensor		[153]
TCS::GFPxOXR2	Line overexpressing *AtOXR2* and expressing a CKs fluorescent sensor		Crossing

TCS::GFPx*oxr2.2*	T-DNA mutant for *AtOXR2* expressing a CKs fluorescent sensor		Crossing
pARR5::GUS	Promotor region of the negative CKs regulator *ARR5* leading *GUS* expression	CS25261	ABRC
pARR5::GUS+OXR2	Line overexpressing *AtOXR2* and expression the promotor region of the negative CKs regulator *ARR5* leading *GUS* expression		Agrobacterium transformation
pARR15::GUS	Promotor region of the negative CKs regulator *ARR15* leading *GUS* expression		ABRC
pARR15::GUS+OXR2	Line overexpressing *AtOXR2* and expression the promotor region of the negative CKs regulator *ARR15* leading *GUS* expression		Agrobacterium transformation
ipt1357	Loss-of-function in CKs syntheses genes *IPT1*, *IPT3*, *IPT5* and *IPT7*		Provided by Dr. Kakimoto, [154]
ipt1357+OXR2	Line overexpressing *AtOXR2* and with loss-of-function in CKs syntheses genes *IPT1*, *IPT3*, *IPT5* and *IPT7*		Agrobacterium transformation
ahp1234	Loss-of-function in CKs signalling genes *AHP1*, *AHP2*, *AHP3* and *AHP4*	CS860163	ABRC
ahp1234+OXR2	Line overexpressing *AtOXR2* and with loss-of-function in CKs signalling genes *AHP1*, *AHP2*, *AHP3* and *AHP4*		Agrobacterium transformation
CKX1	Line overexpressing an enzyme of the CKs catabolic pathway *CKX1*		Provided by Dr. Schmülling [167]
CKX1xOXR2	Line overexpressing an enzyme of the CKs catabolic pathway *CKX1* and *AtOXR2*		Crossing
CKX2	Line overexpressing an enzyme of the CKs catabolic pathway *CKX2*		Provided by Dr. Schmülling [167]
CKX2xOXR2	Line overexpressing an enzyme of the CKs catabolic pathway *CKX2* and *AtOXR2*		Crossing
CKX2x*oxr2.2*	Line overexpressing an enzyme of the CKs catabolic pathway *CKX2* and loss-of-function in *AtOXR2*		Crossing
pm-gk	Line with GPF-marked plasma membrane	CD3-1003	ABRC [116]
AtOXR5-mRFP	Line overexpressing *AtOXR5* fused to mRFP		Agrobacterium transformation

AtOXR5-mRFP+pm-gk	Line overexpressing *AtOXR5* fused to mRFP in background with GFP-marked apoplastic space		Agrobacterium transformation
OXR5	Line overexpressing of *AtOXR5*		Agrobacterium transformation
oxr5.1	T-DNA mutant in *AtOXR5*	SAIL_205_E11.V1	ABRC
oxr2xoxr5	T-DNA double mutant in *AtOXR2 (oxr2.2)* and *AtOXR5 (oxr5.1)*		Crossing

*(https://abrc.osu.edu/researchers)

7.2 List of primers used in this study

Table A2: List of oligonucleotides used in this study.

Primer Name	Sequence (5' to 3')	Description
pSKTAIL-L3	ATACGACGGATCGTAATTTGTCG	Analysis of T-DNA insertion
FLAG176R	CCTCTTAGGAGTAGGTTGCAG	
OX2insF	GCAAATGGATCTTGTTGTATAGG	
SAIL LB1	GCCTTTTCAGAAATGGATAAATAGCCTTGCTTCC	
attbNPR1-F	GGGGACAAGTTTGTACAAAAAAGCAGGCTATGG ACACCACCATTGATGG	35S::NPR1-GFP cloning
attbNPR1-R	GGGGACCACTTTGTACAAGAAAGCTGGGTTCCC GACGACGATG AGAGAG	
OXr5R-Sal	CGCGTCGACCTTTCATTCATTACCTCTCTT	35S::AtOXR5 and 35S::AtOXR5-RFPcloning
OXr5F-Bam	GCCGGATCCATCATCTTCACCACTATGGGT	
qrtOXR2F	GGCAACAAGTGGACCTTCTGAAAC	Detection of AtOXR2 (At2g05990) transcript by RT-qPCR
qrtOXR2R	GAGACGCATGTGCAAATCCCCAG	
qRTOxr5-F	TCCTTGCCTCACTGAGTGCCTT	Detection of AtOXR5 (At5g39590) transcript by RT-qPCR
qRTOxr5-R	TGGTTCACCGCTATTGCCGGG	
qrtAOX1aF	AGCATCATGTTCCAACGACGTTTC	Detection of AOX1a (At3g22370) transcript by RT-qPCR
qrtAOX1aR	GCTCGACATCCATATCTCCTCTGG	
SAL1-qrtF	TTTCATTGGTGGCTGAAGAGGAC	Detection of SAL1 (At5g63980.1) transcript by RT-qPCR
SAL1-qrtR	TTCCTCGGTAGCCAAAGTGTCG	
UGT74E2-qrtF	TTTCCCTTCGTTCCCGATGCTG	Detection of UGT74E2 (At1g05680.1) transcript by RT-qPCR
UGT74E2-qrtR	TTCGGGTATGAGGACGATTCGC	

HRE3-qrtF	GAAGCGTAAACCCGTCTCAGTG	Detection of HRE3 (At2g47520.1) transcript by RT-qPCR
HRE3-qrtR	ACCTTTGCTCGGGTCACGAATC	
HSP23.5-qrtF	ACTCGTGGAATGGGAGCTTCTG	Detection of HSP23.5 (At5g51440.1) transcript by RT-qPCR
HSP23.5-qrtR	GATGCAACGCGTCGTCTTTCTC	
ANAC013-qrtF	CCTGAGGAATTACCTGAGAAAGCG	Detection of ANAC013 (At1g32870.1) transcript by RT-qPCR
ANAC013-qrtR	CCAATAGCCACGTTCAGTAGCTC	
UPOX-qrtF	TGCCTCAATGGATGAACACAAGAC	Detection of UPOX (At2g21640.1) transcript by RT-qPCR
UPOX-qrtR	GAGAAGCTCCCGAATATCTTGTCC	
qrtSID2F	CTTGGCTAGCACAGTTACAGC	Detection of SID2 (At1g74710) transcript by RT-qPCR
qrtSID2R	ACTGCAGACACCTAATTGAGTC	
qrtEDS1F	ACAGACGGGGAGGTAGATGA	Detection of EDS1 (At3g48090) transcript by RT-qPCR
qrtEDS1R	AGTCTCGCAGAGGAGAATGC	
qrtPR1F	tctggcgtctccgccgtgaac	Detection of PR1 (At2g14610) transcript by RT-qPCR
qrtPR1R	TTTGGCACATCCGAGTCTCACTGAC	
qrtNPR3F	GTGAGTTCACGGGTTTGTCA	Detection of NPR3 (At5g45110) transcript by RT-qPCR
qrtNPR3R	AAAACCTTCGACCAGTCTCAA	
qrtPR5F	GCCGTGGAGCTAACGATAAGCCG	Detection of PR5 (At1g75040) transcript by RT-qPCR
qrtPR5R	GCTCCGGTACAAGTGAAGGTGC	
qrtWRKY15F	ATCATCAACGTCCCTCTGAAACGG	Detection of WRKY15 (At2g23320) transcript by RT-qPCR
qrtWRKY15R	TGAGAAAGACGAGACCGTCGTG	
qrtWRKY33F	AGCTGCTATTGCTGGTCACT	Detection of WRKY33 (At2g38470) transcript by RT-qPCR
qrtWRKY33R	AGGCCCGGTATTAGTGTTGT	
qrtWRKY40F	AGCTTCTGACACTACCCTCGTTG	Detection of WRKY40 (At1g80840) transcript by RT-qPCR
qrtWRKY40R	TTGACAGAACAGCTTGGAGCAC	
qrtWRKY60F	AAGGTGCAACGAAGTGCAGAAG	Detection of WRKY60 (At2g25000) transcript by RT-qPCR
qrtWRKY60R	TGTGGTCCGGTGTGGTTATGTG	
qrtWRKY70F	TGAGCTCGAACCCAAGATGTTCAG	Detection of WRKY70 (At3g56400) transcript by RT-qPCR
qrtWRKY70R	TGCTCTTGGGAGTTTCTGCGTTG	
qrtWRKY75F	AGTGGACCAAGAAGTGGTCGTG	Detection of WRKY75 (At5g13080) transcript by RT-qPCR
qrtWRKY75R	TTCTCGATGGGATGCGAATGCAC	
CKX1-qF	TCACAAGCAACAACAACGGTC	Detection of CKX1 (At2g41510) transcript by RT-qPCR
CKX1-qR	TGCAGAGGGGAGAAAGGCTA	

CKX2-qF	CTTCGGGACTCGCTCTTCTC	Detection of CKX2 (At2g19500) transcript by RT-qPCR
CKX2-qR	CCTTTGGGGTAGCGGATTGT	
CKX3-qF	GAATGATCGGATGTCTGCCG	Detection of CKX3 (At5g56970) transcript by RT-qPCR
CKX3-qR	TCAAAAGCCTCCCAATTGTC	
CKX4-qF	TGACAGAACCACCCTTCCCA	Detection of CKX4 (At5g56970) transcript by RT-qPCR
CKX4-qR	TTCGTTTCGGACACGGTTCA	
IPT5-qF	CACTCGCCGTCGAAAAGTTC	Detection of IPT5 (At5g19040) transcript by RT-qPCR
IPT5-qR	TTACCTCACCGGGAAATCGC	
IPT7-qF	CGCCACTGAGGTGTTCTTGA	Detection of IPT7 (At3g23630) transcript by RT-qPCR
IPT7-qR	TCGACGATTCTCTCGCTTG	
qrtARR1-Fw	GCAGACGGAAACGGTGGTTCA	Detection of ARR1 (At3g16857) transcript by RT-qPCR
qrtARR1-Rv	GCCATCAACCGGTGCAATCCCT	
ARR2-qrtF	AAAGAGTGGCGGAGACAGTGAC	Detection of ARR2 (At4g16110) transcript by RT-qPCR
ARR2-qrtR	GGATGGGATGCCTTCCTGTTTG	
qARR5-F	CCGTTCATTACACGAAGACAAGC	Detection of ARR5 (At3g48100) transcript by RT-qPCR
qARR5-R	TGTAAAGTGTTCCAACCAACGC	
ARR7-realF	TGACGGATTACTCAATGCCAGGACT	Detection of ARR7 (At1g19050) transcript by RT-qPCR
ARR7-realR	CTGCTAGCTTCACCGGTTTCAACA	
ARR15-realF	TGAGAGGTGGTGAAGCTGAAGAAGG	Detection of ARR15 (At1g74890) transcript by RT-qPCR
ARR15-realR	TGGAGTGTCGTCATCAAGGGAGGA	
qARR16-F	TGCGCTTAGAGCATTGGAGT	Detection of ARR16 (At2g40670) transcript by RT-qPCR
qARR16-R	CAAAACCTGTCATTCCAGGCA	
qrtACT2/ACT8F	GGTAACATTGTGCTCAGTGGTGG	Detection of ACT2/ACT8 transcript by RT-qPCR
qrtACT2/ACT8R	AACGACCTTAATCTTCATGCTGC	